

**V.I. Il'icev Pacific Oceanological Institute
Far East Branch, Academy of Sciences of Russia
Vladivostok, Russian Federation**

'Approved'
POI FEB RAS Director
Academic V.A. Akulichev
March 2005

**Acoustic Studies on the North East Sakhalin Shelf
Volume 1: Equipment, Methodology and Data**

**30 July to 7 October, 2004
Sakhalin, Russian Federation**

**S.V. Borisov
A.V. Gritsenko
E.V. Dmitrieva
A.A. Karnauhov
M.V. Kruglov
A.N. Rutenko**

**Prepared for:
Exxon Neftegas Limited
&
Sakhalin Energy Investment Company,**

**Yuzhno-Sakhalinsk, Sakhalin,
Russian Federation
June, 2005**

TABLE OF CONTENTS

LIST OF TABLES	III
LIST OF FIGURES.....	III
EXECUTIVE SUMMARY	VI
1 INTRODUCTION.....	1
1.1 Objectives of the acoustic program	5
1.2 Operational strategy and methodology	6
1.3 Terminology and algorithms used in the report.....	9
1.3 Terminology and algorithms used in the report.....	10
1.3 Terminology and algorithms used in the report.....	11
1.4 Units	11
2 ACOUSTIC AND HYDROLOGIC RECORDING AND PROCESSING EQUIPMENT	12
2.1 Autonomous Underwater Acoustic Recorder (AUAR).....	12
2.2 AUAR instrument tests	22
2.2.1 <i>System internal noise test</i>	22
2.2.2 <i>System dynamic range determination</i>	22
2.2.3 <i>Analog channel system filter response</i>	24
2.2.3 <i>Analog channel system filter response</i>	25
2.2.4 <i>Channel to channel crosstalk</i>	28
2.2.5 <i>Results of instrument tests</i>	31
2.3 Calibration of AUARs and cross-calibration error analysis	32
2.4 High Frequency broadband piezoelectric transducer	33
2.5 Low Frequency (LF) electromagnetic resonance transducer.....	34
2.6 Reference amplitude.....	35
2.7 Hydrologic sonde	39
2.7.1 <i>Processing and storage of hydrologic data</i>	41
2.8 Equipment and software for bathymetric profiling	42
2.9 Acoustic data storage, processing and analysis	43
3 ACOUSTIC DATA RECORDED ON THE NE SAKHALIN SHELF DURING THE 2004 FIELD SEASON	46
3.1 Ambient noise studies.....	49
3.1.1 <i>Western gray whale home range</i>	49
3.1.2 <i>Monitor, control and acoustic station locations</i>	50
3.2 Anthropogenic noise studies.....	54

3.3 Behavioral noise studies.....	55
3.3 Behavioral noise studies.....	56
3.3 Behavioral noise studies.....	57
3.4 TL Experiments	57
3.4.1 PA-B and Molikpaq pipeline TL experiments.....	57
3.4.2 Chayvo pipeline TL experiments	58
3.4.3 Orlan TL profiles.....	58
3.4.4 Reference hydrophone.....	60
3.4.5 Methodology used to monitor acoustic levels generated by the transducers	63
3.4.5 Methodology used to monitor acoustic levels generated by the transducers	64
3.5 Bathymetric and hydrologic studies	64
3.5.1 Bathymetry map	65
3.5.2 Data processing for spatial and temporal analysis of the hydrology.....	65
3.5.3 Methodology for building hydrologic sections.....	71
4 ACKNOWLEDGEMENTS	77
5 AUTHORS	77
6 BIBLIOGRAPHY	78
APPENDIX A - CALIBRATION CERTIFICATES	80
APPENDIX B - AUAR INSTRUMENT TESTS.....	117
Instrument Tests for Autonomous Underwater Acoustic Recorder (AUAR).....	117
System Noise Tests	117
System Dynamic Range.....	117
System Filter Response	118
Cross-feed Tests.....	118
Cross-calibration Tests	119
Test Schedule.....	119
APPENDIX C - CROSS-CALIBRATION RESULTS	120
APPENDIX D - METHODOLOGY FOR NORMALIZING AND ANALYZING THE ACOUSTIC DATA	126
Analyzing Transmission Loss (TL) data.....	128
APPENDIX E - DAILY SONOGRAMS FOR AUAR DATA.....	129
APPENDIX F - BATHYMETRIC DATA.....	131

LIST OF TABLES

- Table 2.1. Performance of AUARs on the instrument tests.
- Table 2.2. Technical specifications - Valeport SVXtra sonde.
- Table 3.1(a). Operational times, parameters and locations of AUARs at monitor stations 3 to 8.
- Table 3.1(b). Operational times, parameters and locations of AUARs at monitor stations 8, 10, and 11 as well as acoustic stations A4 to A8.
- Table 3.2. Numbers, names, locations and depths of the proposed stations.
- Table 3.3. Descriptions of the pipeline transmission loss (PTL) profiles.
- Table 3.4. Parameters of hydrology measurements taken on 22 September 2004.
- Table 3.5. Profiles generated using August hydrology measurements.
- Table 3.6. Profiles generated using September hydrology measurements.

LIST OF FIGURES

- Figure 1.1. The research vessel *Academik Oparin*.
- Figure 1.2. Map of the NE Sakhalin Shelf showing the proposed locations of the PA-B and Orlan platforms as well as the AUAR deployment locations.
- Figure 1.3. Map of the NE Sakhalin Shelf showing (a) the bathymetric grid and (b) the locations where vertical hydrologic profiles were acquired.
- Figure 1.4. Deployment of an AUAR from the stern of the *Academik Oparin*.
- Figure 1.5. Retrieval of an AUAR by a boat, zodiac and the *Academik Oparin*.
- Figure 1.6. Deployment of the hydrologic sonde from the *Academik Oparin*.
- Figure 2.1. (a) AUARs designed in 2003 and 2004, (b) spherical (left) and cylindrical (right) hydrophones with pre-amplifiers, (c) schematic of AUAR deployment.
- Figure 2.2. (a) components of the AUAR; (b) deploying an AUAR from the *Academik Oparin*.
- Figure 2.3. AUAR electronics tray showing power supply, disk and electronics.
- Figure 2.4. Inside the titanium AUAR container showing frame holding the batteries.
- Figure 2.5. Hydrophone deployment frame with spherical hydrophone.
- Figure 2.6. Block diagram of the analog channel of the AUAR recording system.
- Figure 2.7. Block diagram of the AUAR recording system.
- Figure 2.8. AUAR electronics (Prometheus board, flash memory and hard drive).

- Figure 2.9. (a) Block diagram showing the experimental schematic for the internal noise estimation test for the LF and HF channels of an AUAR; (b) Spectra of the results for the frequency range 0-15 kHz.
- Figure 2.10. (a) Block diagram showing the experimental schematic for system dynamic range estimation; Spectra of the results for the frequency range 0-15 kHz for (b) the LF channel; (c) the HF channel.
- Figure 2.11. (a) Block diagram showing the experimental schematic for determining the amplitude frequency characteristics of the analog channel.
- Figure 2.12. Amplitude-frequency characteristics of both HF and LF channels measured with broadband white noise; (a) from 0 to 20 kHz; (b) from 0 to 1 kHz; (c) from 0 to 100 Hz and including a plot of the low frequency part of the white noise input signal.
- Figure 2.13. Analog channel system response of all 13 AUARs to a broadband white noise input signal; (Top) the LF channel response plotted in the frequency band from 0 to 16 kHz; (Bottom) the HF channel response plotted in the frequency band from 0 to 20 kHz.
- Figure 2.14. Block diagram showing the experimental schematic for determining the system response of the AUAR.
- Figure 2.15. Top: Block diagram showing the experimental schematic for system filter response estimation; Bottom: System filter response of LF & HF channels measured with broad band white noise.
- Figure 2.16. (a, c) Block diagram showing the experimental schematics for HF to LF channel and LF to HF channel crosstalk estimation; (b) Plot of HF to LF channel crosstalk; (d) Plot of LF to HF channel crosstalk.
- Figure 2.17. Spectral characteristics of the spherical and cylindrical hydrophones.
- Figure 2.18. High frequency broadband piezoelectric transducer.
- Figure 2.19. (a) Low frequency resonance transducer and calibrated monitor hydrophone; (b) Power spectral levels of the acoustic field generated by the transducer recorded by a reference hydrophone at 1 m for a resonance frequency of ~27 Hz.
- Figure 2.20. Laboratory on the *Academik Oparin* showing the equipment for controlling the transducers and recording the reference signal.
- Figure 2.21. Spectra $G(f)$ of signals from the broadband transducer monitored by the reference hydrophone at 2 m; (a) White noise signal (solid line) and vessel noise from the *Academik Oparin* (dotted line); (b) FM signals.
- Figure 2.22. SVXtra Hydrologic sonde being deployed from the *Academik Oparin*.
- Figure 2.23. Main window of the database for the storage and analysis of hydrologic data.
- Figure 2.24. Plot showing the results from a vertical hydrologic profile acquired from the *Academik Oparin*. Note that the density and salinity have been computed from other measurements.
- Figure 2.25. Plot of the sound velocity field along a profile from the proposed Orlan platform location to the Arkutun-Dagi AUAR (#4) location.

- Figure 2.26. Equipment used for continuous recording of bathymetric and positioning data on the *Academik Oparin*.
- Figure 3.1. Map showing the AUAR locations and probability contours showing the density distributions of western gray whales from the 2002 to 2003 aerial surveys.
- Figure 3.2. Sonograms $G(f,t)$ of acoustic energy recorded at acoustic station A5 on from 13 August to 4 September 2004.
- Figure 3.3. Sonograms $G(f,t)$ of acoustic energy recorded at the Odoptu-S-10 monitor station [10] between 10 and 25 September 2004.
- Figure 3.4. Map of the study area showing the locations of the AUARs deployed during the PTL experiments and the profiles surveyed.
- Figure 3.5. Layout of the experiment conducted to investigate the acoustic pressure field from the transducers used for the TL experiments in the near field.
- Figure 3.6. Variation of average Intensity with vertical distance between the transducer and reference hydrophone (a) white noise from broadband transducer (0.8-5 kHz); (b) 27 Hz tonal signal from the LF transducer; (c) variation with horizontal distance between the reference hydrophone and LF transducer (both at 10 m) - 27 Hz tonal signal.
- Figure 3.7. Bathymetric map of the study area with contours, note the dominant NE-SW orientation of the bathymetric structures.
- Figure 3.8. 3D bathymetric map of the study area.
- Figure 3.9. (a) Section of the bathymetric grid used to generate the selected profile; (b) corresponding bathymetric profile.
- Figure 3.10. Result of a request to the hydrology database.
- Figure 3.11. Tide phase for hydrologic measurements made on 22 September 2004 (hydrology measurements are in Table 3.4).
- Figure 3.12. Profiles generated from hydrology acquired in: (a) August and (b) September.
- Figure 3.13. (a) Map showing profile 2.2 generated using data acquired on the 30 August, 2004; (b) Sound velocity field $C(z,r)$ for profile 2.2.
- Figure 3.13. (c) Temperature field $T(z,r)$; (d) Salinity field $S(z,r)$ for profile 2.2.

EXECUTIVE SUMMARY

Acoustic studies in support of the Korean-Okhotsk (western) gray whale monitoring program have been conducted on the NE Sakhalin shelf since 1999, and are designed to evaluate the impact of NE Sakhalin oil and gas developments on the western gray whale population (*Eschrichtius robustus*). These whales are listed as endangered in the Russian Red Book and critically endangered by the International Union for the Conservation of Nature¹.

The key goals of the acoustic monitoring program are threefold. The first goal is to monitor the ambient sound levels on the NE Sakhalin shelf and the temporal variation in anthropogenic noise levels due to oil and gas development activities. The second goal (in conjunction with the behavioral and observational biology programs) is to evaluate the impact of changes in anthropogenic sound on western gray whale behavior, proposing mitigation measures where appropriate. The third goal for the 2004 program was to evaluate the transmission loss from the proposed Exxon Neftegas Limited (ENL) and Sakhalin Energy Investment Company (SEIC) pipeline routes to the Piltun feeding area.

In 2003, The Pacific Oceanological Institute (POI) developed an Autonomous Underwater Acoustic Recorder (AUAR). These AUARs make high fidelity acoustic measurements with an improved dynamic range, increased bandwidth (1 Hz - 15 kHz) and extended recording time (15 days continuous recording), allowing acoustic measurements to be conducted over the entire NE Sakhalin shelf rather than a small range around a base camp or vessel as with sonobuoys. In 2004 eight redesigned AUARs were constructed. Together with the remaining AUARs from 2003 this brought the total number of AUARs available to 13.

In addition to the acoustic studies, a comprehensive sampling program for bathymetry and hydrology was initiated in 2004. The goal of this program was to better understand the temporal and spatial variations in the hydrologic parameters on the NE Sakhalin shelf. This included the short-term and long-term (seasonal) variations as well as changes due to typhoons and strong storms. This data will be used to improve acoustic models and better understand acoustic propagation on the shelf.

¹ Aerial surveys indicate that the gray whales spend most of the ice-free season feeding off the NE Sakhalin coast. They are predominantly located shoreward of the 20 m water depth contour, in an area from the mouth of Piltun bay northwards along the coast as well as south of the Arktun-Dagi license in 30-45 m of water.

1 INTRODUCTION

The acoustic program conducted on the NE shelf of Sakhalin Island in 2004 was an extension to the acoustic monitoring program initiated in 2003. The monitoring program was designed to study temporal and spatial variations in the amplitude and frequency characteristics of ambient and anthropogenic sound at the edge of the Piltun and Offshore gray whale feeding areas. In addition to the program monitoring the background acoustic environment, both ENL and SEIC conducted detailed Transmission Loss (TL) studies along proposed pipeline routes and from proposed facilities. In order to estimate the sound transmission from project activities, it is necessary to understand the characteristics of sound propagation from the proposed production facilities to the limits of the known gray whale feeding areas. These are the areas where the gray whales are concentrated, predominantly feeding in water depths of 5-20 m in the Piltun feeding area and 30-50 m in the Offshore feeding area. Mother-calf pairs have also been seen in the Piltun feeding area in water depths less than 10 m. These studies, in conjunction with the amplitude and spectral content of the background acoustic environment, will be used to assess any potential impacts from the construction and to design more effective mitigation measures.

The acoustic measurements were conducted using digital Autonomous Underwater Acoustic Recorders (AUARs) developed at POI FEB RAS² (POI). The AUARs were designed to accurately record frequencies between 1-15,000 Hz and enable accurate, autonomous, synchronous acoustic measurements over a broad range of frequencies (including infrasounds). A detailed description of this equipment will be given in chapter 2.

During the 2004 field season (30 July to 7 October), AUARs were deployed from the research vessel *Academik Oparin* (Figure 1.1) which also accommodated the biology teams (Benthic, Marine Mammal Observers (MMO) and Photo-ID). Synchronous acoustic measurements were made at stations ranging from north of the Odoptu license area to the center of the Offshore feeding area (Figure 1.2), an area extending 100 km along the NE Sakhalin shelf.

² POI FEB RAS - The Pacific Oceanological Institute, Far East Branch of the Russian Academy of Sciences.

Previous work had shown that the results from acoustic modeling are very sensitive to the hydrologic, bathymetric and sea bottom parameters along the profile of interest. A comprehensive suite of bathymetric and hydrologic measurements was therefore taken using the vessel's sonar and a hydrologic sonde. The total number of measurements undertaken reached 323 vertical hydrologic profiles (comprising sound velocity, temperature and salinity), and 8400 km of bathymetry data. Figure 1.3 gives two maps showing the extent of the bathymetric grid and the points at which vertical hydrologic profiles were acquired.



Figure 1.1 - The research vessel *Academik Oparin*.

The results of the 2004 acoustic program are presented in two separate reports. The first report describes the objectives of the 2004 program, the equipment used, its testing and calibration as well as the operational strategy and methodology for the 2004 field program. This includes the methodology for the TL studies that are analyzed in more detail in the second report. This report contains sonograms (on a CD) in 24-hour segments for all the data recorded in 2004 and listed in the Appendices. This report also contains the bathymetric and hydrologic data acquired during the field season.

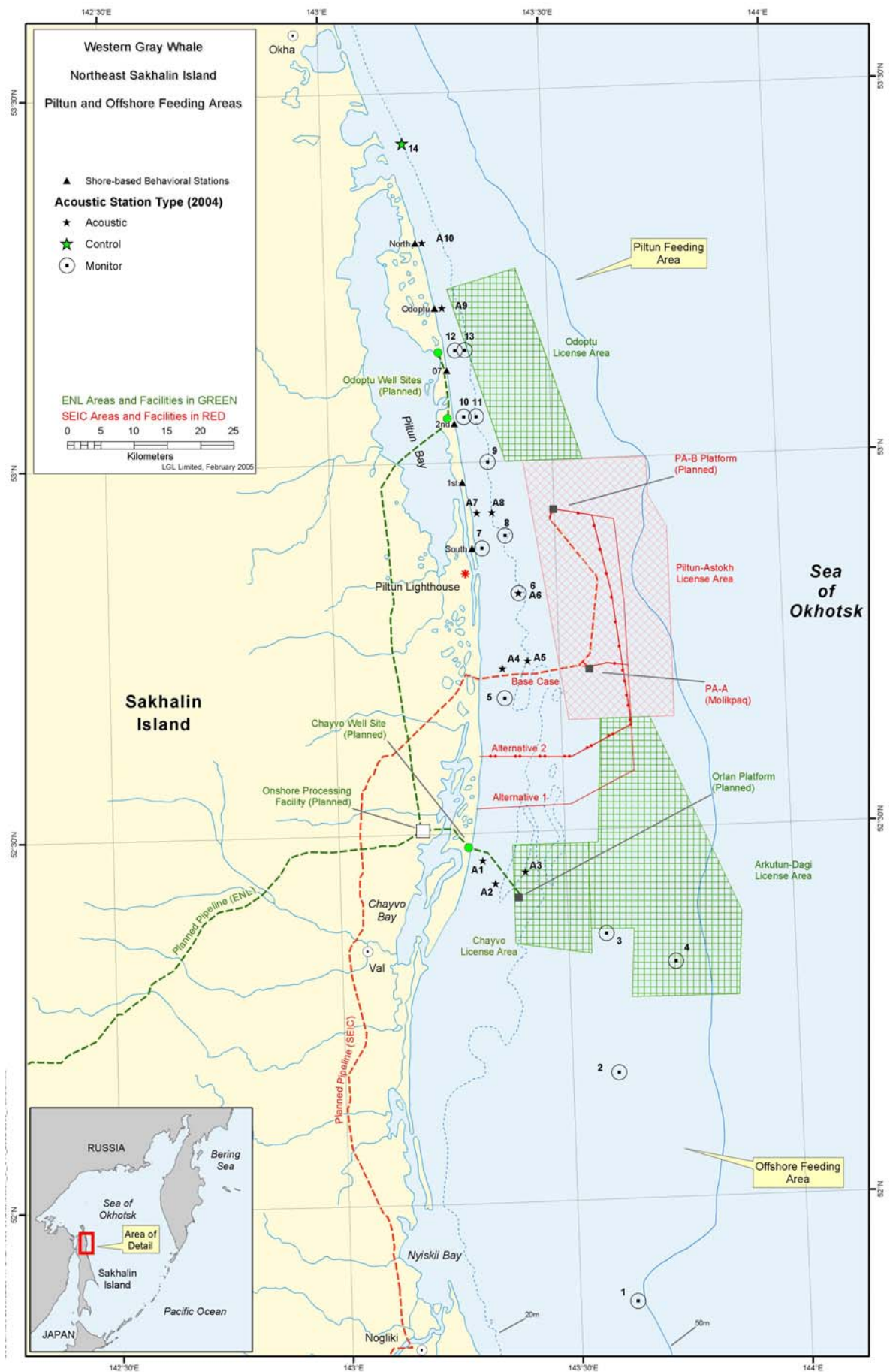


Figure 1.2 - Map of the NE Sakhalin Shelf showing the proposed locations of the PA-B and Orlan platforms as well as the AUAR deployment locations.

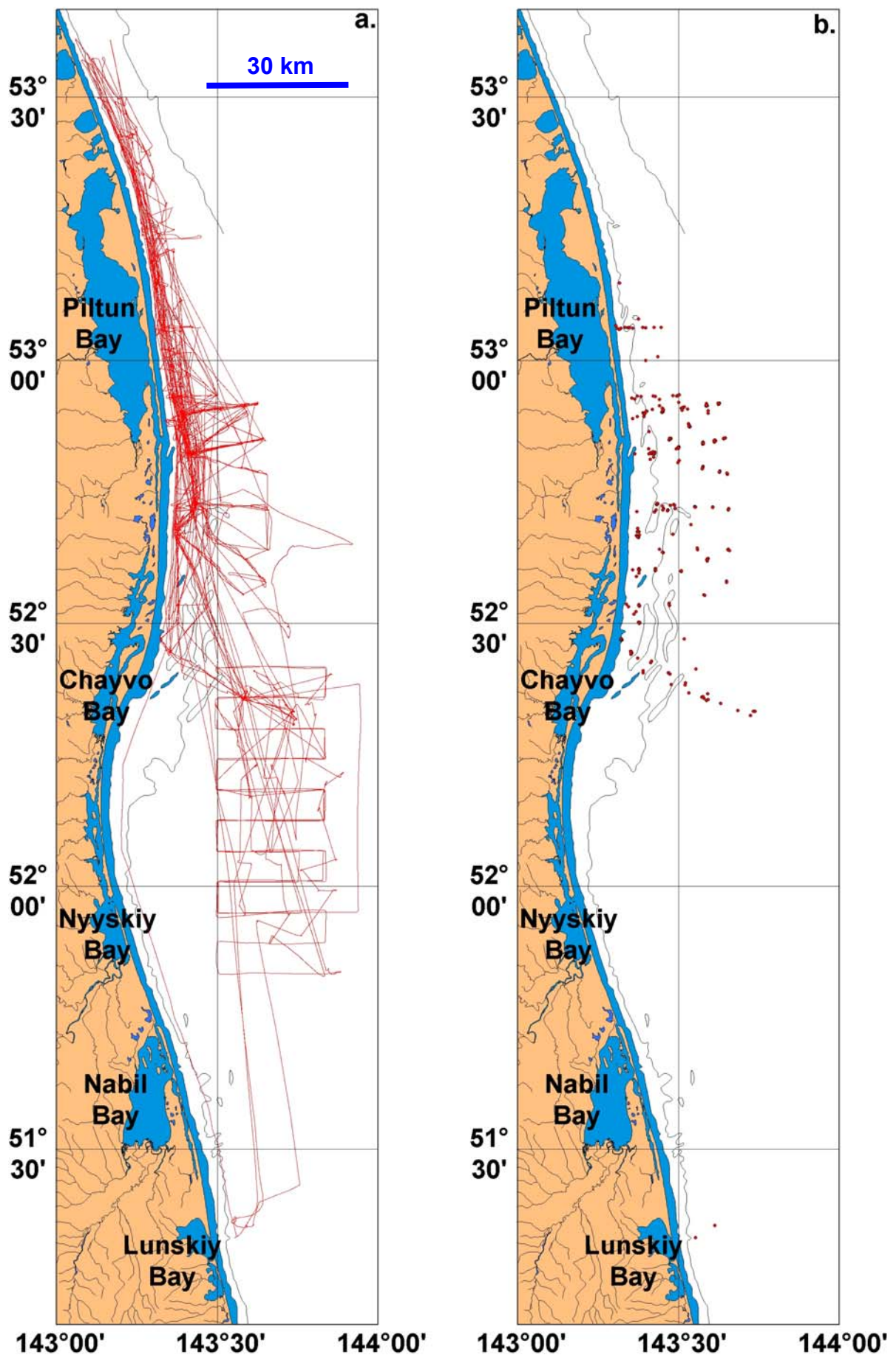


Figure 1.3 - Map of the NE Sakhalin Shelf showing (a) the bathymetric grid and (b) the locations where vertical hydrologic profiles were acquired.

The second report is dedicated to analysis of the data, conclusions and recommendations for future work. This analysis includes the following components:

1. A quantitative spectral analysis of the variation in the ambient acoustic noise level with weather conditions (including typhoons).
2. The results of the comprehensive TL experiments along the proposed pipeline routes from the Moliqpaq and PA-B platforms to the Piltun gray whale feeding area, and from the Orlan platform and Chayvo pipeline route to the Piltun and Offshore feeding areas.
3. A temporal, spectral and spectral-temporal analysis of the acoustic data recorded at different locations on the Sakhalin shelf³.
4. A temporal analysis of acoustic pulses (of anthropogenic, biological and natural seismic origin) recorded on the NE Sakhalin shelf.
5. The results of experiments to measure the noise from the outboard motors on the photo-ID zodiacs and from the *Academik Oparin*.

1.1 Objectives of the acoustic program

The acoustic program conducted on the NE shelf of Sakhalin Island in 2004 had four main objectives:

1. The first was to study both temporal and spatial variations in the amplitude and frequency characteristics of ambient and anthropogenic sound at a series of monitoring stations located throughout the development area. These monitoring stations were positioned to be at the nearest outside edge of a gray whale feeding area to a proposed facility. The goal of this annual acoustic monitoring program is to estimate any increase in the cumulative acoustic level in the gray whale feeding areas due to the oil development and production activities.
2. The second objective was to study sound propagation and the variation in frequency dependent TL from the proposed pipeline routes to the nearest gray whale feeding area. These include the pipelines from Moliqpaq and PA-B as well as from Orlan to Chayvo. The results of these TL profiles will allow the prediction of the potential acoustic footprint from a facility with a defined acoustic signature, installed at the proposed location.

³ The use of AUARs for the 2004 program allowed an unprecedented characterization of the ambient noise at the monitoring stations. However, since the vessel used to house the scientists (*Academik Oparin*) was often a significant distance from the AUAR the identification and specific location of any transient anthropogenic noise source is generally unknown.

3. The third objective was to acquire a comprehensive grid of bathymetric and hydrologic data across the study area, and to investigate the spatial and temporal variations in the hydrology due to weather events (e.g. typhoons).
4. The final objective was to measure the acoustic levels of the two outboard motors used for the photo-ID zodiacs (one two-stroke and one four-stroke) as well as the *Academik Oparin* (under different operational scenarios).

1.2 Operational strategy and methodology

The shallow water (5 - 15 m) part of the NE Sakhalin shelf starting south of the mouth of Piltun Bay and extending northwards up the Sakhalin coast is one of the most important summer feeding areas for the western gray whales. For this reason, acoustic studies have been conducted in the area since 1999. In 2001, a second gray whale feeding area was discovered Offshore in water depths of 30-50 m, approximately 20 km to the south east of the mouth of Chayvo Bay.

In 2004 as in 2003, the entire acoustic program was operated from a vessel. The vessel used in 2004 was the *Academik Oparin*. The *Academik Oparin* was also the operational platform for all the vessel-based biology programs (Photo-ID, benthic, MMO). Dr. Yuri Yakovlev was the expedition leader for the biology-acoustics expedition and managed the overall *Academik Oparin* based operations.

In 2003, POI designed and developed six AUARs in order to capitalize on the enhanced flexibility of a vessel-based program and to allow synchronous acoustic measurements to be conducted over a greatly enlarged spatial area. Each AUAR can be deployed at depths up to 50 m (two to 100 m), can record continuously for 15 days and can measure the absolute acoustic amplitude of a signal over a frequency band from 1-15000 Hz. A detailed description of this equipment is given in chapter 2. In 2004, eight more AUARs were built, 13 AUARs were therefore used for the 2004 field season when the five remaining from 2003 are included (one was lost in 2003).

One of the operational advantages of the *Academik Oparin* is that it can operate in water depths as shallow as 10 m. In water depths greater than 10 m the AUARs were deployed from the stern of the *Academik Oparin* as it sailed slowly along its course (Figure 1.4).

AUARs were retrieved manually using a zodiac or boat deployed from the *Academik Oparin*. When a boat was used the AUAR was pulled to the surface and onto the boat by hand. If a zodiac was used the AUAR was pulled to the surface and towed to the *Academik Oparin*. When the zodiac or boat returned to the *Academik Oparin* the AUAR was transferred to the *Academik Oparin* using its crane (Figures 1.5 and 1.6). Before the expedition the *Academik Oparin* was upgraded with a special electric winch for deploying the hydrologic sonde and transducers to a depth of 10 m.

A low frequency (LF) resonant electromagnetic transducer and high frequency (HF) piezoelectric broadband transducer were deployed from the *Academik Oparin* and used for sound propagation and TL studies at frequencies from 15-15000 Hz. The acoustic level of signals generated by the transducers was monitored using a calibrated hydrophone and recorded on the vessel. As in 2003, the hydrologic characteristics (salinity, velocity, temperature and pressure) of the water layer were acquired using a hydrologic sonde⁴ and were used to more accurately characterize the TL measurements. During the TL experiments, the *Academik Oparin* proceeded at a constant speed along the defined acoustic profiles measuring the depth with a bottom profiler. It was therefore a quasi-stationary noise source of known frequency content and location. A more powerful broadband transducer was built for the 2004 field season.

After the AUAR was recovered, acoustic data from the hard disk was downloaded onto a computer on the *Academik Oparin* and backed up to CDs. The batteries were re-charged prior to redeployment, if a fast turnaround was required (e.g. the AUAR was being re-deployed at the same location) a spare disk and batteries were used. The Received Level (RL) of an acoustic signal depends on the hydrophone deployment depth and the distance between the potential noise source and the AUAR. The gain coefficients of the AUAR must be set to maximize the dynamic range of the recording system⁵. Since the goal of the 2004 season was to measure ambient or low level anthropogenic noise, the gain (and thus sensitivity) of the AUARs was high.

⁴ Model SVXtra manufactured by Valeport Limited, England.

⁵ The minimum acoustic signal that can be measured depends on the gain, the higher the gain the smaller the signals measured, but higher signals are clipped.



Figure 1.4 - Deployment of an AUAR from the stern of the *Academik Oparin*.



Figure 1.5 - Retrieval of an AUAR by a boat, zodiac and the *Academik Oparin*.



Figure 1.6 - Deployment of the hydrologic sonde from the *Academik Oparin*.

1.3 Terminology and algorithms used in the report

Ambient and anthropogenic acoustic data recorded by the AUARs was written to the AUAR disc in a raw format and converted to microPascals (μPa)⁶ after downloading to the computer on the *Academik Oparin* (or during analysis). Acoustic spectra in decibels will be used to describe the variation in acoustic power as a function of frequency. In this report, sound pressure power density spectra $G(f)$ ($\mu\text{Pa}^2/\text{Hz}$)⁷ will be used when spectral data are plotted. The sonograms $G(f,t)$ are plots of power spectral density vs. frequency and time. The scales generally run from ~37 to ~100 dB re 1 $\mu\text{Pa}^2/\text{Hz}$.

The ***Spectral level*** of an acoustic signal relates to the level of acoustic power in a 1 Hz band. This term is only applied to sounds with continuous frequency spectra⁸. These spectra are often averaged over a number of one-second windows⁹ to improve the statistical stability of the ambient noise data¹⁰; the number of one-second windows used in the averaging is given at the top of each plot.

A detailed description of the methodology used for normalizing and calculating both the amplitude and spectral data is given in Appendix D.

1.4 Units

During the course of this report a number of different unit notations have been used. This is due to differences in standard notation between different disciplines and nationalities.

The following are equivalent units using the different standard nomenclatures:

1 mkPa = 1 μPa and 1 mkV = 1 μV .

For spectral density plots: Although the units for power spectral density are $\mu\text{Pa}^2/(\text{s Hz})$, $\mu\text{Pa}^2/\text{s/Hz}$ or μPa^2 , the units for power spectral density are sometimes defined as $\mu\text{Pa}^2/\text{Hz}$ or $\mu\text{Pa}/\sqrt{\text{Hz}}$.

⁶ The data was scaled (after incorporating hydrophone sensitivity, system instrument response and system gain), to convert the data to standard units of pressure (measured through an omni-directional hydrophone).

⁷ Energy and power spectra are scaled to 1 Hz whatever the analysis length.

⁸ A continuous frequency spectrum is a spectrum with signal present at all sampled frequencies.

⁹ Average of X 1-second spectral estimates.

¹⁰ Spectral averaging is used to obtain a lower variance spectral estimate.

2 ACOUSTIC AND HYDROLOGIC RECORDING AND PROCESSING EQUIPMENT

This section describes the Autonomous Underwater Acoustic Recorders (AUAR) developed by POI and used to record acoustic data during the 2004 field program, its instrument testing, calibration and operational deployment. This section further describes the two acoustic transducers utilized for sound propagation studies and the monitoring of the acoustic field generated by them, as well as the hydrologic sonde used to make water column measurements during these studies. It also includes a description of the tools and methodology for analyzing the data.

2.1 Autonomous Underwater Acoustic Recorder (AUAR)

In 2004 POI used the five AUARs designed and constructed in 2003, and eight newly fabricated AUARs¹¹. These individually deployed AUARs were used to make acoustic measurements in the frequency band from 1 Hz to 15 kHz. Figure 2.1(c) shows the major components of an AUAR and how the AUAR and hydrophone are anchored when deployed.

The external shell of the 2003 AUAR is a cylinder 0.8 m long and 0.38 m in diameter constructed from welded titanium alloy; its weight in air is approximately 105 kg. In order to facilitate the deployment and retrieval of the AUARs from a zodiac, the diameter was decreased to 0.32 m and the length increased to 1.2 m in the 2004 design, the weight in air remaining at 105 kg (Figure 2.1(a)). The titanium alloy case of both AUARs can be opened at one end and has been strengthened for deployment in depths of up to 100 m. The open end is used to gain access to the unit and is sealed with o-rings. The lid contains two waterproof connectors that allow external sensors (hydrophones, accelerometers or hydrologic measuring equipment) to be input to the AUAR electronics. Inside the AUAR there are batteries secured in a titanium frame and a tray containing the AUAR electronics and power handling circuitry. The number of batteries depends on the AUAR design, the 2003 AUARs have two sealed batteries can provide continuous operation of the AUAR for over 18 days, the 2004 AUARs have three sealed batteries providing continuous operation of the AUAR for over 15 days¹² (Figures 2.2 to 2.4).

¹¹ The eight new AUARs were designed to improve the operational handling of the units following the experiences of the 2003 field program.

¹² The two sealed batteries (2003) have a capacity of 115 Ampere-hours. The three sealed batteries (2004) have a capacity of 115 Ampere-hours.

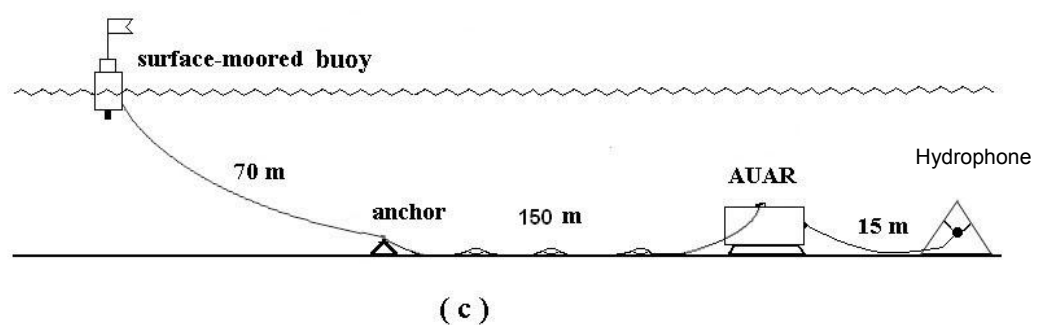
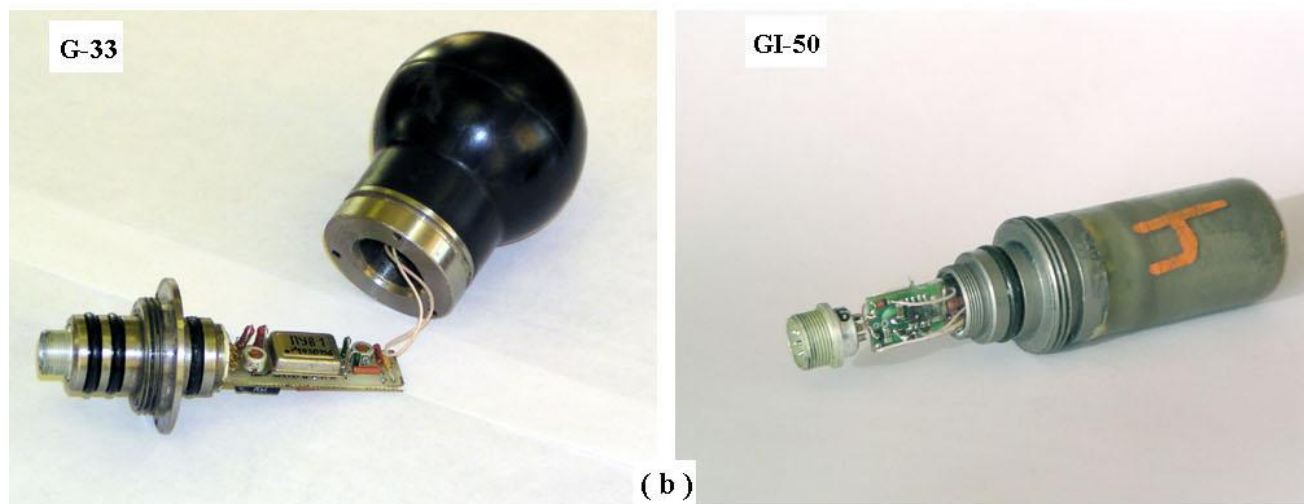


Figure 2.1 - (a) AUARs designed in 2003 and 2004, (b) spherical (left) and cylindrical (right) hydrophones with pre-amplifiers, (c) schematic of AUAR deployment.

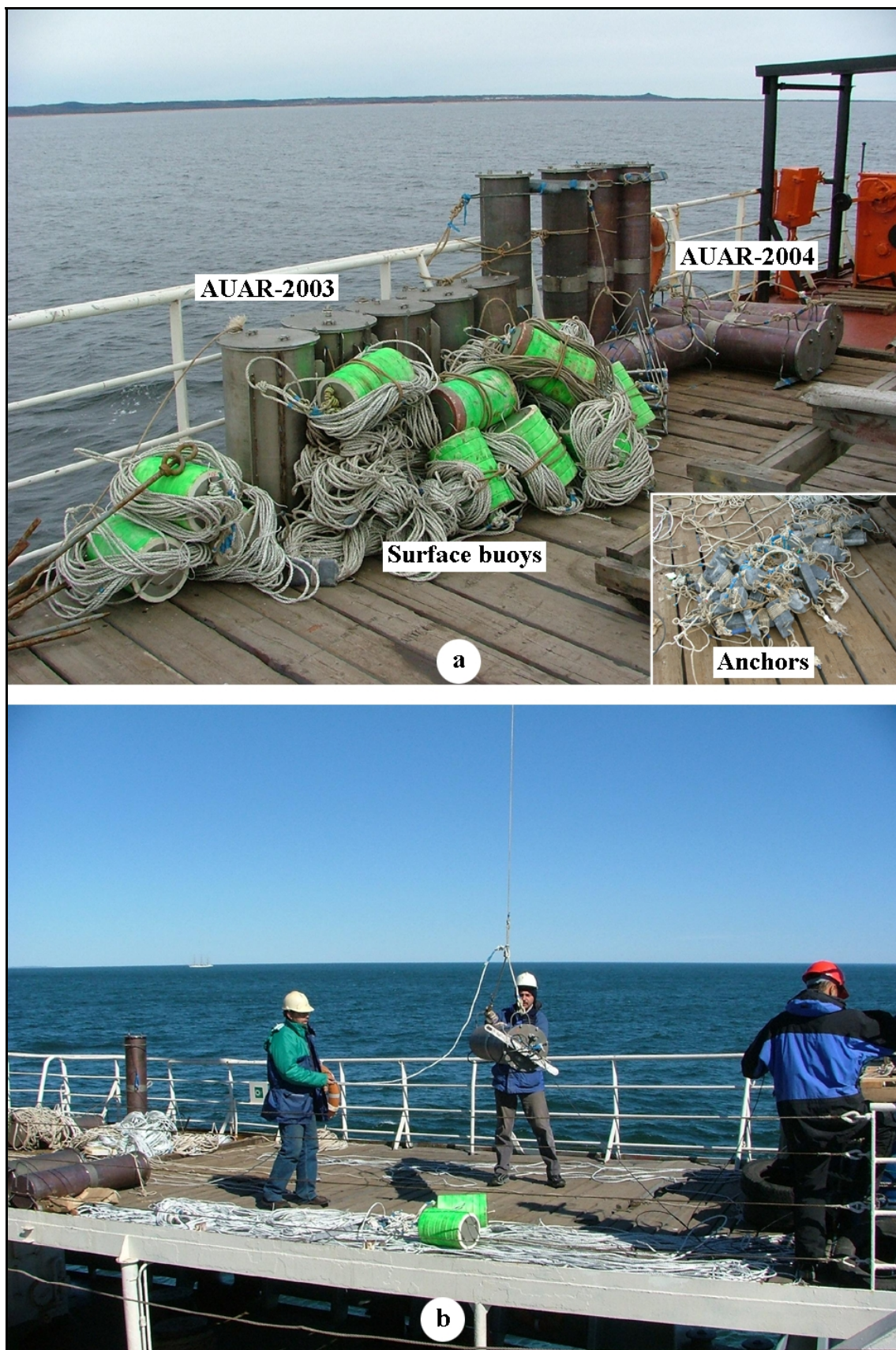


Figure 2.2 - (a) components of the AUAR; (b) deploying an AUAR from the *Academik Oparin*.



Figure 2.3 - AUAR electronics tray showing power supply, disk and electronics.



Figure 2.4 - Inside the titanium AUAR container showing frame holding the batteries.

Figure 2.1(c) shows the layout of the AUAR in the ocean. A surface float connected with a 70 m rope to a 24 kg anchor marks the location of the AUAR on deployment. This anchor is linked to the AUAR by a 150 m long rope weighted down with lead weights. The GPS coordinates of both the anchor and the AUAR are logged during deployment and if necessary the vessel can grapple for the 150 m rope between them, the AUAR can therefore still be recovered in the event that the surface buoy is lost. One AUAR was recovered in this manner during the 2003 field season.

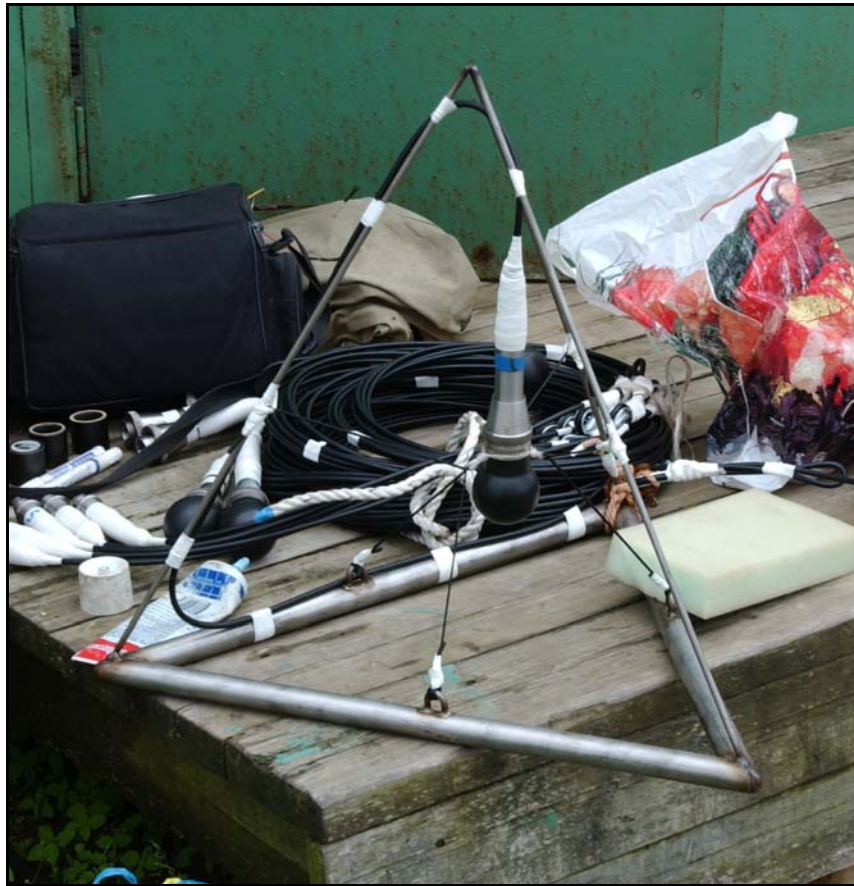


Figure 2.5 - Hydrophone deployment frame with spherical hydrophone.

Practical experience has shown that at shallow deployment depths (10-30 m), movement of the surface buoy due to wave action can be mechanically conducted down the rope to the hydrophone, where this mechanical movement can be recorded as acoustic noise. Interaction of the surface float with waves can generate noise that acoustically propagated to the hydrophone. The AUAR is deployed so as to reduce this noise by isolating the hydrophone from the surface buoy with an anchor, thus reducing the mechanical coupling between the surface buoy and the hydrophone. The hydrophone is also deployed 15 m from the AUAR to prevent scattering or masking by the AUAR container from distorting the

acoustic field at high frequencies. The hydrophone is deployed inside a pyramid shaped wire frame and attached by rubber bands to the frame, isolating it to the best extent possible from the sea floor (Figure 2.5).

Cylindrical hydrophones (model # GI-50 (ГИ-50)) and Spherical hydrophones of type G61H (Г61H) both with integrated pre-amplifiers designed specifically for the hydrophones were used for the AUARs, Figure 2.1(b) shows the hydrophones. The pre-amplifier amplifies the signal prior to transmission along the 15 m connector to the AUAR¹³. The hydrophones were calibrated over the frequency band 1 Hz to 15 kHz. AUARs were deployed at a low speed (3-4 knots) using a crane at the stern of the *Academik Oparin* and were retrieved using a zodiac or boat as discussed earlier.

Figures 2.6 and 2.7 give block diagrams for the AUAR electronics. The output from the hydrophone and pre-amplifier is transmitted along the 15 m cable to the AUAR input connector. The AUAR houses the amplifier, filters and the Analog to Digital Converter (ADC).

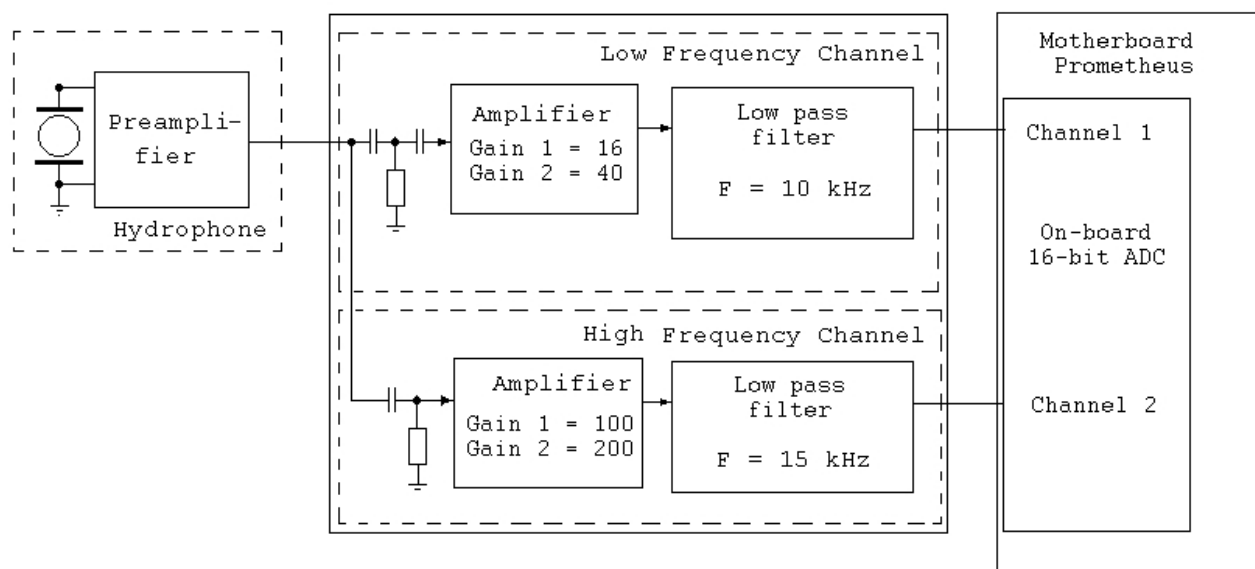


Figure 2.6 - Block diagram of the analog channel of the AUAR recording system.

¹³ The purpose of the pre-amplifier is to amplify the signal as close as possible to the hydrophone. In this way the signal level relative to any noise picked up in the cable and AUAR will be maximized.

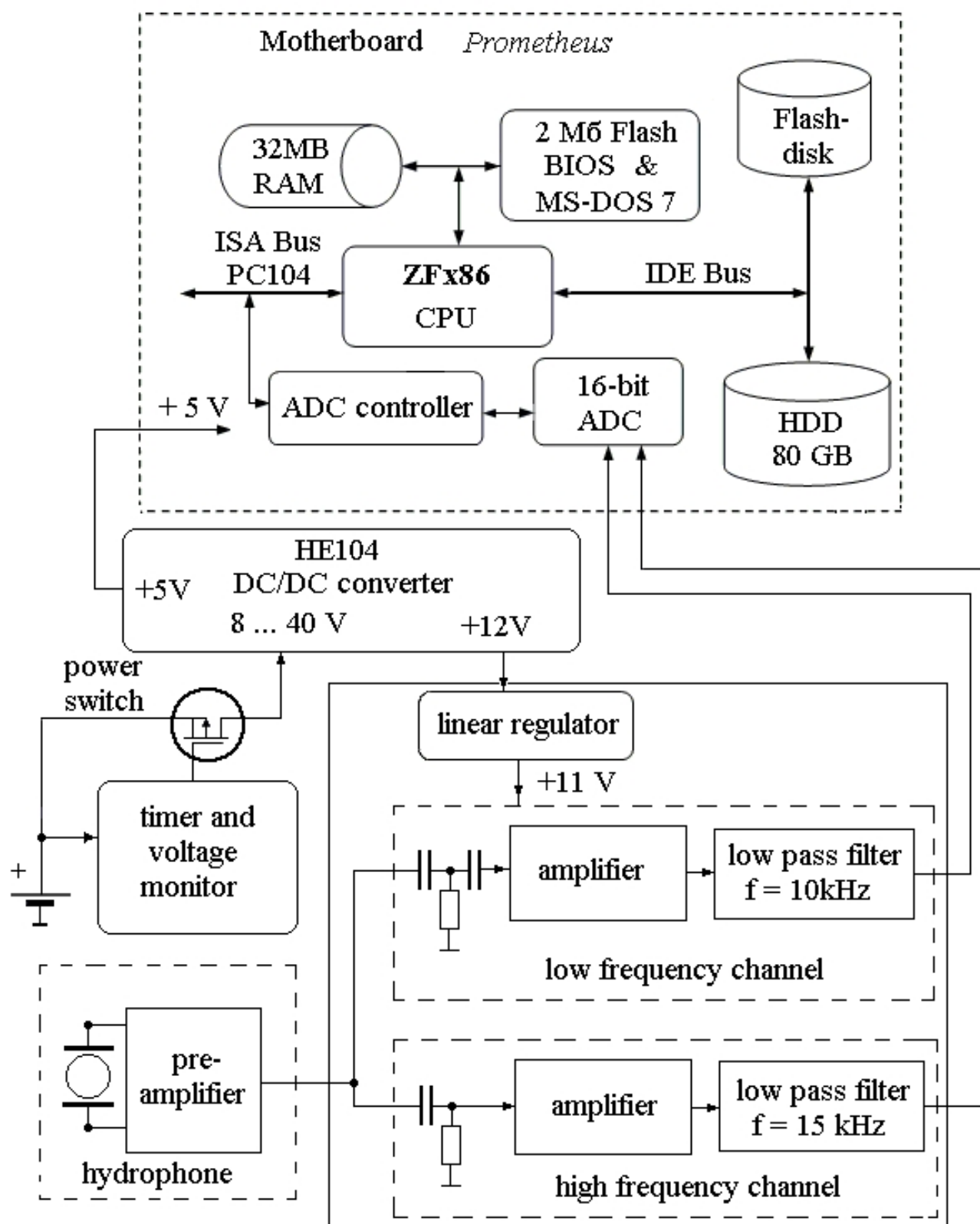


Figure 2.7 - Block diagram of the AUAR recording system.

In order to optimize the dynamic range of the 16 bit ADC¹⁴ the signal amplitudes should be equal across the entire frequency range. However, ambient noise generally has an amplitude maximum at low frequencies and drops off with higher frequencies. The ADC does not have the dynamic range to record frequencies from 1 Hz to 15 kHz. The AUAR therefore has two analog channels, a Low Frequency (LF) channel with only a second order correction for frequencies below 50 Hz and a High Frequency (HF) channel that is processed to maximize the dynamic range. The HF channel has the low frequency component (<3 kHz) removed by a low cut filter, allowing the gain coefficient for frequencies above 1 kHz to be increased without overloading the ADC.



Figure 2.8 - AUAR electronics (Prometheus board, flash memory and hard drive).

The signal from the AUAR input connector is split into two identical data channels. The first is input to the scale amplifier and second order RC filter of the low frequency channel, which has user selectable gain coefficients of 16 or 40. It is then passed into an 8th order elliptic

¹⁴ The ADC is on the Prometheus motherboard and has a maximum sample rate of 100 kHz.

low pass frequency filter with an anti-alias high cut frequency of 10 kHz and slope of 80 dB/Octave. Simultaneously, the signal from the second data channel is input to the scale amplifier and first order RC filter of the high frequency channel, which has user selectable gain coefficients of 100 or 200. The high pass RC-filter has a low cut frequency of 1.5 kHz and slope of 6 dB/Octave. This high passed signal is filtered with the same 8th order elliptic low frequency filter with an anti-alias high cut frequency of 15 kHz and slope of 80 dB/Octave.

The AUARs digital recorder is based on the Prometheus single board computer (Figure 2.7 and Figure 2.8)¹⁵. The 16 bit ADC is connected to the input controller by eight differential inputs and a 48-sample FIFO (First In First Out) buffer. The primary AUAR data storage is a compact laptop 80 GB hard drive¹⁶. To optimize power management and prevent electromagnetic and acoustic noise generated by the rotating hard drive from contaminating the data a 489 MB (2003 AUARs) or 1 GB (2004 AUARs) flash memory drive are used as a buffer. While data is being recorded on the flash drive, the hard drive is in standby mode with its motor off. A voltage converter¹⁷ takes the initial battery voltage (39 V) to a stabilized 12 V to power the computer; the electronic components of the analog devices are powered with an independent linear stabilizer and housed in a shielded container. All units comply with the PC104 specification, having dimensions of 9.1 x 9.7 cm and can work in temperatures from +85 to -40 °C.

The AUAR operating system is MS-DOS 7 and the recording program is written in C++. Acoustic Data are directly recorded to the hard disk by sector, and assembler functions are written for programming the disk controller and writing directly to the hard drive. Data exchange between the RAM and CPU utilizes interrupts. To prevent internal or external errors causing the programs to hang, a WatchDog timer is used¹⁸.

¹⁵The computer, manufactured by Diamond Systems Corporation, consists of a 486-DX2-100 CPU, USB-port, 32 MB RAM, IDE-controller connected to the internal PCI bus, analog and digital input/output unit and 2 MB flash memory containing BIOS, OS and POI recording program.

¹⁶ Although significantly smaller in size than the largest desktop hard drive, the laptop hard drive has better power management and uses dramatically less power.

¹⁷ VE104 - input voltage: 8-40 V (2003 AUARs); HE104 - input voltage: 8-40 V (2004 AUARs).

¹⁸ This system routine checks to ensure that a specific function has been executed within a defined time frame, if the function fails to execute within this time frame the system restarts the function.

The AUAR can be pre-programmed to fulfil a preset recording schedule. This can include a delayed start or an intermittent recording schedule¹⁹. The HF channel is recorded on a schedule selected by the user in order to balance the HF data recorded and the AUARs operational time²⁰. Before the AUAR is deployed its computer is programmed for the desired recording schedules and modes (e.g. how often and for how long will the HF channel be recorded, whether the LF recorder will run continuously or intermittently).

The AUAR recording system operates in a cyclic mode. Each cycle is a sequence of data blocks streaming either from one LF channel (20 kHz sample rate) or synchronously from one LF and one HF channel (20 kHz, 30 kHz sample rates) into the flash memory for storage. Data from the internal memory of the ADC is stored in 2 RAM shoulder buffers; data blocks with sample rates of 20 and 30 kHz are stored in one of the shoulder buffers after each cycle. When one of the shoulder buffers is full the data is transferred to a file on the flash memory drive and the data from the ADC is stored in the second shoulder buffer. The two buffers therefore flip-flop; data being stored in one while the other transfers data to the flash memory. When the flash memory drive is full, the recording cycle stops and the data is moved from the flash memory drive to the hard drive; the number of records in the file being dependent on the size of the flash memory drive. The AUAR hard drive is formatted into FAT32, the program itself modifies the FAT as data are written by sector onto the hard drive. The file name includes the date, start time of the record and number of channels recorded (e.g. d3071218.451 corresponds to - year: 2003; month: 07; day: 12; start time: 18:45; # channels: 1). Since the recording cycle is halted when the flash memory drive is full, and cannot be restarted until the flash memory drive is clear - the data contains controlled gaps. The size of these gaps depends on the size of the flash memory drive and the recording parameters (percentage of time HF channel is recorded)²¹.

Computers on the *Academik Oparin* were used as the main data storage units. The acoustic data on the AUAR hard drive was copied to a removable hard drive as transient

¹⁹ A programmable timer and program executive controls the delayed start or power switching of the AUAR electronics when deployed, the unit is based on the AT90S1200 microcontroller. The delay timer is programmed just before deployment; it can delay recording from 10 minutes to 30 hours.

²⁰ The HF channel can be continuously recorded, however the increased sample rate would fill the hard drive of the AUAR. The HF channel was only periodically recorded to maximize the operation of the AUAR.

²¹ For a 489 MB flash memory drive the gap was approximately 9 minutes, for a 1 GB flash drive it was approximately 24 minutes.

storage before the files on the AUAR drive were deleted prior to redeployment. Periodically data from this transient storage was backed up to DVDs.

2.2 AUAR instrument tests

The AUARs were designed and manufactured by POI in 2003 and 2004. In order to ensure that all of the AUARs adhered to the design specifications, and that the AUARs recorded accurate absolute acoustic measurements, a series of instrument tests were created²². These tests had two goals, to ensure that the AUAR was operating within specifications and to generate an instrument response filter for the analog component of each AUAR. This estimate of the AUAR analog instrument response, measured in the laboratory prior to the field season $K(f)$ and the hydrophone sensitivity $M(f)$ was used to generate an inverse filter; this filter was subsequently applied to the absolute acoustic measurements to back out the system instrument response. These frequency dependent responses correct the acoustic data over the range from 1 Hz - 10 kHz (LF channel) and 10 Hz - 15 kHz (HF channel).

2.2.1 System internal noise test

A $9\ \Omega$ resistor was connected parallel to the hydrophone (Figure 2.9(a)). Data was recorded to flash memory for one writing cycle (60 seconds) and from there to the hard drive. Both LF and HF channels were simultaneously recorded with a 30 kHz sample rate. Figure 2.9(b) displays a spectral analysis of the results showing the internal noise of the LF and HF channels for the frequency range 0-15 kHz. The Internal noise of the AUAR in the frequency range 1.5-15 kHz is approximately 35 dB re $1\ \mu\text{Pa}^2/\text{Hz}$, increasing by up to 20 dB at low frequencies²³.

2.2.2 System dynamic range determination

Figure 2.10(a) gives a block diagram showing the experimental schematic for determining the dynamic range of the LF and HF channels. A sine wave generator model # G3-118 (Γ3-118) was used to generate signals at 20 Hz, 200 Hz, 500 Hz, 2 kHz and 5 kHz into the hydrophone, a $9\ \Omega$ resistor was connected parallel to the hydrophone sensor. The input data should be a smooth sine wave, not clipped or distorted at the peaks, the sine wave amplitude was therefore attenuated to ensure that any non-linear distortion at output was more than 60 dB below the input level. The maximum input acoustic pressure level at which

²² The AUAR instrument tests are given in Appendix B.

²³ This increase in noise at low frequencies could be a result of electromagnetic pick-up during the testing.

the non-linear distortion is 60 dB below the input level is 135 dB re $1 \mu\text{Pa}^2/\text{Hz}$ for the LF channel and 113 dB re $1 \mu\text{Pa}^2/\text{Hz}$ for the HF channel (Figure 2.10(b, c)). Since the instrument noise at approximately 35 dB re $1 \mu\text{Pa}^2/\text{Hz}$ is below the distortion, distortion limits the dynamic range of the AUAR.

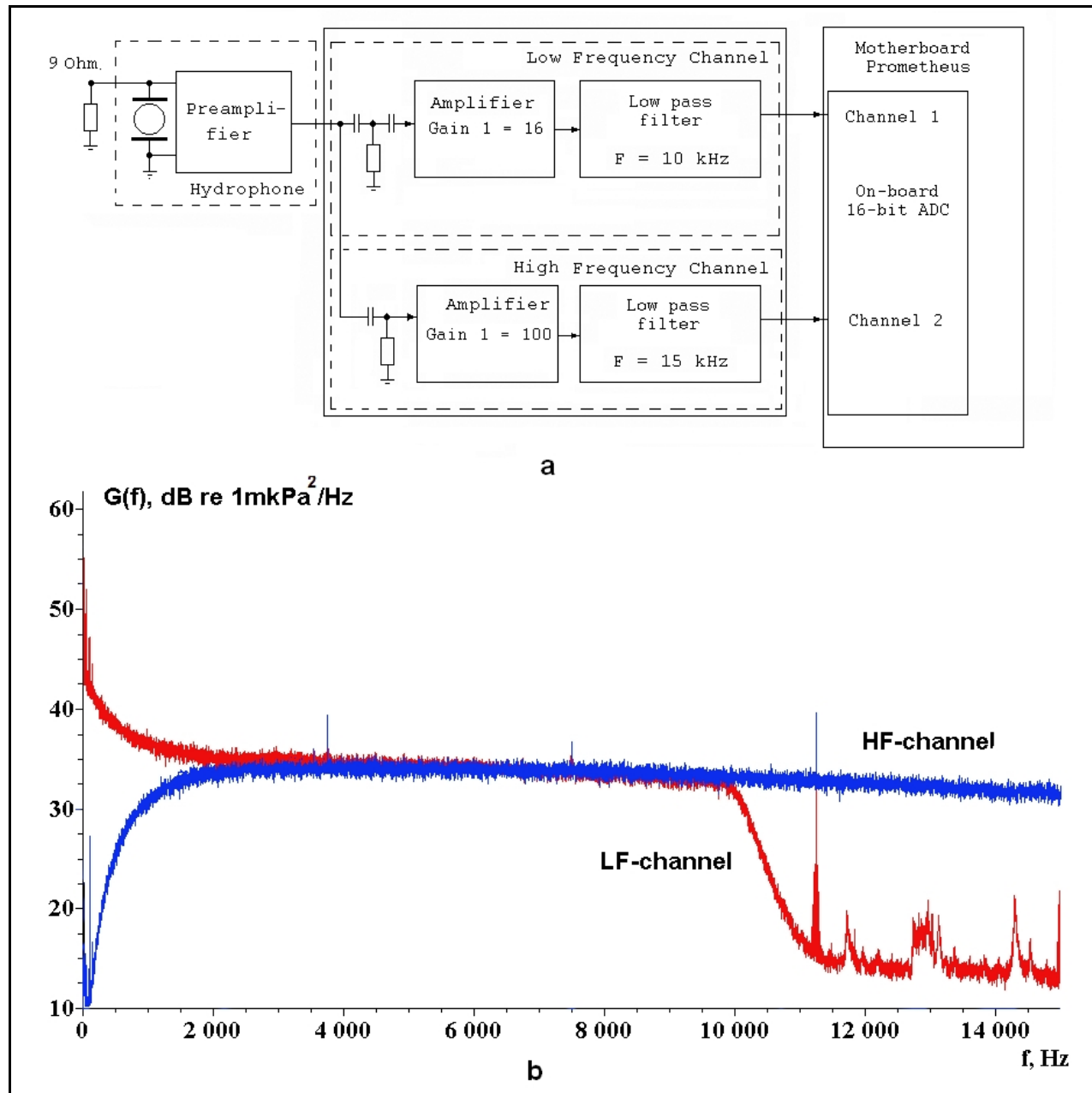


Figure 2.9 - (a) Block diagram showing the experimental schematic for the internal noise estimation test for the LF and HF channels of an AUAR; (b) Spectra of the results for the frequency range 0-15 kHz.

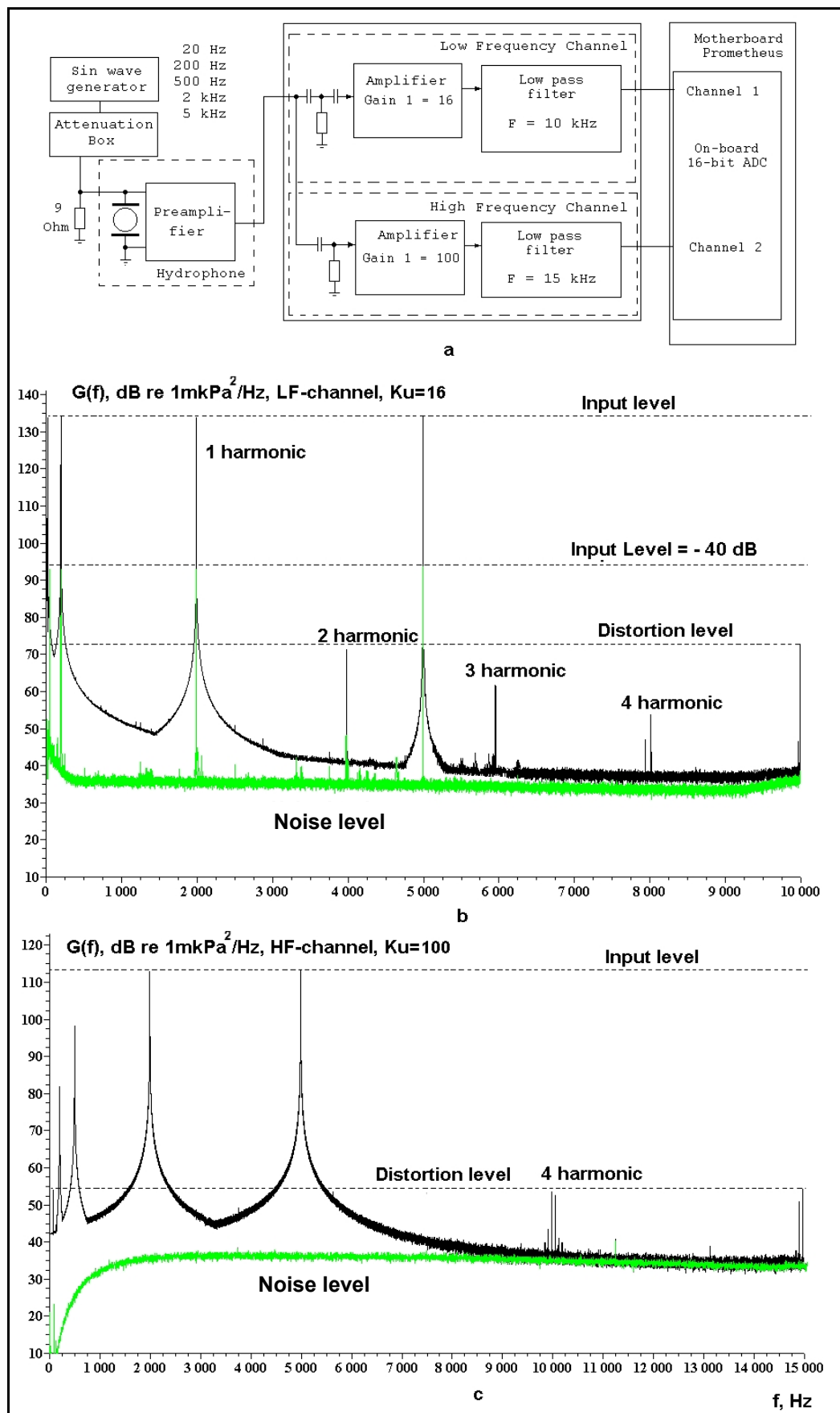


Figure 2.10 - (a) Block diagram showing the experimental schematic for system dynamic range estimation; Spectra of the results for the frequency range 0-15 kHz for (b) the LF channel; (c) the HF channel.

2.2.3 Analog channel system filter response

Figure 2.11 shows a block diagram giving the experimental schematic for determining the filter response of the LF and HF channels, verifying the amplitude response of the system and identifying aliasing. A white noise generator was attached to the input of the AUAR amplifier through an attenuator. A National Instruments 16 bit ADC card and 8 channel 8th order Bessel filter²⁴ were used to record the data. Figure 2.12(a) shows the filter response of both the LF and HF channels in the frequency band from 0 to 20 kHz. The remaining figures show the same response over a more limited frequency band, 0 to 1 kHz (Figure 2.12(b)) and 0 to 100 Hz (Figure 2.12(c)). Figure 2.12(c) also shows the white noise signal from the test generator. Figure 2.13 shows the analog channel system response of all 13 AUARs to a broadband white noise input signal. The LF channel response is plotted in the frequency band from 0 to 16 kHz and the HF channel in the band from 0 to 20 kHz.

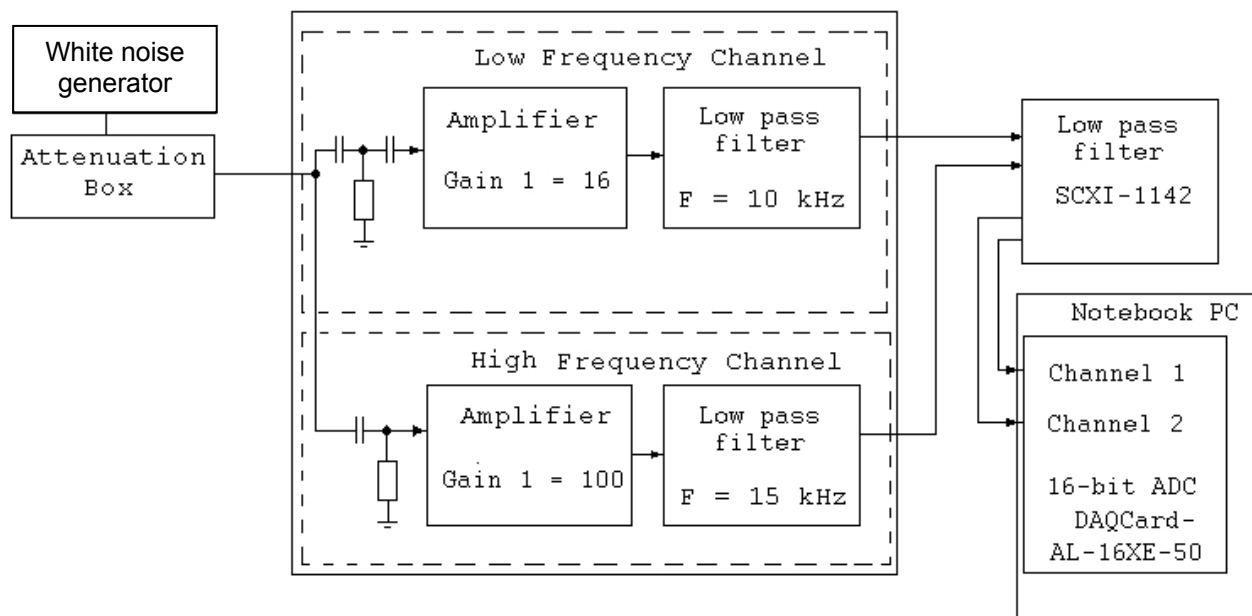


Figure 2.11 - (a) Block diagram showing the experimental schematic for determining the amplitude frequency characteristics of the analog channel.

Figure 2.14 shows a block diagram giving the experimental schematic for verifying the amplitude response of the AUAR. A white noise generator was attached to the preamplifier of the hydrophone through a precision attenuator, a 9Ω resistor was connected parallel to the hydrophone sensor and the output was recorded by the AUAR computer.

²⁴ National Instruments model # DAQCard-AL-16XE-50 and National Instruments model # SCXI-1142.

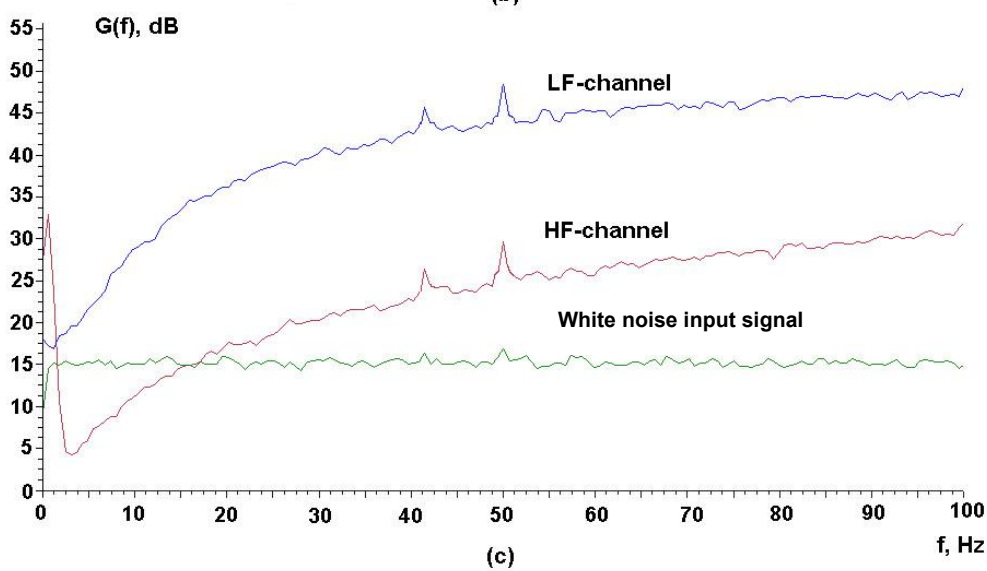
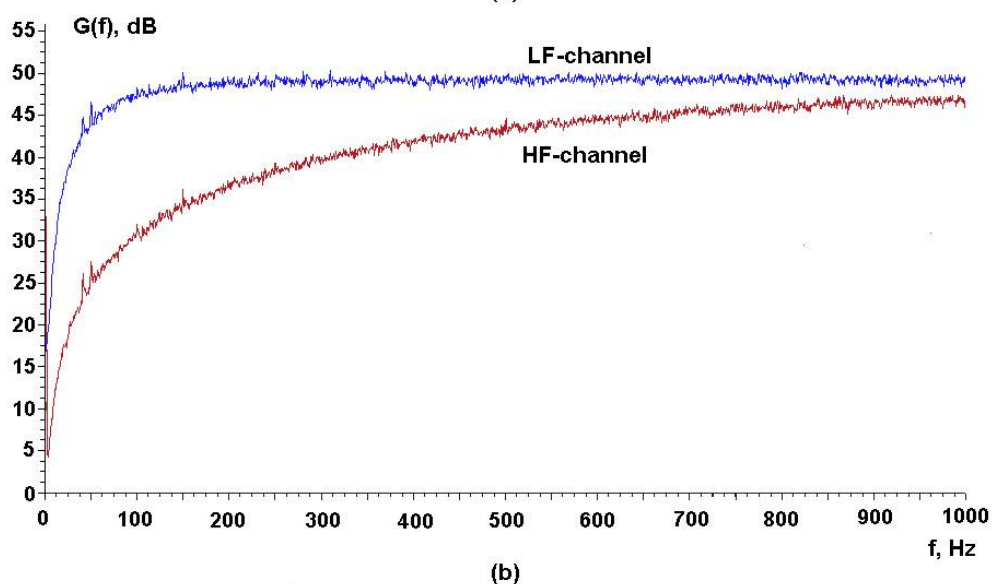
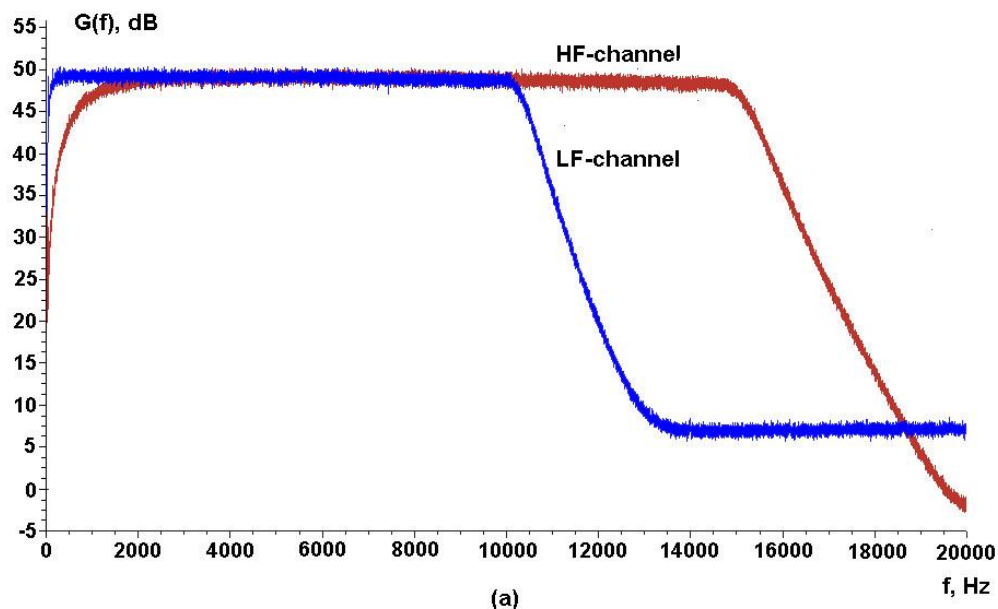


Figure 2.12 - Amplitude-frequency characteristics of both HF and LF channels measured with broadband white noise; (a) from 0 to 20 kHz; (b) from 0 to 1 kHz; (c) from 0 to 100 Hz and including a plot of the low frequency part of the white noise input signal.

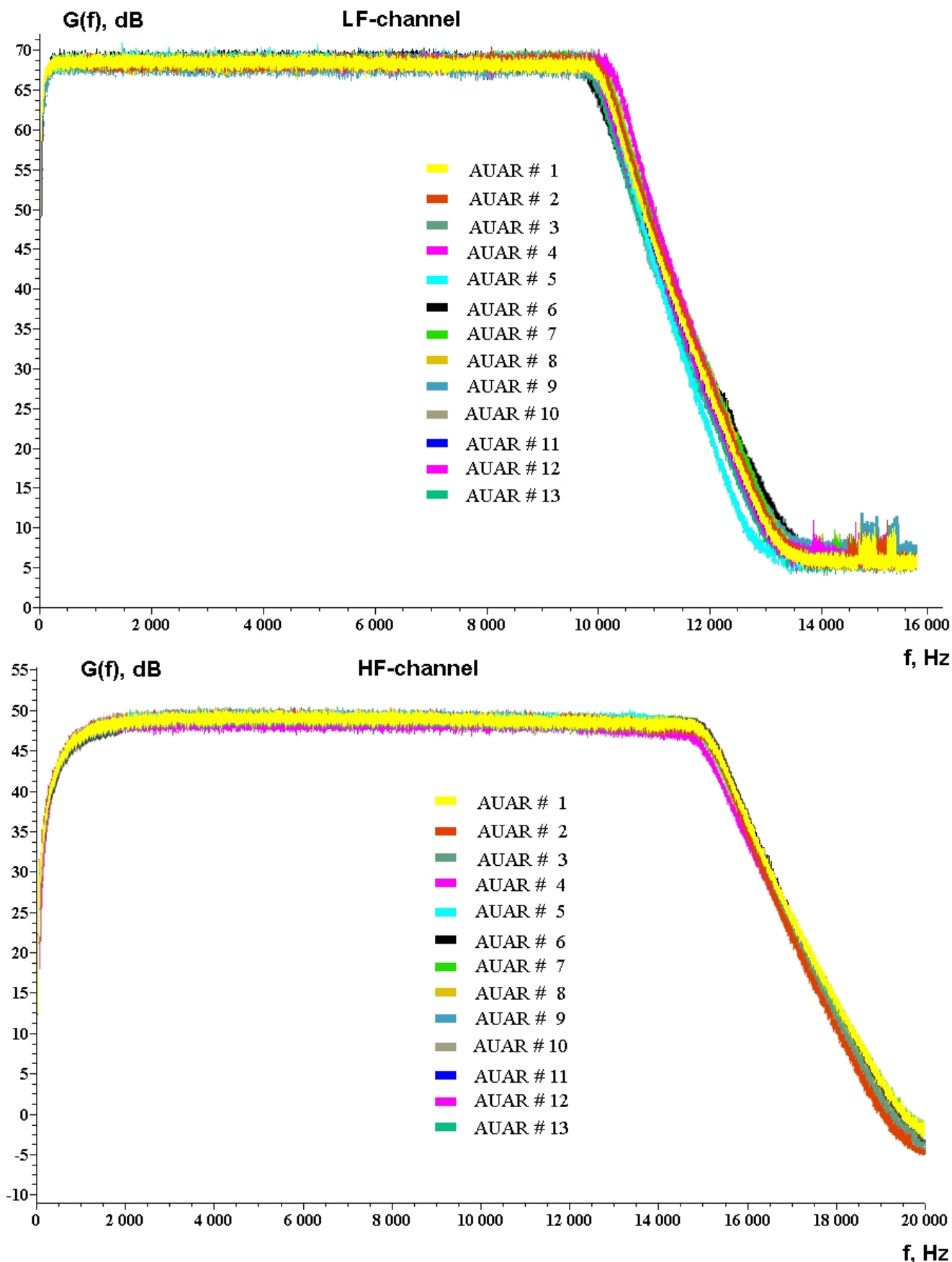


Figure 2.13 - Analog channel system response of all 13 AUARs to a broadband white noise input signal; (Top) the LF channel response plotted in the frequency band from 0 to 16 kHz; (Bottom) the HF channel response plotted in the frequency band from 0 to 20 kHz.

Figure 2.15 shows the measured LF and HF channel system filter response to a broadband white noise input signal for one of the AUARs.

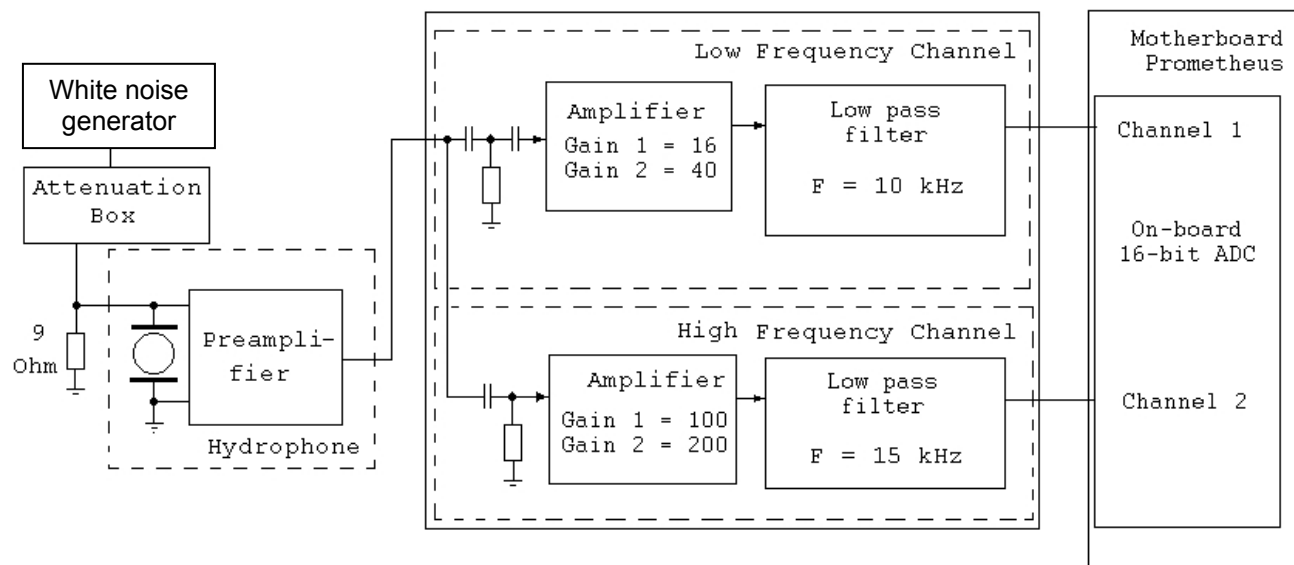


Figure 2.14 - Block diagram showing the experimental schematic for determining the system response of the AUAR.

The broadband white noise test is the standard filter response test used for the AUARs; tonal signal tests are conducted once per AUAR to determine a system filter response. The combined results from the tonal signal test and broadband white noise test are used to estimate an analog instrument filter response for each AUAR. This filter response is used to correct the data as it is processed and to compensate for the slope of the HF channel at frequencies lower than 3 kHz and the LF channel at frequencies lower than 100 Hz.

2.2.4 Channel to channel crosstalk

Figure 2.16(a, c) shows a block diagram giving the experimental schematics for determining the crosstalk between the LF and HF channels²⁵. A known signal with input amplitude just below that required to overload the system was selected for the test. To measure the HF to LF channel crosstalk a 9 Ω resistor was used to terminate the inputs to the LF channel. Figure 2.16(b) shows that the crosstalk levels are ~65 dB lower than the input level of the HF channel. Above 10 kHz the crosstalk levels increase slightly (by ~3 dB).

²⁵ Since an AUAR has 2 inputs to the ADC (a high frequency and a low frequency channel) it is possible that a signal from one channel can crossfeed into the other channel.

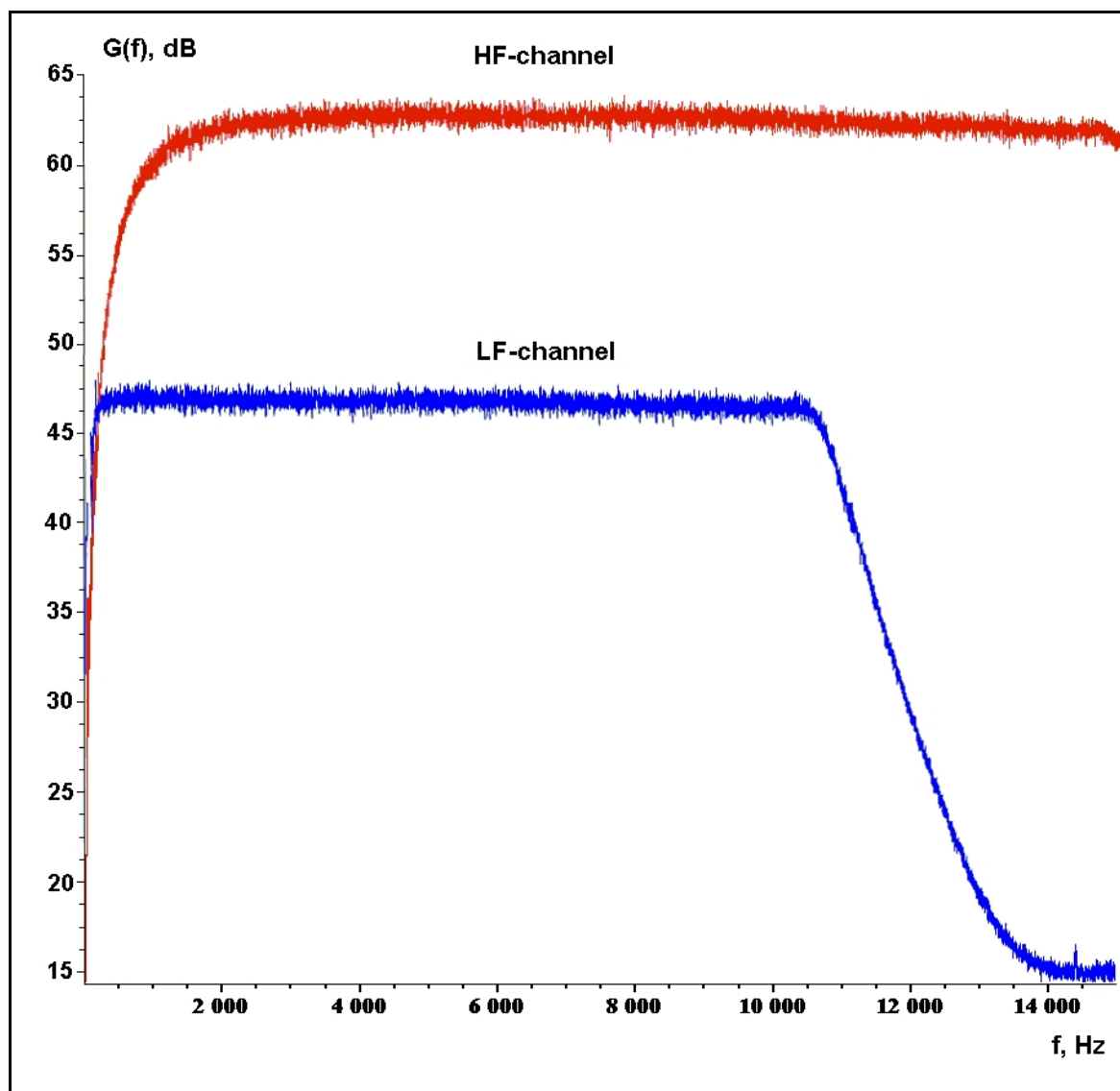
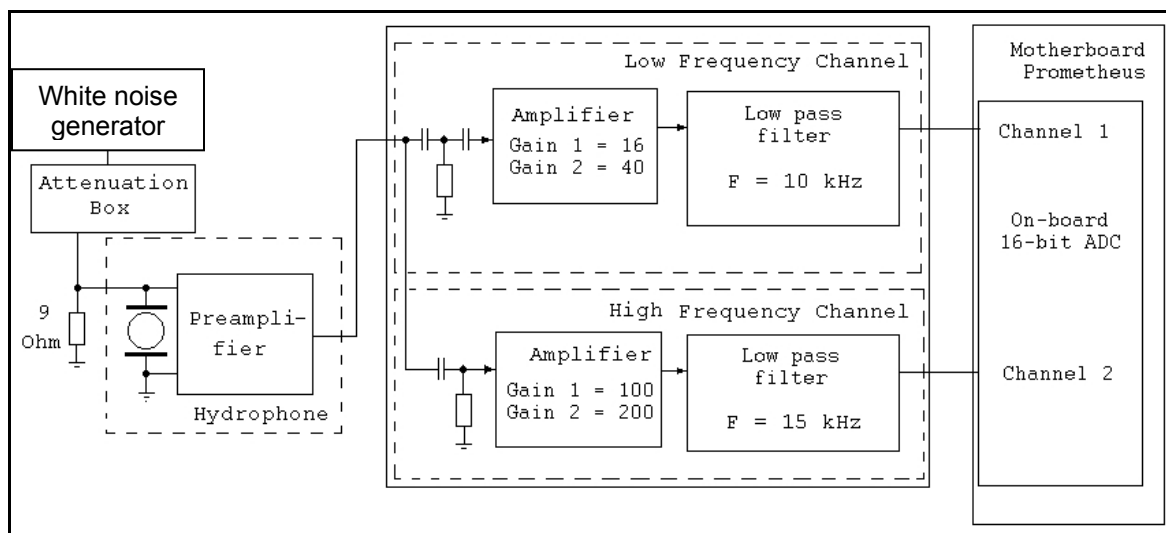


Figure 2.15 - Top: Block diagram showing the experimental schematic for system filter response estimation; Bottom: System filter response of LF & HF channels measured with broad band white noise.

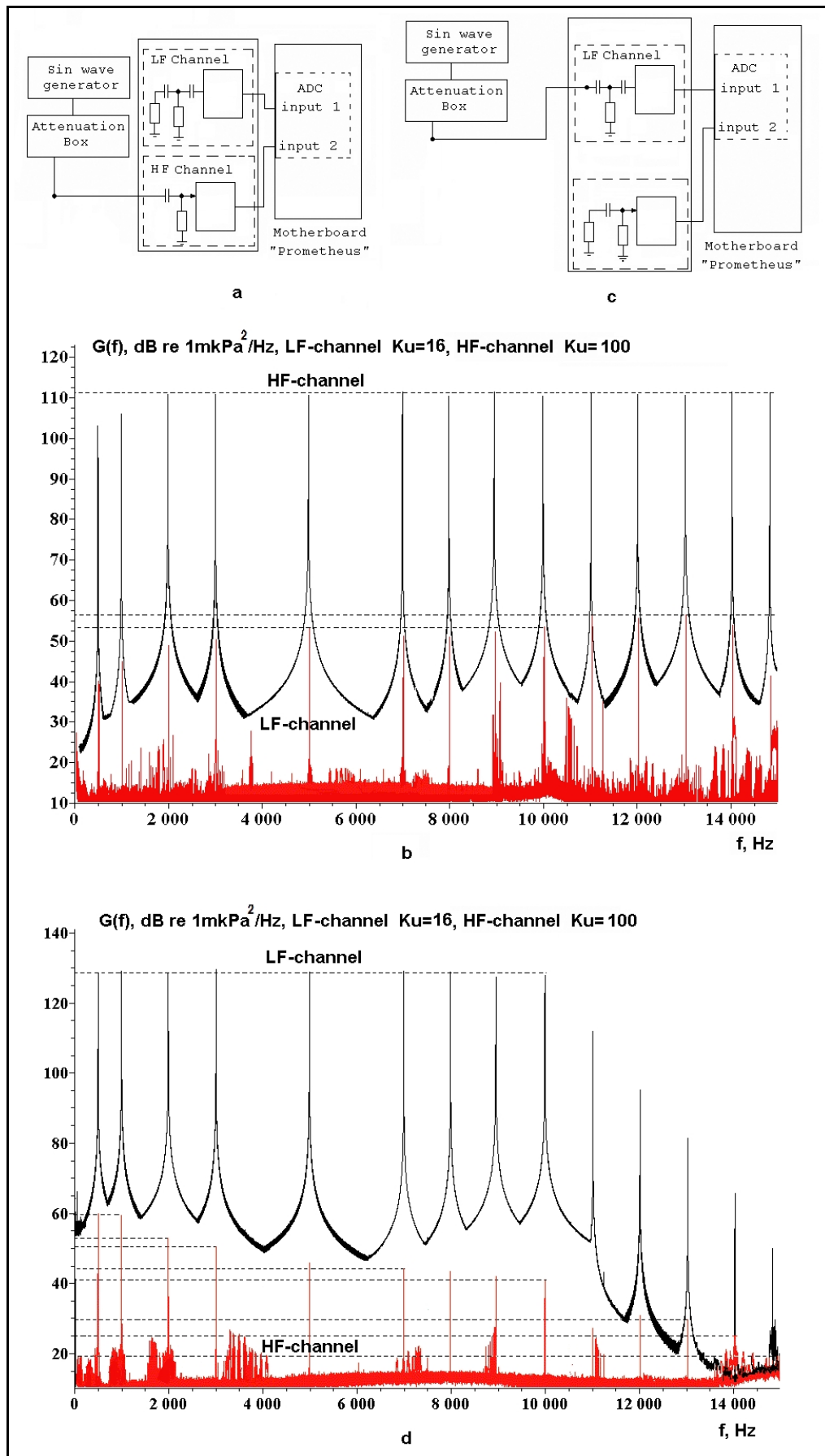


Figure 2.16 - (a, c) Block diagram showing the experimental schematics for HF to LF channel and LF to HF channel crosstalk estimation; (b) Plot of HF to LF channel crosstalk; (d) Plot of LF to HF channel crosstalk.

LF to HF channel crosstalk was measured in the same way. A $9\ \Omega$ resistor was used to terminate the inputs to the HF channel and known signals were input to the LF channel. Figure 2.16(d) shows that the crosstalk is at least 65 dB lower than the input level of LF channel at all frequencies.

2.2.5 Results of instrument tests

The unit to unit performance of all the AUARs was confirmed by regular testing. All the AUARs were subject to the tests listed in Appendix B; Table 2.1 gives the individual test results for all thirteen AUARs. All AUARs performed within specifications.

Table 2.1 - Performance of AUARs on the instrument tests.

AUAR serial number	Internal noise (dB re $1\ \mu\text{Pa}^2/\text{Hz}$)				Dynamic range , dB	Crossfeed (dB)	
	LF channel (1 – 500 Hz)	LF channel (0.5 – 10 kHz)	HF channel (1 – 500 Hz)	HF channel (0.5 – 15 kHz)		Drive LF, record HF	Drive HF, record LF
01	64	36.3	23.7	36.1	98.1	-66	-66
02	64.1	36.5	24	36.2	98.2	-66	-66
03	64	36.3	23.9	36.1	98	-66.3	-66
04	63.8	36	23.6	35.8	98.4	-65.9	-65.9
05	64	36	23.7	35.8	99	-66.1	-65.8
06	64	36.1	23.9	36	98.6	-66.3	-65.8
07	63.7	35.9	23.8	35.9	98.6	-66	-66
08	64.1	36	23.8	36	98.2	-66.1	-66.1
09	64	36.4	24	36.2	99	-66.2	-66
10	63.9	36.3	23.9	35.9	98.7	-66.1	-66
11	63.9	36.1	23.7	35.9	98.8	-66.2	-65.8
12	64	36.4	24.1	36	98	-65.9	-66.1
13	64.1	36.1	23.8	35.8	98	-66.2	-65.8

2.3 Calibration of AUARs and cross-calibration error analysis

In order to compare the acoustic measurements made on the NE Sakhalin shelf to previous or future work, the data has to be calibrated to an absolute pressure standard. The hydrophones were manufactured with nominal sensitivities and the gains were set in the field. In order to confirm the calibration of the equipment a field cross-calibration was conducted.

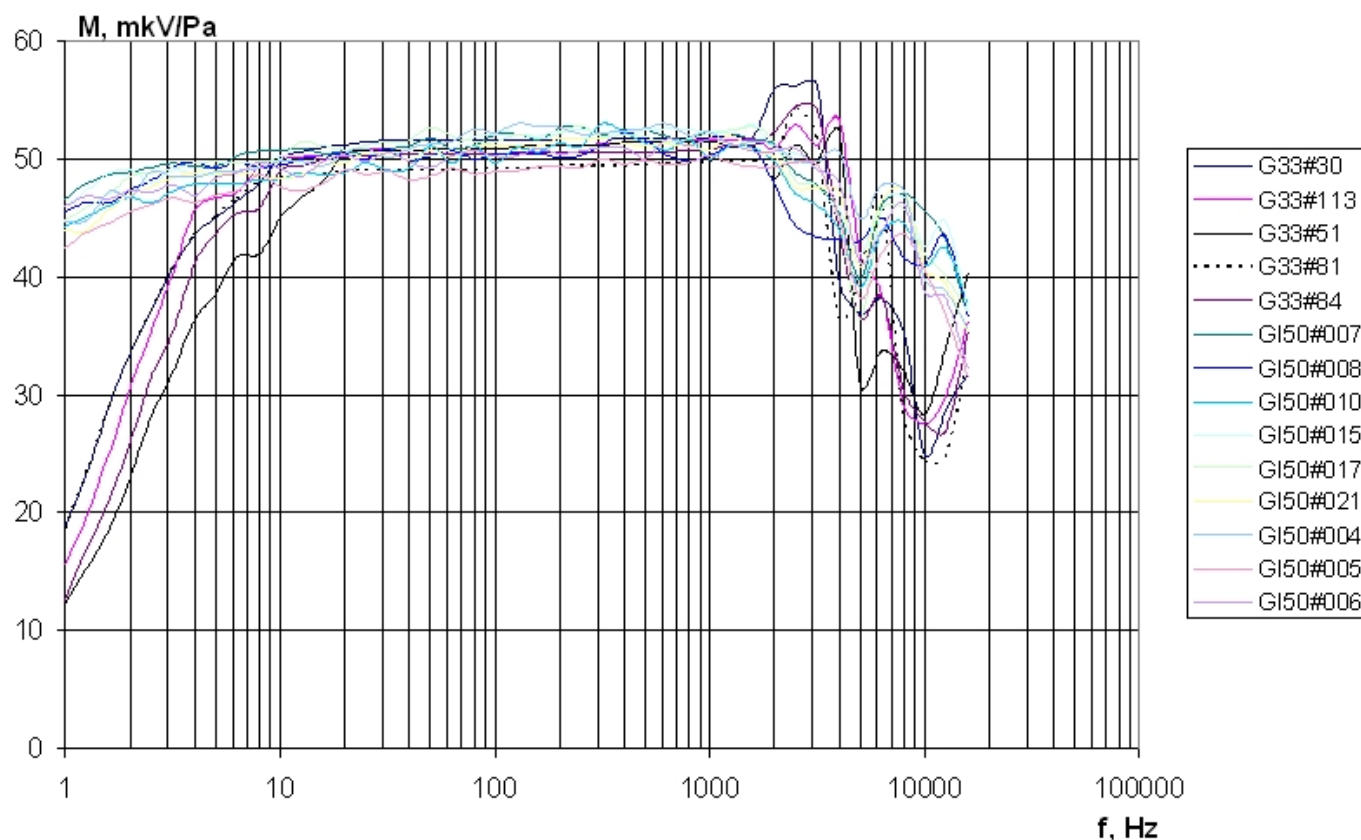


Figure 2.17 - Spectral characteristics of the spherical and cylindrical hydrophones.

The hydrophone calibrations were conducted over the frequency band 1 Hz to 15 kHz in compliance with state standard MI 2098-90 at SMCHM²⁶ located at RSSRIPRTM²⁷ (Moscow). The sensitivities of the hydrophones were determined by comparative calibration

²⁶ SMCHM - State's Meteorological Center of Hydro-acoustical Measurements.

²⁷ RSSRIPRTM - Russian State's Scientific Research Institute of Physical Radio Technical Measurements.

against a reference hydrophone in acoustical calibration chambers²⁸ and have a relative error of less than 1.5 dB (95% probability)²⁹. Figure 2.17 shows the frequency dependence of the hydrophone sensitivity over frequencies from 1 Hz-15 kHz. Calibration certificates for the hydrophones are shown in Appendix A.

At the end of the 2004 field season a cross-calibration of the 13 AUARs was conducted on the *Academik Oparin* in 30 m water depth. The AUARs were cross-calibrated by comparing noises generated by the *Academik Oparin* and tonal signals generated by the LF and broadband sound transducers. The hydrophones were divided into groups due to the number of hydrophones being calibrated. One hydrophone was used as a control for all the groups.

The field cross-calibration procedure is described in detail in Appendix C. The maximum absolute error from the mean for any AUAR was 1.07 dB³⁰. These values were within the expected relative error limits for the equipment and the absolute calibration of the data was therefore confirmed.

2.4 High Frequency broadband piezoelectric transducer

Broadband noise and tonal signals in the frequency band from 400-15000 Hz were used for high frequency propagation studies, TL measurements and cross-calibrations. Figure 2.18(a) shows the broadband piezoelectric (ceramic) transducer that generated these signals. The transducer is cylindrical³¹ and consists of seven piezoelectric rings connected in parallel, coated with a composite material and sealed at the ends with a metal shield. A marine connector at one end connects the transducer to the power supply and control system. A 1500 Watt power amplifier drives the transducer³².

Figure 2.18(b) is a block diagram giving a schematic of the control system for the transducer. Three signal generators produce tonal signals from 10 Hz - 20 kHz, broadband

²⁸ A Model UVT 71-a-90 calibration chamber to 600 Hz and an acoustically muted chamber above 600 Hz.

²⁹ This error includes the approximately 1 dB error associated with estimation of absolute pressure for the calibration of the reference hydrophone.

³⁰ The highest errors were due to the low signal level of the calibration signal (Appendix C).

³¹ Dimensions are diameter 28 cm, Height 136 cm; Weight ~ 60 kg in air, ~ 15 kg in water.

³² Phonic MAX-2500 1500 Watt power amplifier.

noise signals or linearly frequency modulated signals (with adjustable frequency range and frequency of modulation). A precise signal generator (Г3-122) was used as modulator and provides a stable sin wave with controllable amplitude at frequencies from 0.001 Hz to 3 MHz. This output was input to a frequency-modulating generator (GFG-8216A). The output of this generator was therefore a FM signal whose carrier signal was determined by the GFG-8216A and whose modulation was controlled by the Г3-122 signal generator. White noise from a white noise generator (RFT-1123) can also be input to the transducer instead of a FM signal. The manufacturers specifications indicate that the white noise signal had a signal variation of <0.1 dB in the band from 1 Hz to 200 kHz.

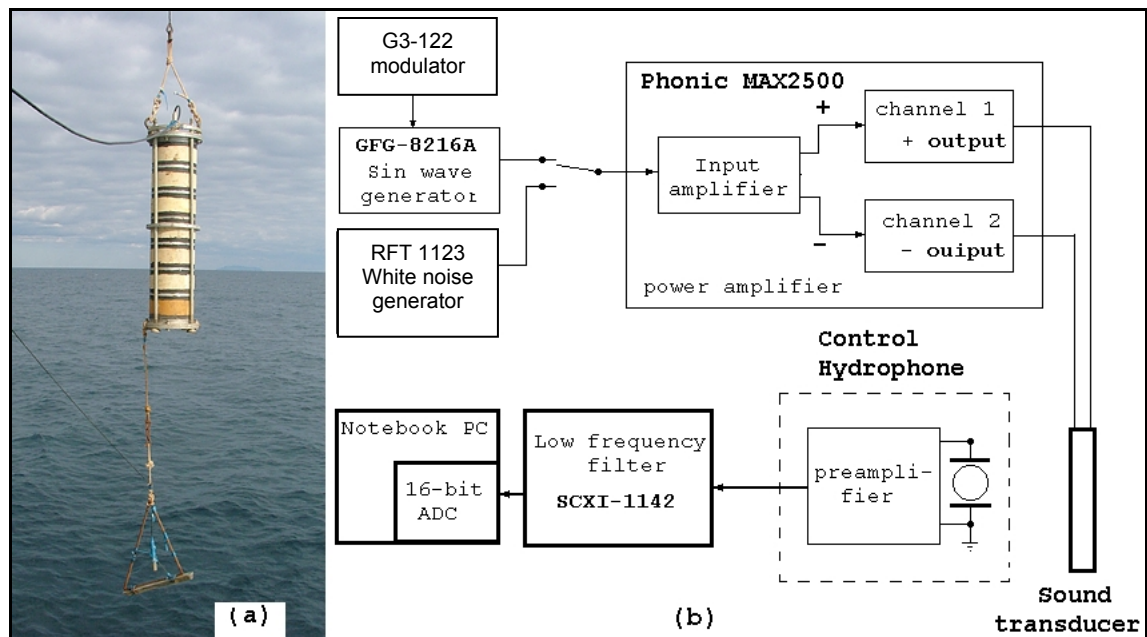


Figure 2.18 - High frequency broadband piezoelectric transducer.

2.5 Low Frequency (LF) electromagnetic resonance transducer

A Low frequency resonance transducer was used for propagation studies, TL measurements and cross-calibrations. The LF transducer has a cylindrical container filled with gas³³, and a pair of identical closely spaced radiating pistons oscillating in opposite directions creating a volume displacement. An electromagnetic controller controls the motion of the pistons; the ends of the pistons are connected together by cylindrical springs and to the edge of the cylindrical container with rubber gaskets. A bridge thyristor inverter connected to the transducer by a 4-line 34 m long cable drives the transducer. Hydrostatic

³³ Dimensions are Diameter 58 cm, Height 15 cm; Weight 48 kg in air, ~ 6 kg in water.

compensation is achieved using an air pump and control manometer connected to the transducer by a 27 m hose³⁴. In order to achieve electric resonance, a battery of electric capacitors and solenoids located on board the *Academik Oparin* are connected sequentially with the solenoid of the transducer. Figure 2.19(a) shows the LF resonance transducer and reference hydrophone being deployed over the side of the *Academik Oparin*.

2.6 Reference amplitude

The acoustic pressure level generated by both the HF and LF transducers were monitored by a calibrated reference hydrophone located a fixed distance from the transducer³⁵. The monitor data could be contaminated by flow noise, vibration from currents, surface waves, rocking of the vessel and noise from the *Academik Oparin*. In order to prevent contamination of the reference signal by this noise it was monitored by a reference hydrophone and preamplifier located a distance of 2 m from the center of the broadband transducer and 1 m from the edge of the LF transducer. The reference hydrophone was isolated from mechanical noise using a rubber suspension system inside a weighted pyramidal frame. Data from the reference hydrophone was recorded on a laptop using a system based on National Instruments equipment, and housed in a power chassis³⁶ powered by a 12V battery. It contained a low pass filter module³⁷ with eight preamplifiers and 8th order Bessel filters, which were used to limit the frequency range of the input signal to within the Nyquist frequency for the sample rate of the Analog to Digital Converter (ADC). The data was then converted to digital data by a multi-channel gain ranging 16 bit ADC data acquisition card³⁸ housed in a notebook computer.

This system was described in greater detail in [Borisov et. al., 2003]. Figure 2.20 shows the laboratory on the *Academik Oparin* with the equipment used to control the transducers and record the reference signals.

³⁴ During calibration tests in the Sea of Japan the amplitude of the piston motion at the resonance frequency was 3.3 mm. The amplitude of the volumetric oscillation was therefore 0.0012 cubic meters. The tests using calibrated accelerometers, and conducted at a depth of 2 m, indicated that when the maximum number of springs (30) are used, the resonance frequency of the transducer is 20.2 Hz with marginal frequencies of 15.2 and 30.6 Hz (-3 dB).

³⁵ The calibration certificates for the reference hydrophones are given in Appendix A.

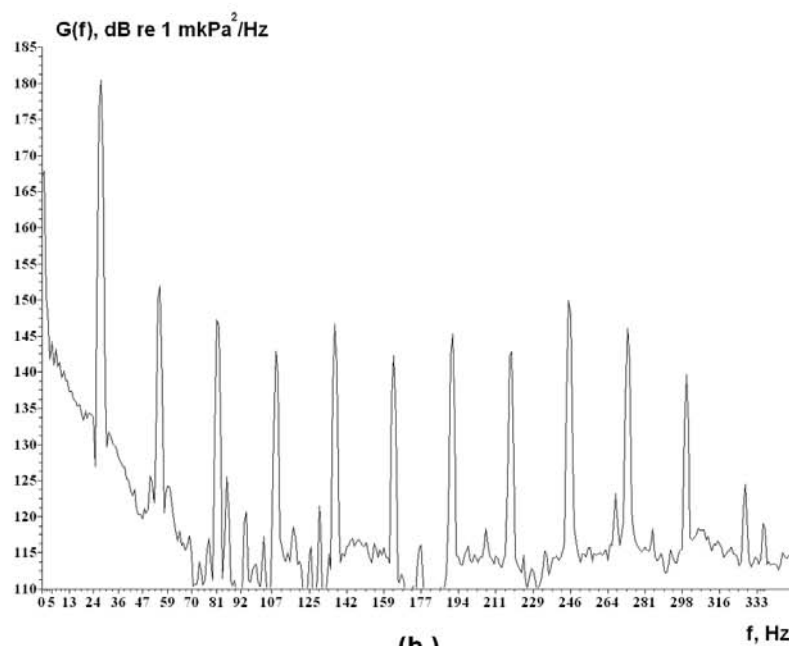
³⁶ National Instruments SCXI-1000DC.

³⁷ National Instruments SCXI-1142.

³⁸ National instruments DAQCard-AL-16XE-50.



(a.)



(b.)

Figure 2.19 - (a) Low frequency resonance transducer and calibrated monitor hydrophone; (b) Power spectral levels of the acoustic field generated by the transducer recorded by a reference hydrophone at 1 m for a resonance frequency of ~27 Hz.

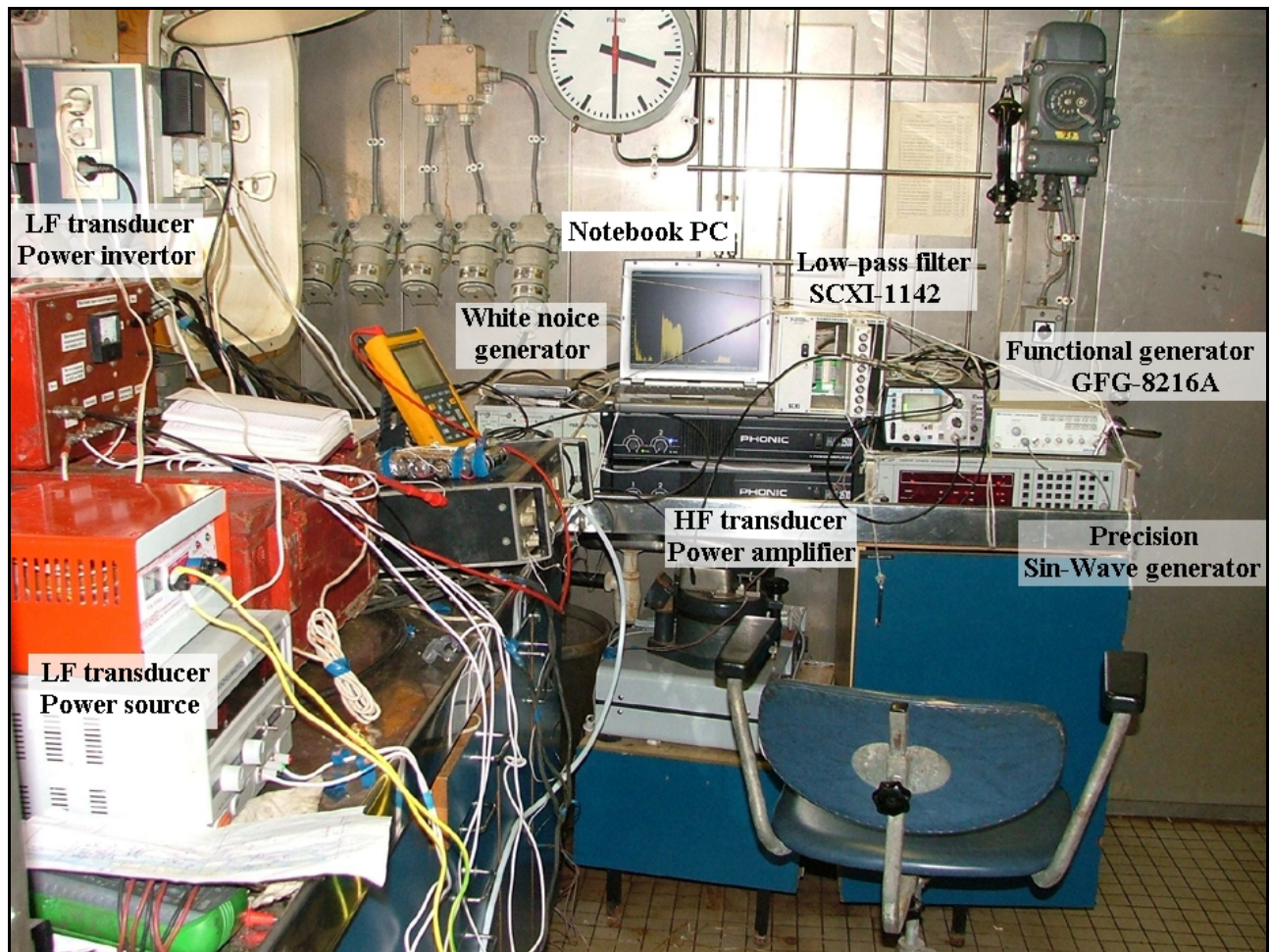
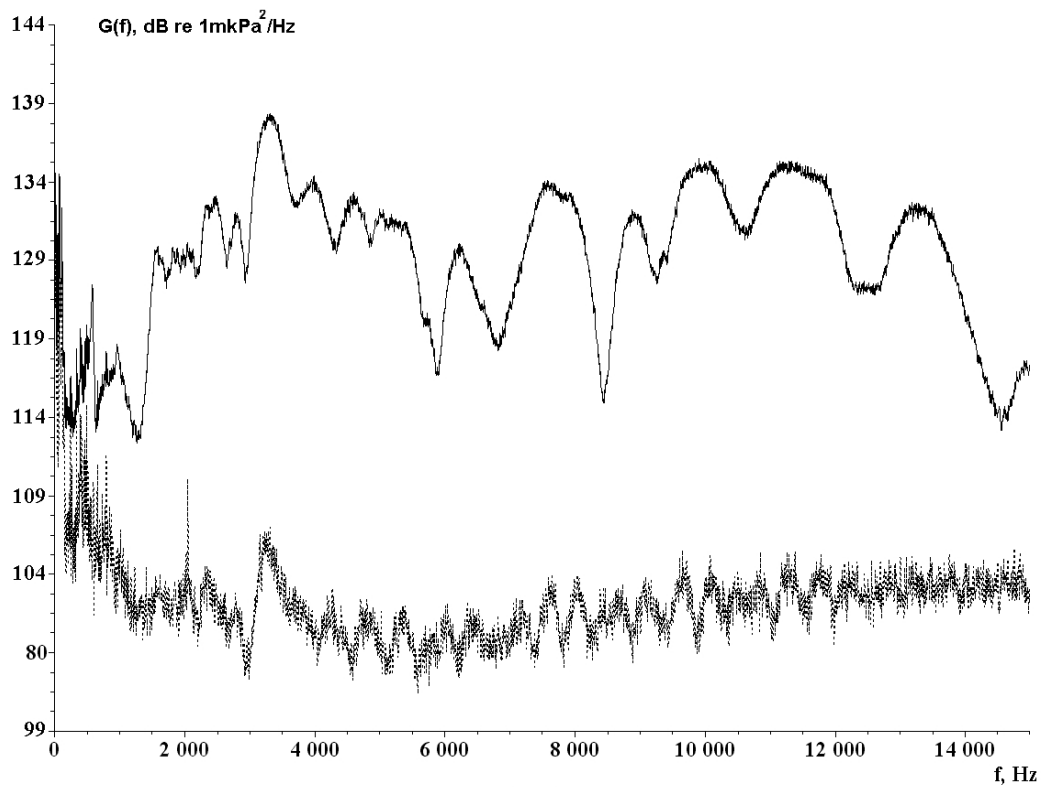
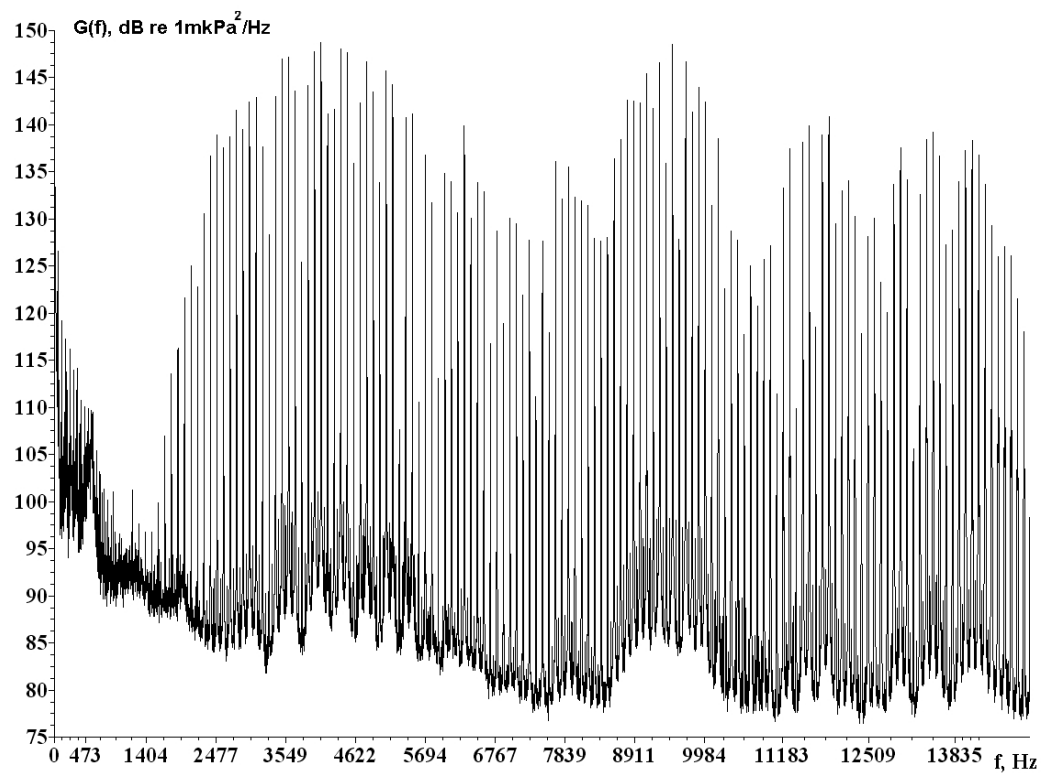


Figure 2.20 - Laboratory on the *Academik Oparin* showing the equipment for controlling the transducers and recording the reference signal.

Figure 2.21 shows the spectra of signals produced by the HF transducer and monitored by the reference hydrophone located 2 m from the center of the transducer. Figure 2.21(a) shows the spectra $G(f)$ when the transducer is driven by a white noise signal, the dotted line gives a measure of the noise from the *Academik Oparin* recorded between transmissions. Figure 2.21(b) gives the spectra when the transducer is driven by a FM signal. The 25 dB variation in the output spectrum is a function both of the output of the transducer and interference between the direct and reflected waves from the vessel and the sea floor. The signal was recorded by the 12 m deep reference hydrophone in 30 m water depth; the vessel hull was 4.5 m deep.



(a)



(b)

Figure 2.21 - Spectra $G(f)$ of signals from the broadband transducer monitored by the reference hydrophone at 2 m; (a) White noise signal (solid line) and vessel noise from the *Academik Oparin* (dotted line); (b) FM signals.

The LF resonance transducer was deployed at a depth of 8 m from the anchored *Academik Oparin*. Figure 2.19(b) displays the spectral levels, recorded by a control hydrophone at 1 m, of the acoustic field generated by the transducer at a resonance frequency of ~27 Hz and its harmonics. The ~27 Hz acoustic signal has a spectral level of ~180 dB re 1 $\mu\text{Pa}^2/\text{Hz}$ at 1 m from the transducer.

2.7 Hydrologic sonde

Modeling work, conducted in conjunction with TL experiments in order to more effectively characterize the variation in TL over time have shown that the hydrologic properties of the water column should be measured in addition to the acoustic properties. A hydrologic sonde³⁹ was used to determine the hydrologic properties of the water layer. The *Academik Oparin* was upgraded with an electric winch in order to deploy the sonde (and transducers), Figure 2.22 shows the sonde being deployed. The sonde can independently measure conductivity, sound velocity, temperature and pressure. The main characteristics of the sonde are given in Table 2.2; the calibration certificates for the sonde sensors are given in Appendix A.

Table 2.2 - Technical specifications - Valeport SVXtra sonde.

Parameter	Type	Range	Accuracy	Resolution	Response time
Conductivity	Pressure balanced inductive coils	0.1-60 mS/sm	± 0.01 mS/sm	0.003 mS/sm	100 ms
Speed of sound	Time of flight	1400-1600 m/s	± 0.05 m/s (± 0.03 m/s rms)	0.001 m/s	Single pulse. Maximum time of flight 145 μs
Temperature	Fast response PRT	-5°C +35°C	$\pm 0.01^\circ\text{C}$	0.002°C	100 ms
Pressure	Strain gauge pressure sensor	5000 dBar	$\pm 0.1\%$ FS	$\pm 0.005\%$ FS	20 ms

The sensors can be programmed with a sample rate of 1, 2, 4 or 8 Hz; all parameter values are measured synchronously and stored in the Sonde's internal 8 MB flash memory. Once the measurements are complete the data can be transferred to a computer via a RS232

³⁹ Model SVXtra manufactured by Valeport Limited, England.

port⁴⁰. The sonde is powered by a set of eight D-cells, providing approximately 180 hours of continuous operation.

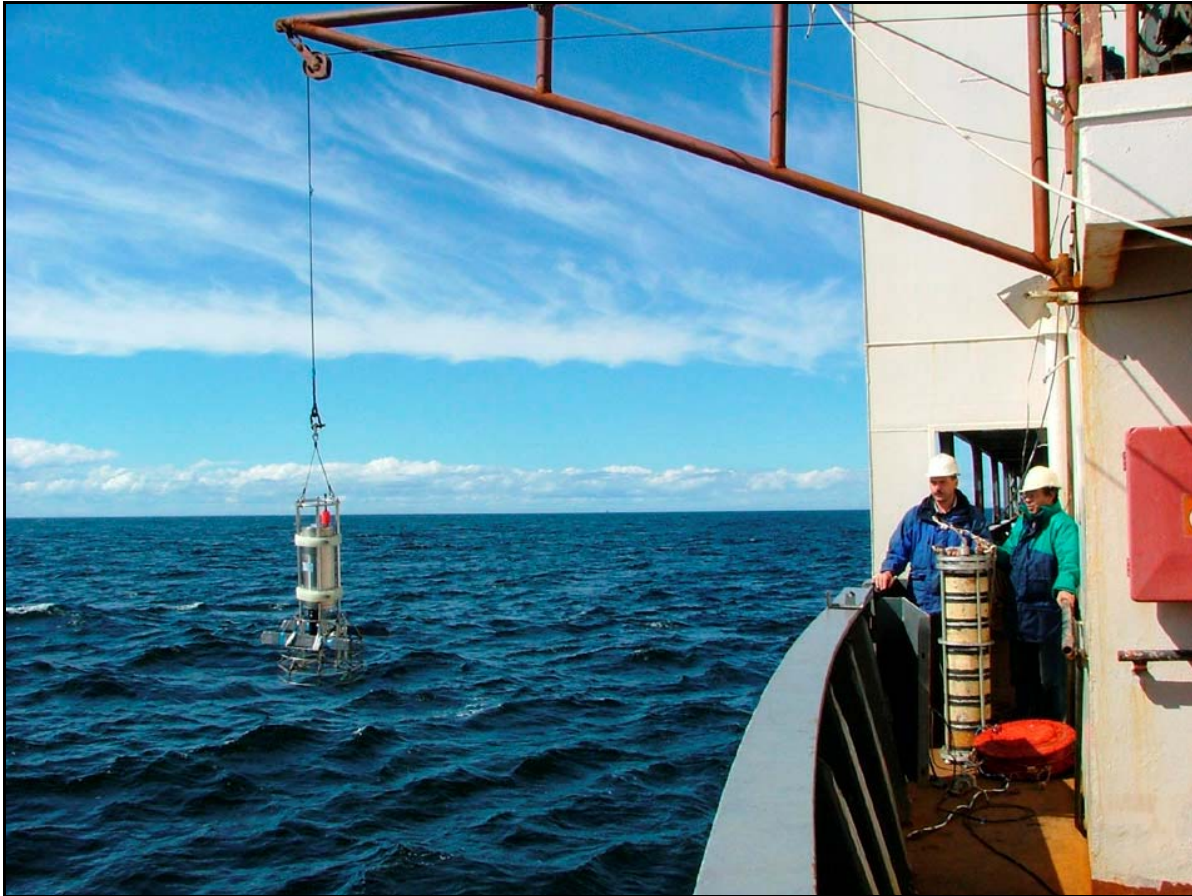


Figure 2.22 - SVXtra Hydrologic sonde being deployed from the *Academik Oparin*.

In order to estimate the cumulative effect of developments on the NE Sakhalin shelf, it is necessary to understand the transmission characteristics between the oil and gas facilities and operations and the gray whale feeding areas. Detailed bathymetric and hydrologic measurements are required to improve the accuracy of the acoustic models used for this task. In 2004, the schedule of hydrologic measurements was significantly expanded to include a set of bathymetric profiles with associated vertical hydrologic profiles. 8400 km of bathymetric data and 323 vertical hydrologic profiles were acquired in 2004; Figure 1.3 shows these profiles.

⁴⁰ The DataLog400 program included with the sonde is used to adjust measurement modes, to transfer data to a computer, for data visualization and relative density calculation from the other parameters.

2.7.1 Processing and storage of hydrologic data

To more effectively manage the quantity of acoustic data acquired during the 2004 expedition and expected in the future, the acoustic team developed a database for the storage and analysis of hydrologic data. The main window of the database is on Figure 2.23. Data is read from the sonde using the DataLog400 program, converted into text and input into the database. Since the crane on the *Academik Oparin* deploys the sonde slowly and the sonde samples the hydrologic parameters eight times a second, a large number of depth samples are acquired during each vertical profile. Data is collected into depth bins (the depth horizons stored in the database are 2.5 cm thick) and averaged. Extra information, for example the experiment and profile name and coordinates is added. Every entry in the database contains the measurement date, experiment, profile and point name, as well as the coordinates and depth (max depth recorded by the sonde) of the point, the sensor readings and the number of depth bins measured.

Время зондирования	Название рейса (эксперимента)	Название гидрологического разреза	Название точки зондирования	Широта точки	Долгота точки
07.09.2004 11:33:04	Sakhalin2004	Arkutun-Dagi - P-Orlan	A	52.324617	143.72289
07.09.2004 12:58:12	Sakhalin2004	Arkutun-Dagi - P-Orlan	C	52.334567	143.68401
07.09.2004 13:25:35	Sakhalin2004	Arkutun-Dagi - P-Orlan	D	52.3477	143.6300
07.09.2004 14:37:01	Sakhalin2004	Arkutun-Dagi - P-Orlan	D	52.3477	143.6300
07.09.2004 15:08:45	Sakhalin2004	Arkutun-Dagi - P-Orlan	E	52.36	143.571
07.09.2004 16:25:25	Sakhalin2004	Arkutun-Dagi - P-Orlan	G	52.3674	143.5310
07.09.2004 16:52:12	Sakhalin2004	Arkutun-Dagi - P-Orlan	H	52.3835	143.4764
07.09.2004 18:45:16	Sakhalin2004	Arkutun-Dagi - P-Orlan	P-Orlan	52.40555	143.3890

Время	Название точки
07.09.2004 18:45:16	P-Orlan
07.09.2004 16:52:12	H
07.09.2004 16:25:25	G
07.09.2004 15:08:45	E
07.09.2004 14:37:01	D
07.09.2004 12:58:12	C
07.09.2004 11:33:04	A

Время	Название точки	Сим	Разм	Цвет
07.09.2004 18:45:16	P-Orlan	34	12	Черный
07.09.2004 16:52:12	H	34	12	Черный
07.09.2004 16:25:25	G	34	12	Черный
07.09.2004 15:08:45	E	34	12	Черный
07.09.2004 14:37:01	D	34	12	Черный
07.09.2004 12:58:12	C	34	12	Черный
07.09.2004 11:33:04	A	34	12	Черный

Figure 2.23 - Main window of the database for the storage and analysis of hydrologic data.

The software can output data in tables or plots (Figure 2.24), it can sort the data by date, experiment, profile or point name and can export data into MS Word and Excel.

Additionally, data can be exported into Surfer⁴¹ to better visualize the spatial variation of the acoustic velocity, temperature, salinity and density fields). Figure 2.25 shows an example of

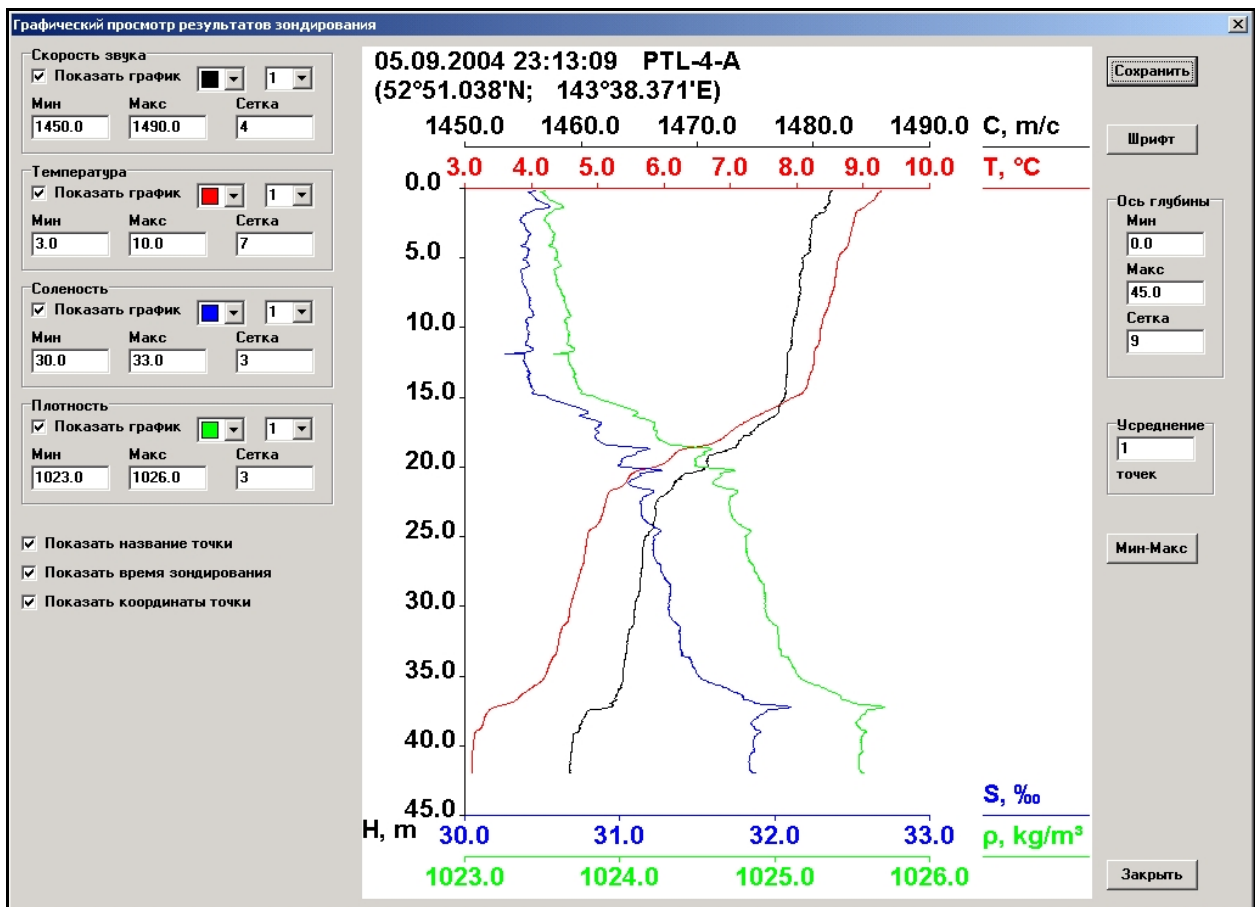


Figure 2.24 - Plot showing the results from a vertical hydrologic profile acquired from the *Academik Oparin*. Note that the density and salinity have been computed from other measurements.

a sound velocity section plotted in Surfer. The data can also be input into MapInfo to plot the experimental profiles on a map.

2.8 Equipment and software for bathymetric profiling

NMEA (National Marine Electronics Association) standard format signals from the sonar⁴² and GPS receiver⁴³ on the *Academik Oparin* are input into an NMEA hub⁴⁴ attached to COM

⁴¹ Golden software.

⁴² Wesmar, operating frequency 20 kHz, beam width 7°.

⁴³ Furuno.

⁴⁴ HUB51MK.

port of a computer. The computer is running dKart Navigator⁴⁵ that can handle the NMEA format, computing and plotting a vessel's course.

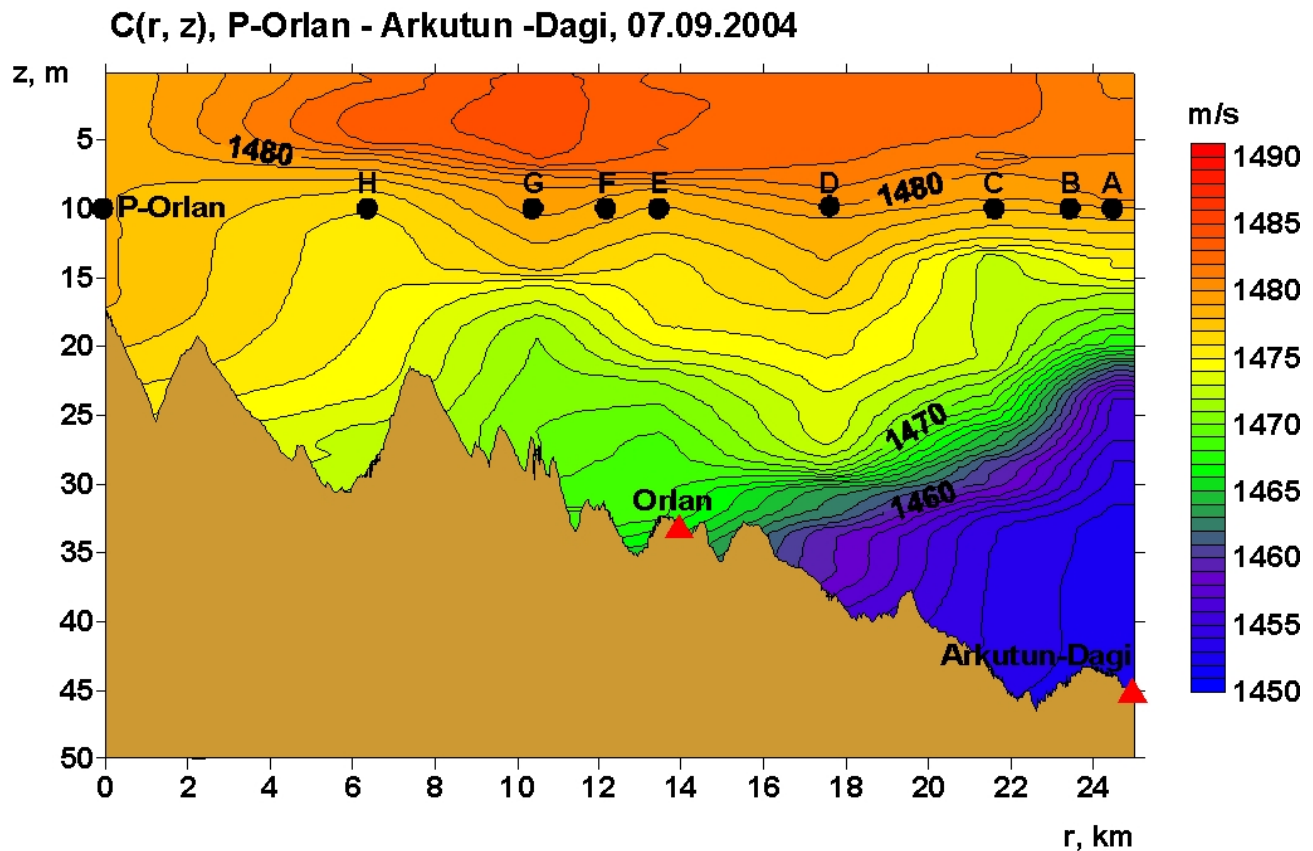


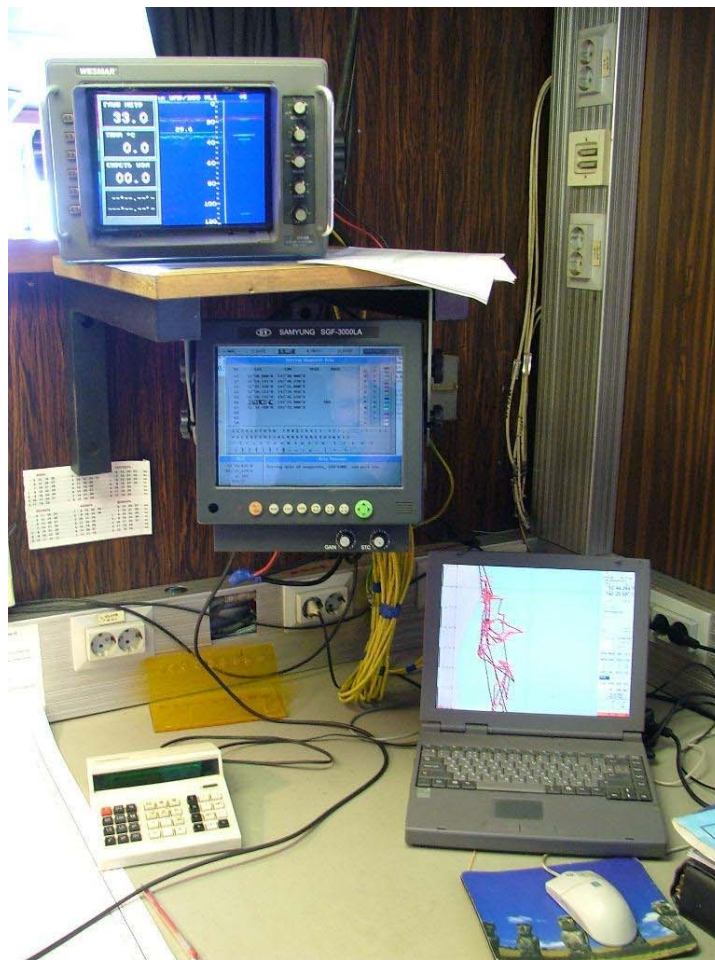
Figure 2.25 - Plot of the sound velocity field along a profile from the proposed Orlan platform location to the Arkutun-Dagi AUAR (#4) location.

Figure 2.26(a) shows the equipment used for continuous bathymetric recording on the *Academik Oparin*, Figure 2.26(b) is a schematic of the bathymetric equipment. Navigation information (time, coordinates, depth, speed, and course (from compass)) was recorded every 10 seconds.

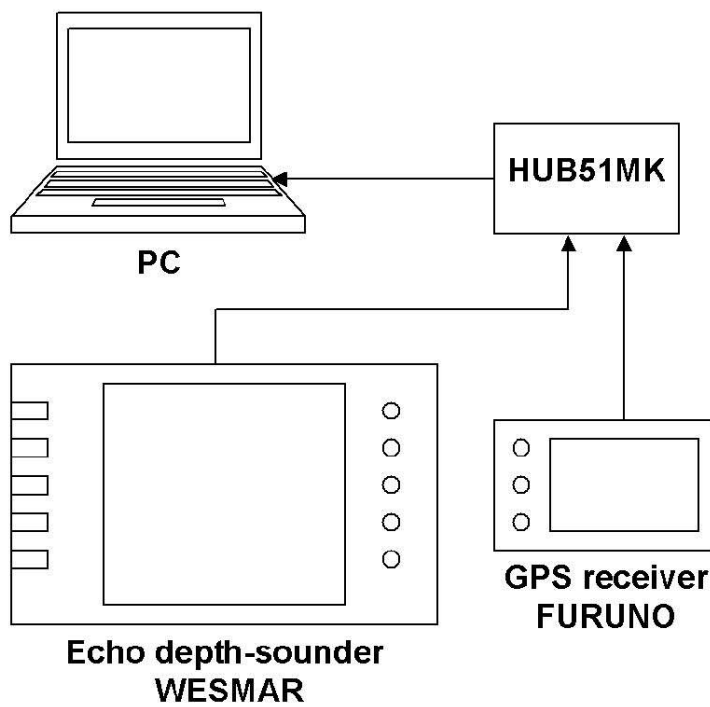
2.9 Acoustic data storage, processing and analysis

When an AUAR was recovered, the data from its hard drive was downloaded to a removable hard drive in a computer on the *Academik Oparin*. The batteries of the AUAR were recharged and the disk then wiped clean prior to redeployment. During the 2004 field season over 1.4 TB of data was accumulated.

⁴⁵ dKart Navigator (version 6.32) is a professional navigation solution for communication with navigation equipment such as GPS, sonar, AIS, radar, compass, log etc.



(a.)



(b.)

Figure 2.26 - Equipment used for continuous recording of bathymetric and positioning data on the *Academik Oparin*.

The raw data recorded by the AUAR was stored in a raw format, the data from the AUAR disk was downloaded to the computer on the *Academik Oparin* and was archived to DVD. The data was then converted to absolute amplitude (μPa) and written to a second removable hard drive. The data was corrected for the hydrophone sensitivity at 1 kHz and for gain⁴⁶. The program uses equation (D1) in Appendix D to convert the data, the inputs are the analog response of each channel of the AUAR (measured in the laboratory) K_v and the hydrophone calibrations made in Moscow (and confirmed by cross-calibration) S_H .

Software was specifically designed for the experimental data processing required for this work in order to more effectively evaluate the acoustic data. Sonograms and spectra were computed for the data. Additional programs were written for cross-calibration, calculating spectra and applying correction factors (from cross-calibrations). The instrument responses of the analog electronics of the AUARs were determined and the response removed from the final data.

⁴⁶ Correction for the instrument response of the two channels of the AUAR is made prior to spectral analysis.

3 ACOUSTIC DATA RECORDED ON THE NE SAKHALIN SHELF DURING THE 2004 FIELD SEASON

This section discusses the acoustic data recorded on the NE Sakhalin shelf during the 2004 field season. It describes the deployment dates, recording times, hydrophone depths and locations of the AUARs as well as their operational characteristics. Table 3.1 gives these details for the thirteen AUARs used in the study. The POI acoustic team undertook five distinct studies in 2004, these were:

1. Ambient noise measurements;
2. Anthropogenic noise measurements (especially noise from vessels involved in the western gray whale surveys such as noise from the outboard motors on the photo-ID zodiacs and from the *Academik Oparin*);
3. TL experiments along the proposed pipeline routes from the Moliqpaq and PA-B platforms to the Piltun gray whale feeding area, and from the Orlan platform and Chayvo pipeline route to the Piltun and Offshore feeding areas;
4. Bathymetric and hydrologic studies of the survey area; and
5. Studies of noise levels near behavioral monitoring stations.

This section will not discuss the analysis of these experiments, which will be the subject of the second volume of this report; it will however present all the acoustic data from the 2004 field program. This data will be presented as sonograms⁴⁷, where the spectral density values $G(f,t)$ are represented by different colors⁴⁸, one sonogram representing the acoustic data for one AUAR for one day. The spectral density plots $G(f,t)$ cover a narrow (1-1000 Hz) and a broad (1-10,000 Hz and 1-15,000 Hz) band of frequencies to aid in the visual analysis of the data. For the narrow band plots, a linear frequency axis is used, for the broad band plots, a logarithmic axis is used. These sonograms $G(f,t)$ show the variation in the spectral levels of ambient and anthropogenic noise with frequency and time due to changing meteorological conditions, vessel movements and industrial activity. All sonograms $G(f,t)$ will be in absolute amplitude (dB re 1 $\mu\text{Pa}^2/\text{Hz}$), all instrument and sensor corrections having been applied to the data. Appendix E shows the days on which data was acquired at each station. Sonograms for all the data are available on a CD at the back of the report.

⁴⁷ A sonogram is a plot showing the variation in acoustic power spectral density level with frequency and time.

⁴⁸ The scale of the sonograms varies from 37 to 100 dB re 1 $\mu\text{Pa}^2/\text{Hz}$ in 3 dB increments.

Table 3.1(a) - Operational times, parameters and locations of AUARs at monitor stations 3 to 8.

Station		Date		Time		Time	AUAR	Location		Z	Gain		Sens.
Name	#	Start	End	Start	End		#	Latitude	Longitude	(m)	LF	HF	(mV/Pa)
Orlan	3	3-Aug	18-Aug	22:00	23:50	362.0	№ 6	52°21.217	143°35.325	32	16	100	50.8
Orlan	3	7-Sep	20-Sep	10:00	6:30	308.5	№ 10	52°21.803	143°35.201	32	40	200	51.5
Orlan	3	21-Sep	24-Sep	21:00	2:10	53.2	№ 9	52°21.752	143°35.246	34.5	40	200	54.4
Orlan	3	27-Sep	30-Sep	17:00	9:10	64.2	№ 3	52°21.576	143°34.681	32	40	200	50.1
Arkutun-Dagi	4	3-Aug	18-Aug	22:00	17:30	338.0	№ 1	52°19.857	143°43.942	42	16	100	50.1
Arkutun-Dagi	4	19-Aug	1-Sep	6:38	2:00	283.4	№ 10	52°20.088	143°44.086	43	40	200	51.5
Arkutun-Dagi	4	7-Sep	19-Sep	11:30	14:30	276.5	№ 4	52°19.156	143°44.072	43.5	40	200	51.46
Piltun-S	5	28-Aug	1-Sep	17:00	09:20	81.3	№ 2	52°40.180	143°22.078	17.5	40	200	51.6
Piltun-S	5	24-Sep	28-Sep	17:30	15:30	94.0	№ 4	52°40.242	143°22.375	18	40	200	52.1
Piltun-S	5.1	4-Sep	7-Sep	17:00	11:04	66.1	№ 13	52°40.760	143°22.588	18	40	200	51.1
Piltun-S	5.2	24-Sep	25-Sep	17:30	00:00	24.0	№ 8	52°40.657	143°22.354	17	40	200	52.3
Piltun	6	6-Aug	19-Aug	13:00	07:40	299.0	№ 7	52°49.180	143°25.570	20.7	16	100	52.4
Piltun	6	27-Aug	8-Sep	20:00	11:30	255.5	№ 1	52°49.421	143°24.450	20	40	200	50.8
Piltun	6	18-Sep	20-Sep	16:39	06:08	37.5	№ 9	52°49.517	143°24.420	19.5	40	200	54.4
Piltun	6.1	27-Aug	31-Aug	21:00	07:30	75.0	№ 7	52°49.142	143°24.827	22	40	200	52.4
PA-B-10	7	6-Aug	21-Aug	22:20	12:00	337.7	№ 3	52°52.982	143°20.576	11.5	16	100	50.8
PA-B-10	7	22-Sep	1-Oct	9:15	9:00	215.8	№ 10	52°53.018	143°20.270	9	40	200	51.5
PA-B-20	8	4-Sep	16-Sep	15:00	16:30	289.5	№ 5	52°53.955	143°23.270	19.5	40	200	50.31
PA-B-20	8	18-Sep	19-Sep	17:50	23:24	29.6	№ 1	52°53.921	143°23.282	20	40	200	50.8

Table 3.1(b) - Operational times, parameters and locations of AUARs at monitor stations 8, 10, and 11 as well as acoustic stations A4 to A8.

Station Name	#	Date		Time		Time	AUAR #	Location		Z (m)	Gain		Sens. (mV/Pa)
		Start	End	Start	End			Latitude	Longitude		LF	HF	
PA-B-20	8.1	18-Sep	19-Sep	17:37	02:38	9.0	№ 11	52°53.986	143°23.481	21	40	200	50.8
Odoptu-S-10	10	10-Sep	25-Sep	21:17	5:48	344.5	№ 2	53°03.685	143°18.281	11	40	200	51.6
Odoptu-S-10	10	24-Sep	1-Oct	14:00	11:00	165.0	№ 6	53°03.630	143°19.000	14.3	40	200	52.3
Odoptu-S-20	11	9-Aug	21-Aug	14:00	19:40	274.0	№ 8	53°03.763	143°20.097	20.9	16	100	52.1
Odoptu-S-20	11	10-Sep	12-Sep	21:05	00:52	27.8	№ 12	53°03.521	143°19.725	20	40	200	52.8
Odoptu-S-20	11	23-Sep	1-Oct	17:00	11:30	186.5	№ 11	53°03.660	143°19.858	20.5	40	200	52.4
Piltun-1	A.4	6-Aug	14-Aug	22:20	01:00	169.7	№ 12	52°43.100	143°22.466	15.5	16	100	52.8
Piltun-1	A.4	28-Aug	1-Sep	17:00	23:30	78.5	№ 8	52°42.781	143°22.027	17	40	200	51.72
Piltun-1	A.4	24-Sep	28-Sep	16:00	16:20	96.3	№ 7	52°42.913	143°22.353	15	40	200	52.4
Piltun-2	A.5	6-Aug	18-Aug	08:00	05:16	288.0	№ 5	52°43.409	143°25.635	23.5	16	100	50.31
Piltun-2	A.5	28-Aug	8-Sep	15:00	10:00	235.0	№ 12	52°42.900	143°25.600	21	40	200	52.8
Piltun-2	A.5	4-Sep	11-Sep	16:38	18:26	169.8	№ 9	52°43.785	143°25.815	22	40	200	52.3
Piltun-2	A.5.1	28-Aug	31-Aug	17:00	24:00	55.0	№ 5	52°42.864	143°25.762	21.5	40	200	50.31
Piltun-2	A.5.1	22-Sep	23-Sep	13:00	18:40	29.7	№ 4	52°43.344	143°26.016	22	40	200	52.1
Piltun-3	A.6	6-Aug	17-Aug	13:00	08:00	251.0	№ 10	52°49.286	143°25.040	20.7	16	100	51.5
Piltun-3	A.6	14-Sep	16-Sep	21:00	16:15	43.3	№ 1	52°49.493	143°24.436	20	40	200	50.8
Piltun-3	A.6.1	14-Sep	16-Sep	21:00	10:10	37.2	№ 11	52°49.232	143°24.950	21	40	200	50.8
PA-B-1	A.7	6-Aug	21-Aug	15:00	10:30	345.0	№ 2	52°55.810	143°20.470	13.7	16	100	51.6
PA-B-2	A.8	6-Aug	21-Aug	14:00	08:30	346.0	№ 4	52°55.897	143°21.711	22.2	16	100	52.1

3.1 Ambient noise studies

One of the key goals of the acoustic studies in the western gray whale research program has been to measure and characterize the ambient noise field on the NE Sakhalin shelf. This ongoing program commenced in 2003 and continued in 2004. This data, in conjunction with the measurement of the acoustic signature of present and future facilities, will allow the cumulative effect of oil development and production operations on the acoustic background in the area, as well as the gray whale population to be more effectively estimated.

3.1.1 Western gray whale home range

In order to strategically plan the location of the monitoring stations for the 2003, 2004 and future programs, it was critical to estimate the home range of the gray whales on the NE Sakhalin shelf. In 2003, the home range was estimated and the acoustic monitoring locations selected using all the 2001 and 2002 aerial surveys [Borisov et al., 2004], however in 2001, many more aerial surveys were acquired and they were concentrated in a reduced seasonal range. Further, no correction was made for survey effort. In 2004, the home range was estimated using the 2003 and 2004 aerial survey data and the sighting data was weighted by the observation effort⁴⁹.

In 2003, the probability contours were estimated using a conventional kernel density method⁵⁰. Kernel density methods employ a gridding process, which is robust for small sample sizes unless the variances of the north-south and east-west components of the distribution are very different. However, for the Piltun feeding area the distribution of whale sightings is oriented parallel to the coast with significantly greater variance in the along-shore direction than in the perpendicular-to-shore direction. For this reason, in 2004, a grid was constructed for the Piltun feeding area that was oriented along-shore and with an along-shore grid cell dimension greater than the perpendicular-to-shore dimension, (i.e. each cell was 4 km by 0.5 km). Density was then computed for each cell as the number of whales normalized by the observation effort and divided by the cell area.

⁴⁹ The sighting data was normalized for observation effort by dividing the number of whales in a cell by the line kilometers of sighting effort for that cell.

⁵⁰ The kernel density contours were mapped using the Arcview© 3.1 extension Animal Movement 2.04 [Hooge et. al., 1997]. Kernel density contours are an estimator that assesses an animal's probability of occurrence at each point in space using a utilization distribution. It is a non-parametric estimator that has no underlying assumptions of how animals use space.

Probability contours were then computed for the density grid by sorting the cells by density and sequentially selecting cells in increasing density order until the desired probability threshold was achieved. For example, the 50% probability contour involves selecting cells until the cumulative sum of density times area equals 50% of the population (the sum of density times area for all cells). Internal boundaries between contiguous grid cells were eliminated to produce bounding polygons. Internal voids (e.g. 'donut' holes), consisting of up to two cells were then eliminated. The final contour line was then generated with a spline fit to the resultant polygons using a Bezier method. Probability contours were computed independently for the Piltun and Offshore feeding areas

The same methodology was employed for the Offshore feeding area except that in this case, the conventional assumptions about distribution were satisfied and a regular grid of 1 km by 1 km cells was employed. In this analysis, probability contours are used to visualize areas with the greatest density of normalized gray whale sightings, and examine shifts in the 'centers of activity' of gray whales over time. Probability contours of 50% and 95% were arbitrarily chosen and generated to visualize the aggregation of 2002-2003 gray whale sightings over time.

3.1.2 Monitor, control and acoustic station locations

A systematic acoustic monitoring framework was developed in 2003 and extended in 2004. The goal was to monitor changes in the acoustic field on the NE Sakhalin shelf and most importantly those changes in the anthropogenic noise level that could cause a significant increase in the Received Level (RL) in either the Piltun or Offshore feeding areas.

Three types of stations for recording acoustic data were designated:

- **Monitor stations** - These are locations that will be systematically monitored to gain an understanding of the changes in the acoustic field over time. They will be reoccupied multiple times in a season and over multiple seasons. The monitor stations will generally be located at the edge of a gray whale feeding area nearest to a proposed facility or in a location where the greatest cumulative impact from multiple facilities could be expected.
- **Control station(s)** - Dr. John Richardson (LGL) recommended that a control station or stations be set up far enough away from the proposed development operations that the

anthropogenic noise field would not be expected to increase. This station would reflect any changes to the ambient noise field unrelated to the oil development activities.

- **Acoustic stations** - These locations will be infrequently monitored, their purpose is to gain an understanding of the anthropogenic noise field from a location at a specific time or to conduct TL experiments.

Prior to the start of the 2003 field season, 11 stations were designated; seven were monitor stations, three were acoustic stations and one was a control station. For the 2004 season, a further six monitor stations and seven acoustic stations were designated. Table 3.2 gives the proposed names, numbers and locations of these stations⁵¹.

The locations of the monitor stations were determined with reference to the major gray whale concentrations in the area (Figure 3.1)⁵². Probability contour maps were made from the aerial surveys flown in 2002 and 2003⁵³. For the Offshore feeding area, the locations of the stations (except the OFA station) were chosen to be on the 95% probability contour at the point closest to a current or proposed facility. In 2004, the Orlan and Lunskeye stations remained⁵⁴ and two new monitor stations were designated. The OFA (Offshore Feeding Area) station is approximately in the center of the Offshore feeding area and the Arkutun-Dagi station is at the North Eastern edge of the Offshore feeding area.

The Piltun feeding area is strongly defined by bathymetry, most whales feeding in water depths between ~8-12 m. Mother-calf pairs have been seen in the Piltun feeding area, often in water depths of 5-10 m, but few whales have been seen outside the 20 m contour. Here the two key monitor points are the 20 m contour and the 10 m contour (regarded as the edge and center of the distribution). Five monitor stations remain from 2003⁵⁵.

⁵¹ Where possible the numbers and names of the monitor stations will be maintained year to year for clarity.

⁵² Various vessel based (MMO, Photo-ID, Benthic) and land based (vehicle surveys, behavioral) biology programs were being conducted over the same range, so an evaluation of the effect of any changes in the acoustic field on the distribution of gray whales can be evaluated.

⁵³ In 2005 a method is being evaluated to use all whale survey data (aerial, vessel and land based surveys) using statistical techniques to normalize for the observation effort.

⁵⁴ The Orlan station is on the 95% Kernel probability contour (from 2003) closest to the proposed location of the Orlan platform and the Lunskeye station at the southern edge of the Offshore feeding area.

⁵⁵ The Odoptu-S-10 and Odoptu-N-10 stations were at the 10 m bathymetry contour off the coast from the two proposed Odoptu well pads, while the Piltun station was at the 20 m bathymetry contour between the Molikpaq platform and the major gray whale concentration off Piltun lighthouse. The PA-B stations were at the 10 m (PA-B-10) and 20 m (PA-B-20) bathymetry contours closest to the proposed PA-B location.

Table 3.2 - Numbers, names, locations and depths of the proposed stations.

#	Station		Latitude	Longitude	Depth
Monitor Stations:					
1	Lunskoye	Лунское	51° 51' 45" N	143° 37' 27.3" E	50 m
2	OFA (Offshore Feeding area)	ГЗК (Глубоководная зона кормления)	52° 10' 18" N	143° 36' 1.8" E	~40 m
3	Orlan	Орлан	52° 21.6' N	143° 35.0' E	32 m
4	Arkutun-Dagi	Аркутун-Даги	52° 19' 9.6" N	143° 44' 4.6" E	~40 m
5	Piltun-S	Пильтун-Ю	52° 40' 51" N	143° 22' 34" E	10 m
6	Piltun	Пильтун	52° 49.3' N	143° 24.9' E	20 m
7	PA-B-10	ПА-Б-10	52° 53' 2.1" N	143° 20' 10.6" E	10 m
8	PA-B-20	ПА-Б-20	52° 54' 00" N	143° 23' 20.5" E	20 m
9	Odoptu-PA-B	Одопту-ПА-Б	53° 00' 00" N	143° 21' 18" E	20 m
10	Odoptu-S-10	Одопту-Ю-10	53° 03.7' N	143° 18.3' E	10 m
11	Odoptu-S-20	Одопту-Ю-20	53° 03' 42" N	143° 19' 58" E	20 m
12	Odoptu-N-10	Одопту-С-10	53° 09.1' N	143° 17.4' E	10.5 m
13	Odoptu-N-20	Одопту-С-20	53° 09' 6" N	143° 18' 42" E	20 m
14	Control	Контрольная	53° 25.95' N	143° 11.1' E	20 m
Acoustic Stations:					
A1	#1 (Chayvo-1)	#1 (Чайво-1)	52° 27.8' N	143° 19.0' E	11 m
A2	#2 (Chayvo-2)	#2 (Чайво-2)	52° 25.9' N	143° 20.6' E	11 m
A3	#3 (Chayvo-3)	#3 (Чайво-3)	52° 26.8' N	143° 24.6' E	17 m
A4	#4 (Piltun-1)	#4 (Пильтун-1)	52° 43' 14.4" N	143° 22' 26.7" E	10 m
A5	#5 (Piltun-2)	#5 (Пильтун-2)	52° 43' 48" N	143° 25' 49" E	20 m
A6	#6 (Piltun-3)	#6 (Пильтун-3)	52° 49.3' N	143° 24.9' E	20 m
A7	#7 (PA-B-1)	#7 (ПА-Б-1)	52° 55' 54" N	143° 19' 39" E	10 m
A8	#8 (PA-B-2)	#8 (ПА-Б-2)	52° 55' 54" N	143° 21' 42.4" E	20 m
A9	#9 (BEH-Odoptu)	#9 (Одопту (Пов))	53° 12' 33.1" N	143° 15' 51" E	10 m
A10	#10 (BEH-north)	#10 (Пов-север)	53° 17' 52.4" N	143° 13' 25.4" E	10 m

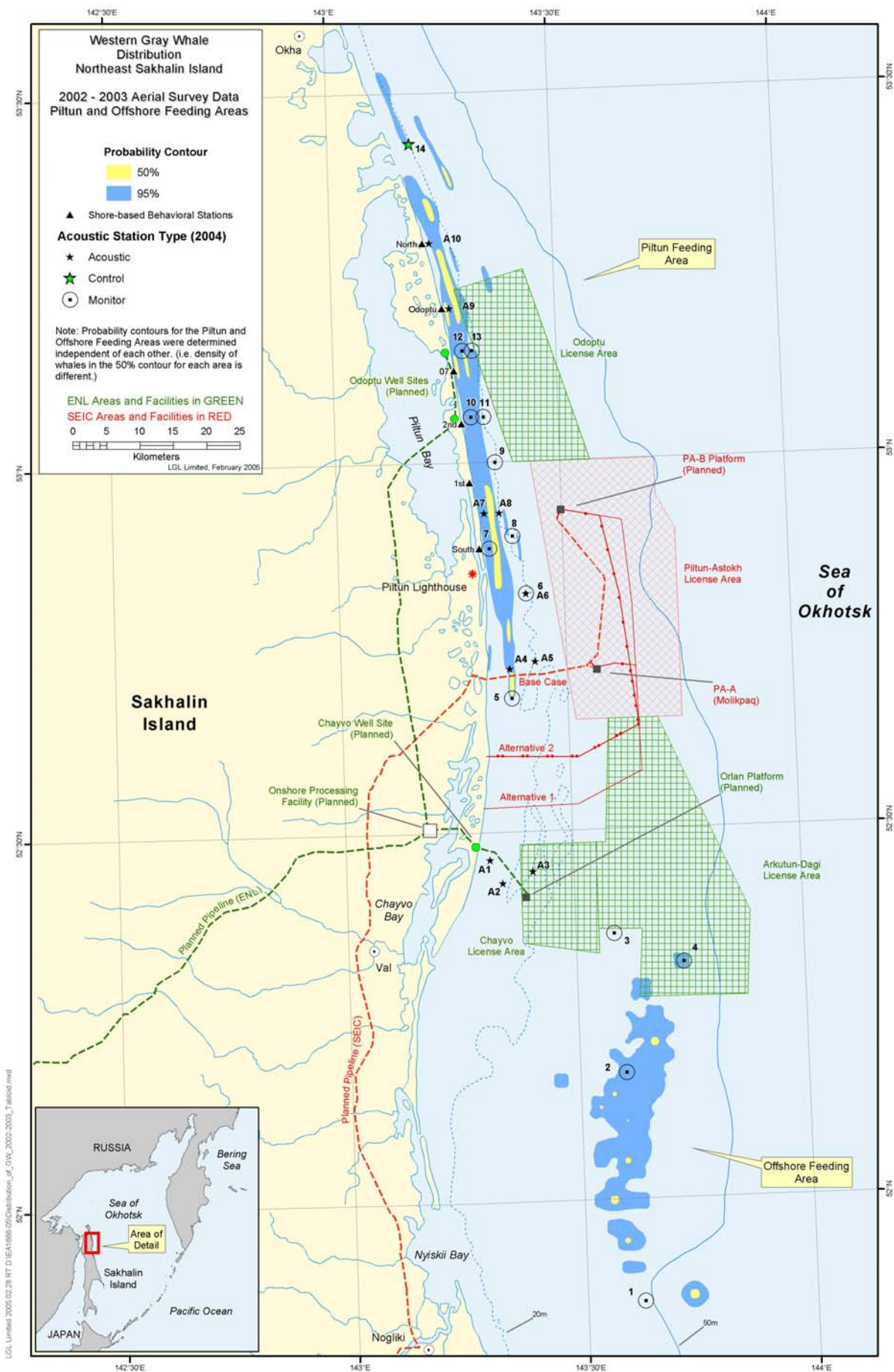


Figure 3.1 - Map showing the AUAR locations and probability contours showing the density distributions of western gray whales from the 2002 to 2003 aerial surveys.

In 2004, four new monitor stations were designated. These were the Piltun-S station at the southern edge of the Piltun feeding area and the Odoptu-PA-B station at the 20 m bathymetry contour between the proposed locations of the Odoptu-S well pad and the PA-B platform. The Odoptu-S-20 and Odoptu-N-20 stations were located at the 20 m bathymetry contour off the coast from the two proposed Odoptu well pads as well as the Odoptu-S-10 and Odoptu-N-10 stations.

The control station location remained the same as in 2003⁵⁶. This location had a similar bathymetric character to the Piltun feeding area, but was not so far away that operational support would be difficult.

Seven new acoustic stations were added in 2004 and were designated stations A4 to A10, Stations A1 to A3 were not occupied in 2004. All the acoustic stations occupied in 2004 were used for TL experiments, most along the proposed pipeline routes from PA-B and Molikpaq.

The AUARs were deployed as shown in Table 3.1. This data represents acoustic noise synchronously recorded over 100 km along the NE Sakhalin coast from the control station to the OFA monitor station. Figures 3.2 and 3.3 shows sonograms $G(f,t)$ of acoustic measurements made by the AUARs at the A5 and Odoptu-S-10 monitor stations, the full set of sonograms for the data is supplied on CD and listed in Appendix E. The logarithmic scale on the frequency axis clearly shows the pseudo-noise signals below 16 Hz on Figure 3.3, these are flow noise caused by a tidal current with a velocity exceeding 3 m/s and recorded twice a day. The acoustic data for the infrasonic band should therefore be analyzed during slack tide periods when flow noise is absent (approximately 4 hours - Figure 3.3).

3.2 Anthropogenic noise studies

In addition to the monitoring of ambient noise, one of the goals of the 2004 program was to measure the acoustic signature of both the 2-stroke and 4-stroke outboard motors on the zodiacs used by the Photo-ID team. The second was to determine the acoustic signature of the *Academik Oparin* the mother ship used to house the biology and acoustic teams.

⁵⁶ The control station was located on the 20 m bathymetry contour approximately 40 km north of the Odoptu North pad site.

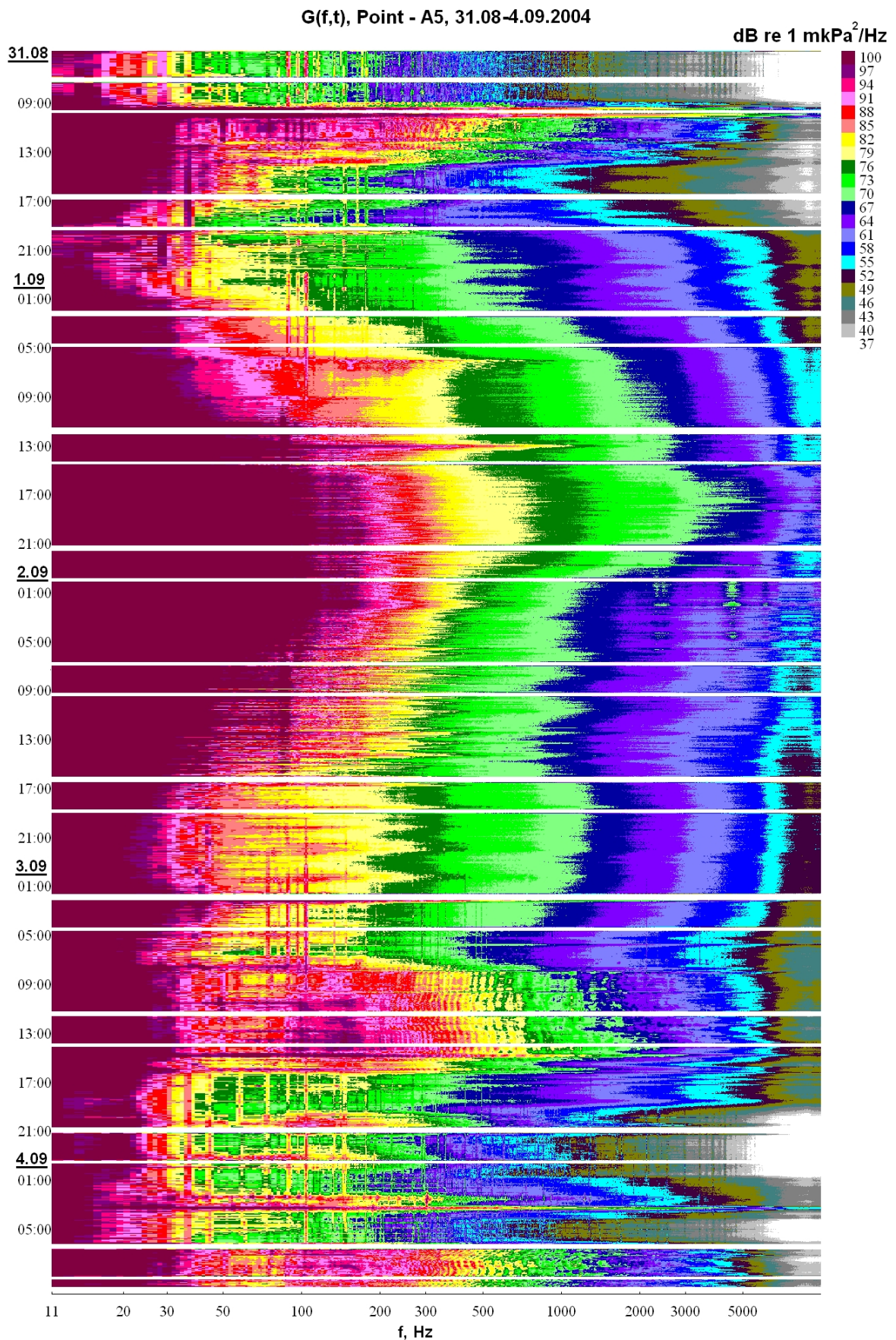


Figure 3.2 - Sonograms $G(f,t)$ of acoustic energy recorded at acoustic station A5 on from 13 August to 4 September 2004.

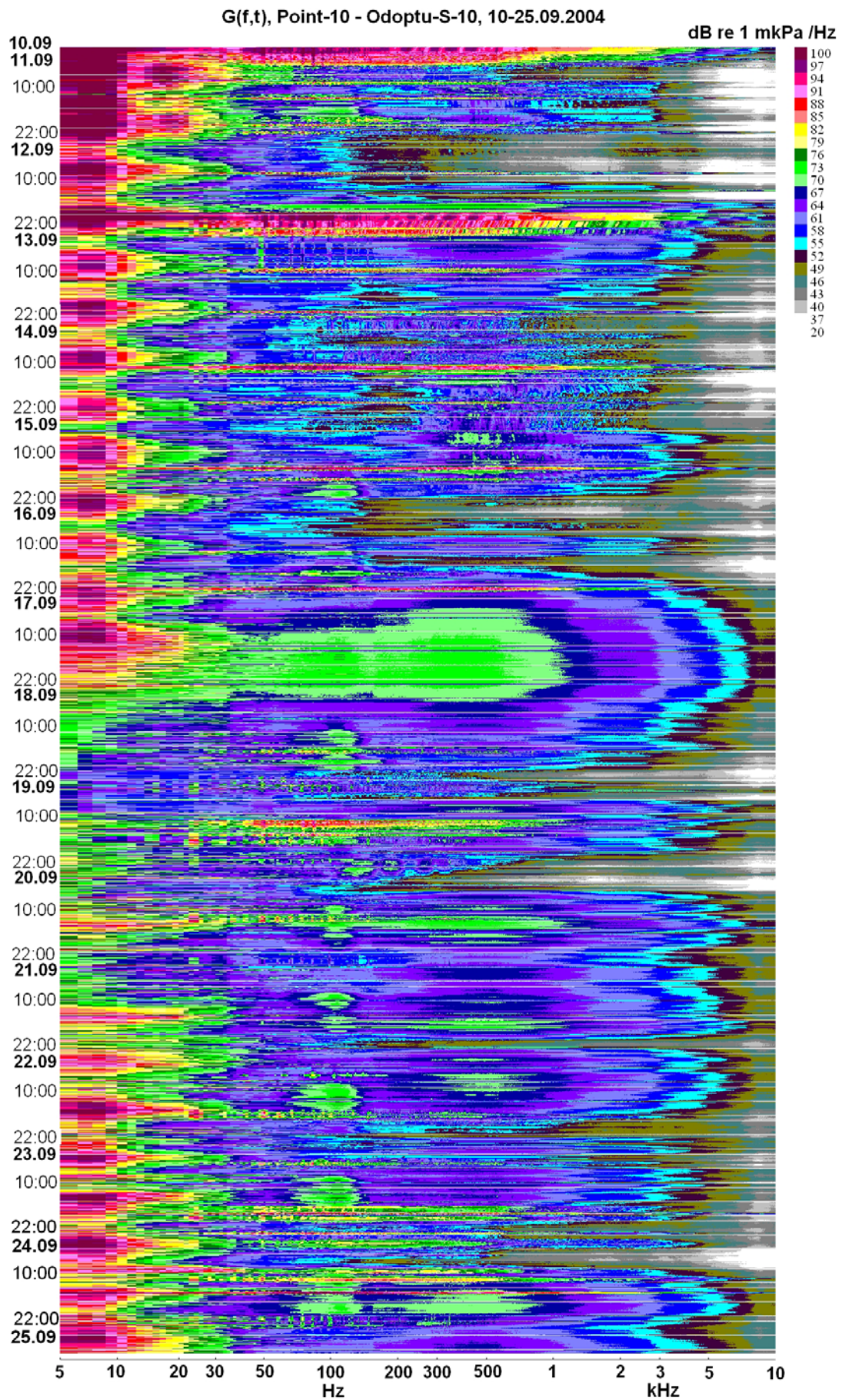


Figure 3.3 - Sonograms $G(f,t)$ of acoustic energy recorded at the Odoptu-S-10 monitor station [101] between 10 and 25 September 2004.

3.3 Behavioral noise studies

Figure 3.1 shows the location of the behavioral stations (marked with triangles), as well as the acoustic monitor station locations. One of the goals of the 2004 program was to measure the acoustic levels at monitor stations 7 and 10 synchronously with behavioral observations at the south and 2nd behavioral stations. There were three days where synchronous behavioral measurements were taken, these were:

- 16 August - Measurements taken at the South behavioral and acoustic #7 stations.
- 11 September - Measurements taken at the 2nd behavioral and acoustic #10 stations.
- 19 September - Measurements taken at the 2nd behavioral and acoustic #10 stations.

For each of these days broad band sound pressure levels were estimated in 1-minute windows and energy levels were estimated in 10-minute windows.

3.4 TL Experiments

A key component of the 2004 acoustic monitoring program was detailed Transmission Loss (TL) studies conducted along both the proposed ENL and SEIC pipeline routes and from proposed facilities to the western gray whale feeding areas. This would allow the acoustic impact of construction activities at Moliqpaq, PA-B and Orlan to be more effectively estimated. These studies will be used to more effectively analyze any potential impacts from the construction and to design more effective mitigation measures.

3.4.1 PA-B and Moliqpaq pipeline TL experiments

A series of 11 Pipeline Transmission Loss (PTL) experiments were conducted from the three proposed pipeline routes from PA-B and Moliqpaq (Table 3.3, Figure 3.4). These TL experiments were used to determine the frequency dependent Transmission Loss (TL) from the proposed pipeline routes to the nearest 20 m bathymetric contour enclosing the Piltun feeding area.

To conduct the measurements, AUARs were deployed at the specified monitoring stations for each profile. Tonal and broadband noise signals were then transmitted from the source locations for each profile. At the beginning and on completion of the transmission, hydrologic measurements were taken with the sonde. The profile was then sailed by the *Academik Oparin* with bathymetric and hydrologic data measurements being taken along the profile from the TL source locations to the recording station locations.

Table 3.3 - Descriptions of the pipeline transmission loss (PTL) profiles.

TL Profile	Source Locations	Receiver Locations
Piltun: PTL1	PTL1-A	Acoustic stations # 7 and 8
Piltun: PTL2	PTL2-A, B, C	PA-B-20, Piltun, (PA-B-10)
Piltun: PTL3	PTL3- B, C	Piltun
Piltun: PTL4	PTL4-A, B, C	Piltun
Piltun: PTL5	PTL5-A, B, C	Piltun
Piltun: PTL6	PTL6-A, B, C	Acoustic station # 5
Piltun: PTL7	PTL7-A, C	Acoustic station # 5
Piltun: PTL8	PTL8-A, B, C	Acoustic station # 5, (Arkutun-Dagi)
Piltun: PTL9	PTL9-A, B	Piltun-S, (Orlan)
Piltun: PTL10	PTL10-A, B	Piltun-S, Orlan
Piltun: PTL11	PTL11-A, B, C	Piltun-S, Acoustic station # 4, Orlan
Chayvo: PTL12	PTL12-A	Piltun-S, Acoustic station # 4, Orlan
Chayvo: PTL13	PTL13-A	Piltun-S, Acoustic station # 4, Orlan

3.4.2 Chayvo pipeline TL experiments

Two PTL profiles were acquired for each of the Chayvo PTL source locations PTL12A and PTL13A. One profile ran north to the Piltun feeding area and the other to the Orlan station (#3) at the edge of the Offshore feeding area. These PTL measurements were acquired in a similar fashion to those described in section 3.4.1 above.

3.4.3 Orlan TL profiles

Two TL profiles were acquired from the Orlan platform. TLP-6 was a profile from the Orlan platform to the Piltun-S and A4 stations at the edge of the Piltun feeding area. The four source locations on this profile were acquired on 26 September 2004. TLP-2 was a 25.5 km profile from the Orlan platform through the Orlan station (#3) to the Arkutun-Dagi station (#4) at the northern edge of the Offshore feeding area. There were nine source locations on this profile⁵⁷; the profile and associated hydrology were acquired on 7 September 2004.

⁵⁷ TLP-2I (25.5 km from Arkutun-Dagi station), -2H (19.3 km), -2G (15.3), -2F (13.3 km), -2E (12.3 km, 1 km from Orlan station), -2D (8 km), -2C (4 km), -2B (2 km), -2A (1 km).

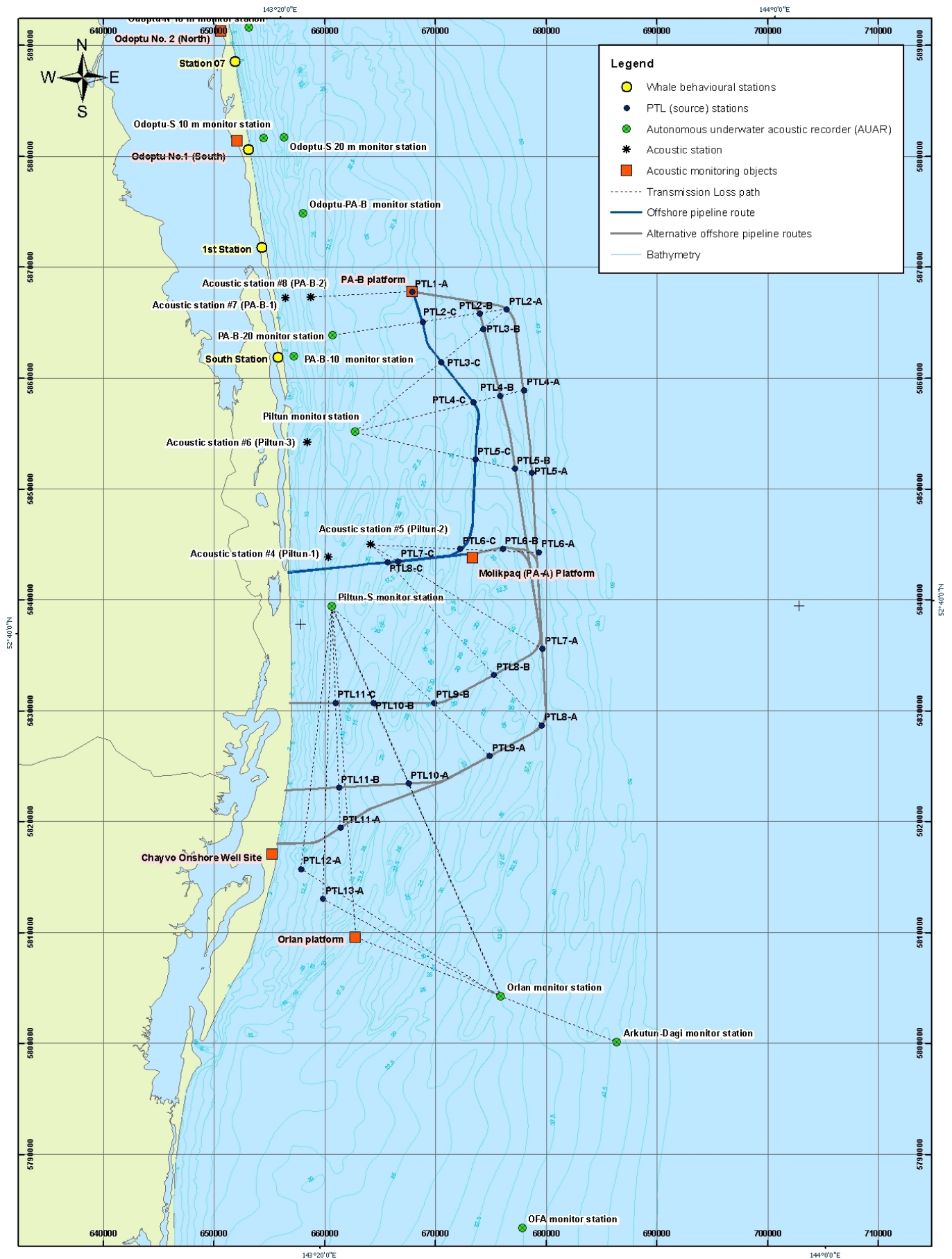


Figure 3.4 - Map of the study area showing the locations of the AUARs deployed during the PTL experiments and the profiles surveyed.

3.4.4 Reference hydrophone

Ideally the reference hydrophone used to monitor the output of the transducer would in the far field of the transducer. However, on the NE Sakhalin shelf, the water depths are too shallow to allow the reference hydrophone to be placed in the far field without propagation effects making the output of the transducer impossible to determine. The optimum location for the reference hydrophone in these TL experiments is therefore difficult to determine.

The frequency and range dependent TL is estimated by subtracting the power spectral density level (dB) of the acoustic signal at 1 m from the transducer from the power spectral density of the acoustic signal as recorded at the AUAR:

$$TL(f, r) = 10 \log G_r(f) - 10 \log G_{1m}(f) \quad (3.1)$$

Where:

$TL(f, r)$ is the frequency and range dependent TL,

$G_r(f)$ is the power spectral density of the acoustic signal at range r from the transducer,

$G_{1m}(f)$ is the power spectral density of the acoustic signal at 1 m from the transducer.

It is therefore critical to obtain a quantitative estimate of the pressure field generated by the transducer at 1 m. To better understand the near field acoustic pressure field of the transducers used for the shallow water TL studies, an experiment was conducted in deeper water (28 m). The layout of the experiment is shown in Figure 3.5.

During the experiment the power spectral density of the acoustic signal $G_z(f)$ was recorded by the reference hydrophone at different distances from the source levels. The reference hydrophone was moved in 1 m steps along the rope supporting the transducer. This experiment was conducted for the broadband transducer while transmitting white noise (800-5000 Hz), and for the LF resonant transducer while transmitting a 27 Hz tonal signal. Additionally, with the LF transducer, the reference hydrophone was moved along the side of the *Academik Oparin* at a depth of 10 m.

The average Intensity \bar{I} of the acoustic field from the broadband transducer measured using a hydrophone at a distance z is shown in Figure 3.6. The average value of Intensity was estimated using Equation (3.2).

$$\bar{I}(f_n; f_m) = 10 \log \left(\frac{G(f_n) + \dots + G(f_m)}{m - n + 1} \right) \quad (3.2)$$

Where:

$f_n = 800$ Hz,

$f_m = 5000$ Hz.

The points on Figure 3.6 show the results from each experiment and the curves show the variation in average Intensity with distance for a number of different divergence schemes. Figure 3.6(a) (HF transducer - 800-5000 Hz white noise) and Figure 3.6(b) (LF transducer - 27 Hz tonal signal) show the results of the vertical separation experiments (as shown in Figure 3.5(a)). Figure 3.6(c) corresponds to the experiment when the reference hydrophone was placed at a depth 10 m, but moved horizontally away from the transducer (Figure 3.5(b)). Linear regressions (using the least squares method) of the data from each experiment are shown in black on each plot. The regressions estimate the logarithmic rate of change of Intensity with increase in range (r):

$$\bar{I}(r) = A - B \log(r) \quad (3.3)$$

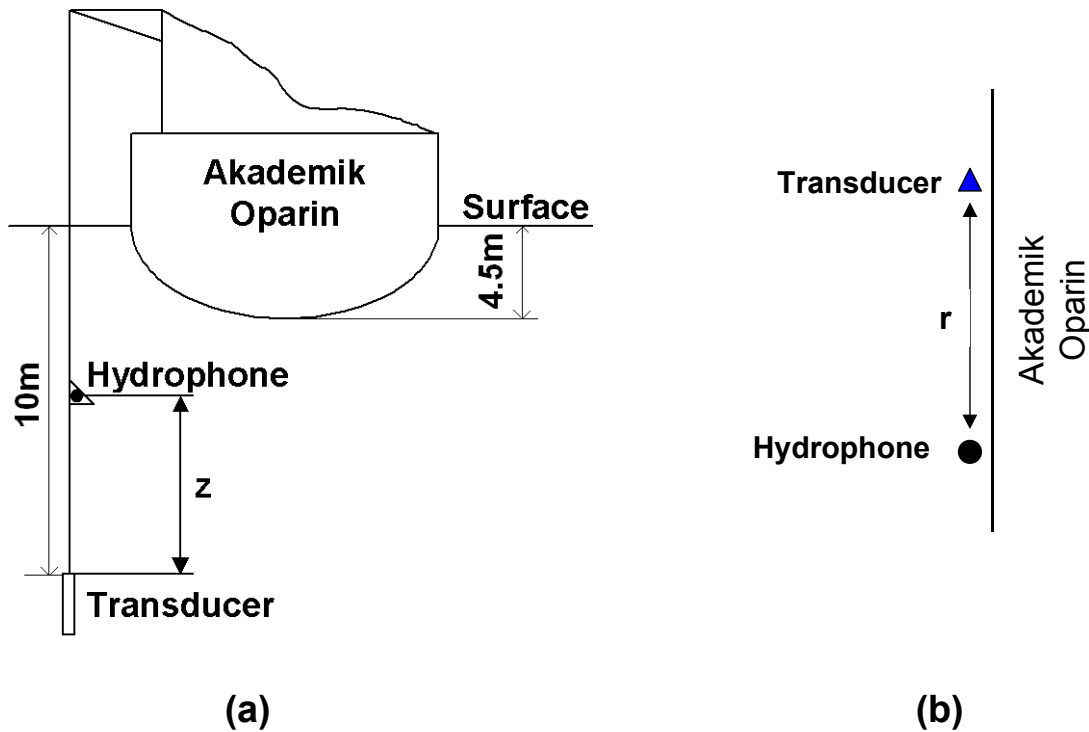


Figure 3.5 - Layout of the experiment conducted to investigate the acoustic pressure field from the transducers used for the TL experiments in the near field.

It can be seen from Figure 3.6(a) that the average Intensity of the acoustic field produced by the broadband transducer decreases with distance at a rate between spherical spreading (green curve) and cylindrical spreading (violet curve). A value of $16.31\log(r)$ was estimated by the regression. The wavelength (0.3 - 2 m) at these frequencies is approximately the same as the dimensions of the cylindrical transducer (136 cm height, 28 cm diameter). The transducer cannot therefore be considered to be a point source and in the near field its acoustic field will differ from the spherical spreading expected from a point source.

Figures 3.6(b) and 3.6(c) show that in both cases the average Intensity of a 27 Hz tonal signal decreases more rapidly than would be expected by spherical spreading ($20\log(r)$). The intensity decreases faster in the vertical direction than in horizontal. This could be expected due to the interaction of the acoustic field with the free surface; as the hydrophone approaches the sea surface the acoustic field will suffer additional attenuation.

That the amplitude decreases faster than would be expected due to spherical spreading can probably be explained by the fact that at a frequency of 27 Hz the wavelength (≈ 50 m) is significantly larger than the diameter of the transducer pistons. Thus, near the transducer the acoustic field can have a reactive component that is significantly larger than the active component. The ratio between the reactive and active components changes with distance, the reactive component decreasing and the active increasing. In the far field the active component is significantly larger than the reactive. In the near field, unlike the far field, intensity cannot be determined from pressure squared due to the phase difference between the pressure and oscillating velocity fields. Since the hydrophone measures pressure, it is measuring both the active and reactive components of the field. Therefore, in the near field of the transducer the spreading loss can be greater than expected since only the active component has a spreading loss due to spherical spreading. The spreading loss for the reactive component exceeds that for the active component in the near field.

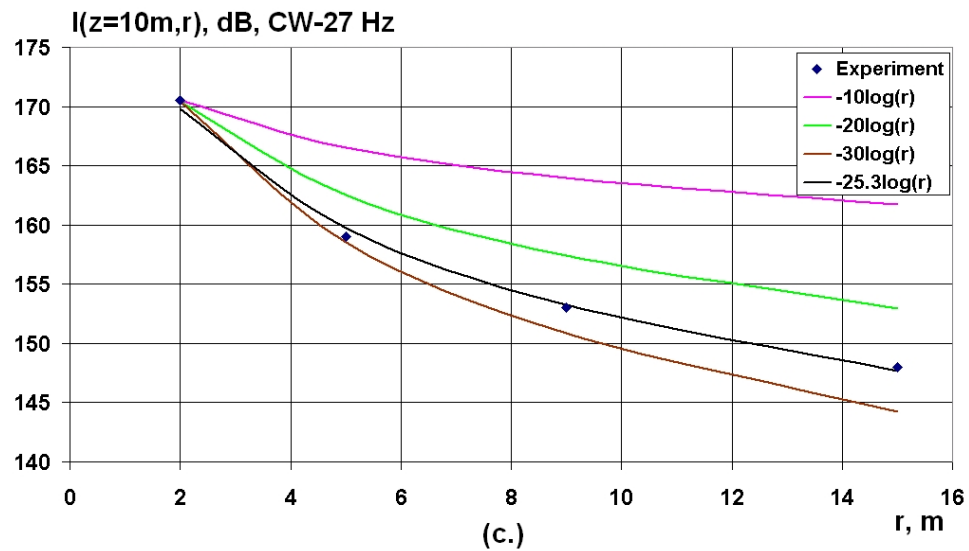
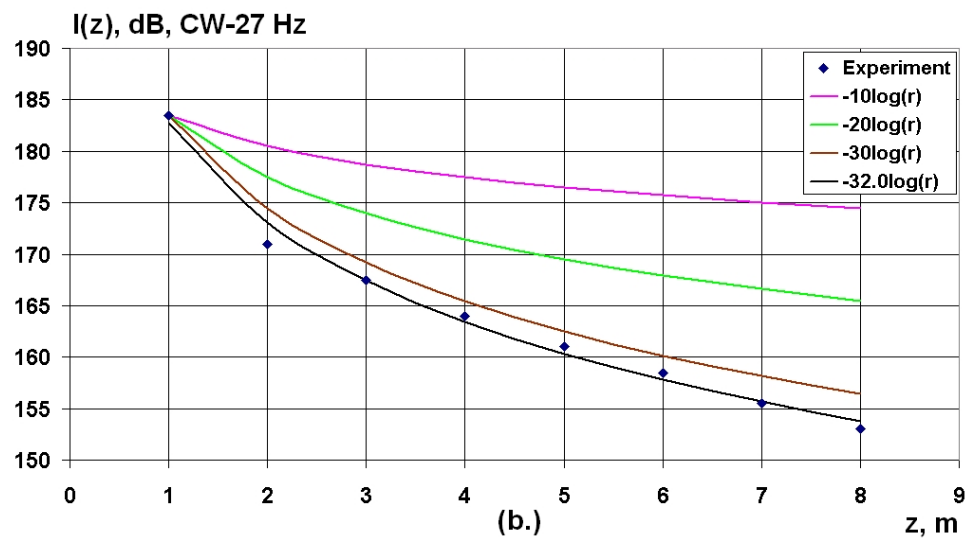
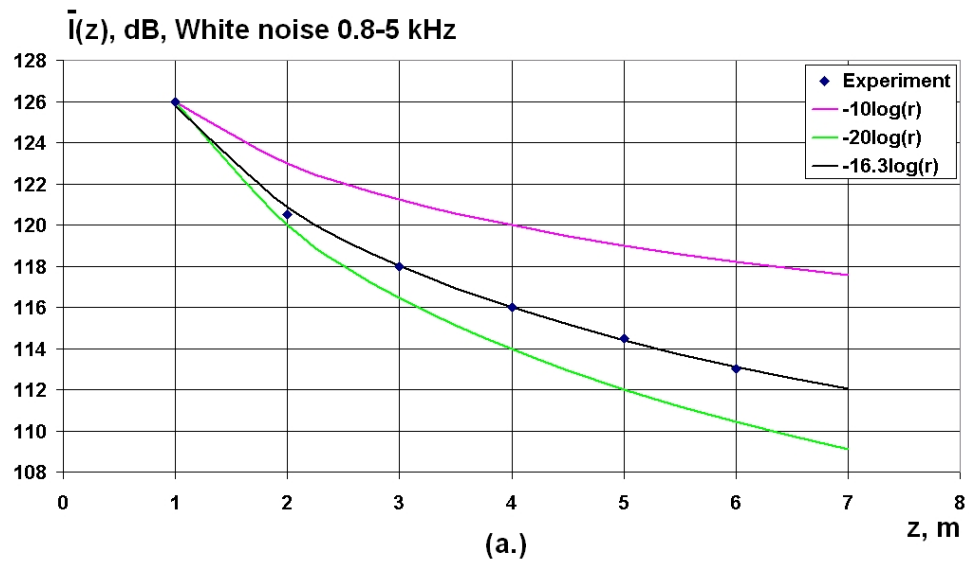


Figure 3.6 - Variation of average Intensity with vertical distance between the transducer and reference hydrophone (a) white noise from broadband transducer (0.8-5 kHz); (b) 27 Hz tonal signal from the LF transducer; (c) variation with horizontal distance between the reference hydrophone and LF transducer (both at 10 m) - 27 Hz tonal signal.

3.4.5 Methodology used to monitor acoustic levels generated by the transducers

Ideally, in order to eliminate the near field phenomena described in the previous section the reference hydrophone used to monitor the output should be located several wavelengths from the transducer (in the far field). However, this is impractical since for the study area on the NE Sakhalin shelf, the water depths are too shallow (10-40 m). The length of *the Akademik Oparin* (75 m) limits the horizontal distance; additionally the stern area of the ship is noisier since it is near the engine compartment. Also, as the range increases, interference between the direct arrival and reflections from the sea floor, the sea surface and the hull of the *Academik Oparin* can complicate the interpretation of the results.

The reference hydrophone was located at a distance of 2 m from the center of the broadband transducer and at 1 m from the edge of LF transducer. The reference hydrophone was isolated from vibration using a rubber suspension system (see section 2.6). The goal of the system was to minimize contamination of the data by flow noise, vibration from currents and surface waves, as well as noise from equipment on and the rocking of the *Academik Oparin*. The previous studies indicate that the source level of the transducers could be slightly lower than the reference level for the LF transducer (~4 dB) and slightly higher than the reference level for the LF transducer (~2 dB).

3.5 Bathymetric and hydrologic studies

In addition to the basic processing of the bathymetry and hydrology data described in section 2.7, the Oceanology department of POI undertook an independent analysis of the data using their own methods and algorithms. The oceanologists brought their expertise to the development of a hydrological model of the area. This section describes how the bathymetric and hydrologic data acquired on the NE Sakhalin shelf was processed to enable the creation of a bathymetric map that was used for research on the temporal-spatial variations of hydrology in the study area. This data will be used to build acoustic models which will be used to model the acoustic fields generated by known sources and to analyze the impact of bathymetry and hydrology on the propagation of these fields. The data will also be used to investigate the impact of temperature and salinity variations on benthos development.

3.5.1 Bathymetry map

Figure 1.3 shows the profiles along which the bathymetric data was acquired using the sonar on the *Academik Oparin*. 252000 depth measurements were taken in 2004 and were used to build the map⁵⁸. The data points were interpolated into an even grid using a kriging algorithm⁵⁹ [Allen, 1973]. Figure 3.7 shows a bathymetric map with contours and Figure 3.8 is a 3D rendering of the same data. A notable feature of the bathymetry is the NE orientation of the bathymetric channels in the area; this will be discussed further in the second report. This grid of interpolated data was used to determine the bathymetric structure along selected profiles⁶⁰. Figure 3.9(b) shows an example of a bathymetric profile, extracted from the interpolated grid along the line shown in Figure 3.9(a).

3.5.2 Data processing for spatial and temporal analysis of the hydrology

Prior to analyzing the spatial and temporal variation of hydrology in the study area, the acquired data set was translated into new smoothed or averaged parameters in order to:

- Make the data selection for different depths and vertical sections faster and easier;
- Have the capability to operate on averaged one-meter level values of temperature (T), salinity (S) and sound velocity (C); and
- Classify the hydrologic profiles by phase of the tide at acquisition.

To complete the first goal, a relational database was designed [Атлас океанов. Тихий океан - М, 1974]. The core of the database design is a logical hydrologic data model; the input data values are then used to populate the model parameters. The model consists of a set of inter-linked tables. The next paragraph describes the three main tables; columns giving the table parameters and descriptions follow the name of the table. Data selection and parameter computation was accomplished within the PARADOX database system [Yozhida, 1967]. Figure 3.10 gives an example of a request to the database for data from a given time and area. The table **STATION** contains the data about the hydrologic measurement at a location. The table **DATA_TSC** contains the measurements of T, S, and C as acquired by the sonde, and the table **AVERAGE_TSC** contains the T, S, and C measurements averaged over 1 m intervals. The parameter Nom is common to all tables and can therefore be used to link the tables.

⁵⁸ There was a 4.5 m depth correction from the transducer to the sea surface, but none for tidal variation.

⁵⁹ This kriging algorithm was part of the Surfer mapping package developed by Golden Software.

⁶⁰ Using the slice function from the Surfer mapping package (Golden Software).

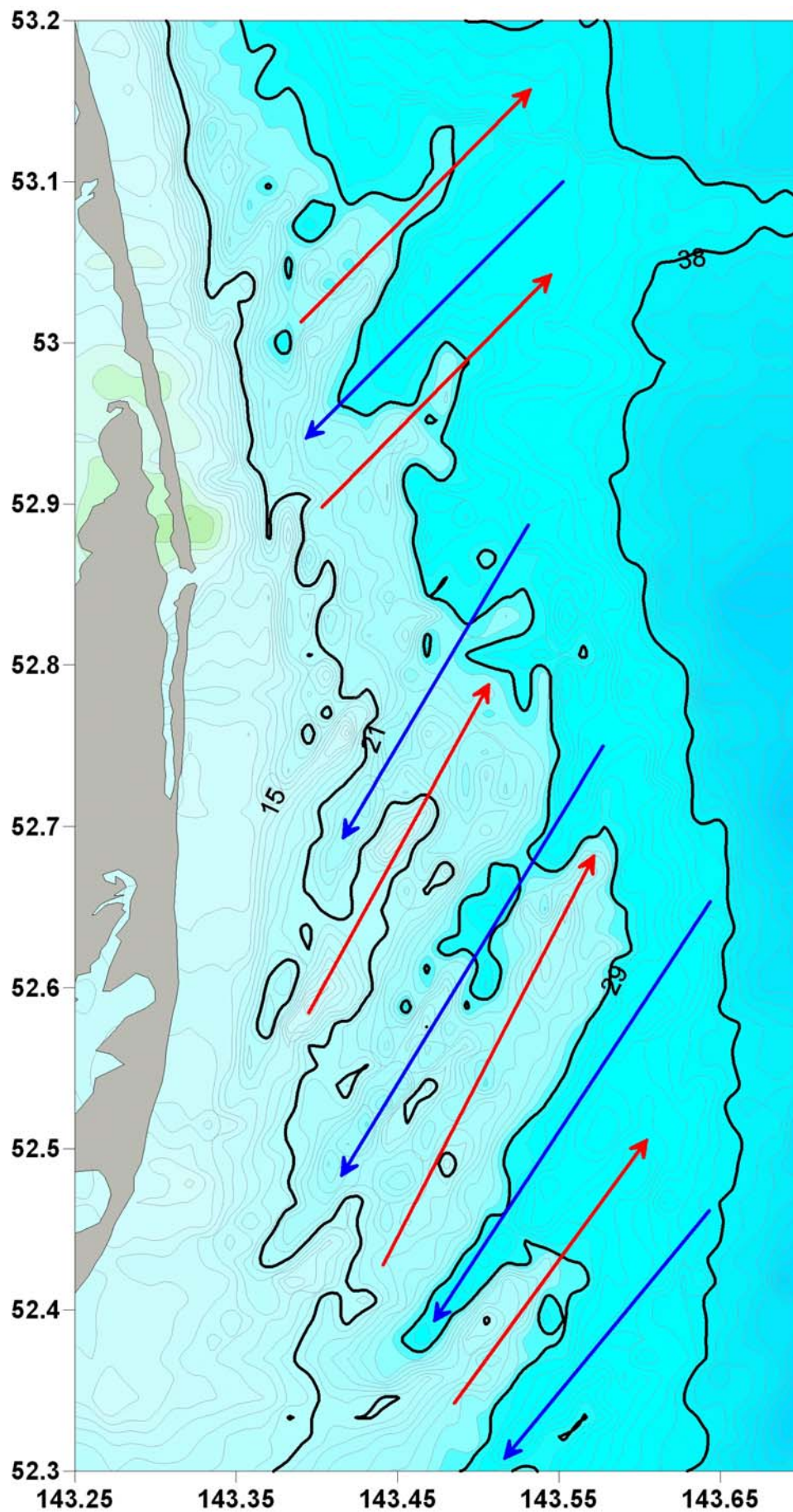


Figure 3.7 - Bathymetric map of the study area with contours, note the dominant NE-SW orientation of the bathymetric structures.

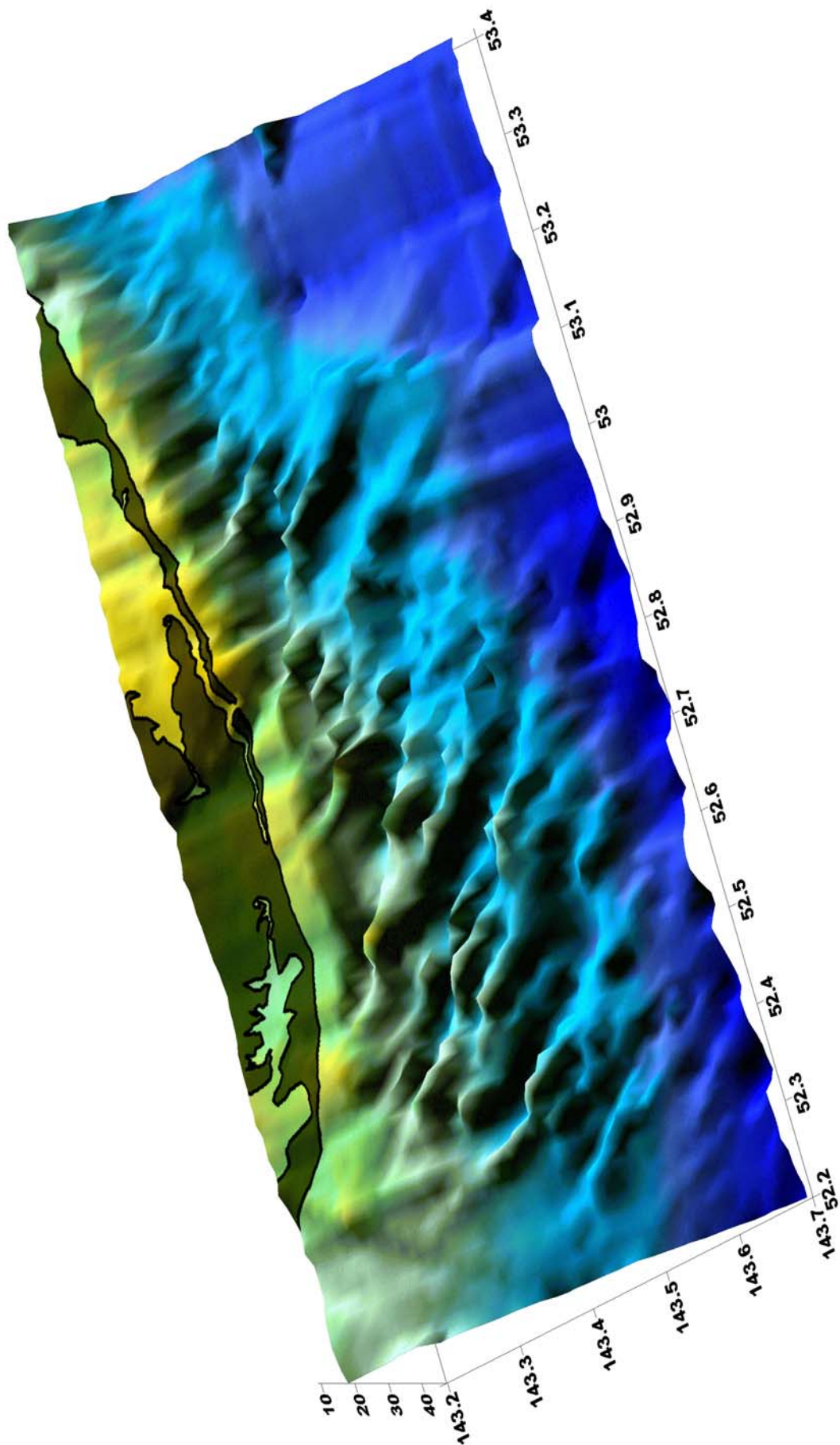


Figure 3.8 - 3D bathymetric map of the study area.

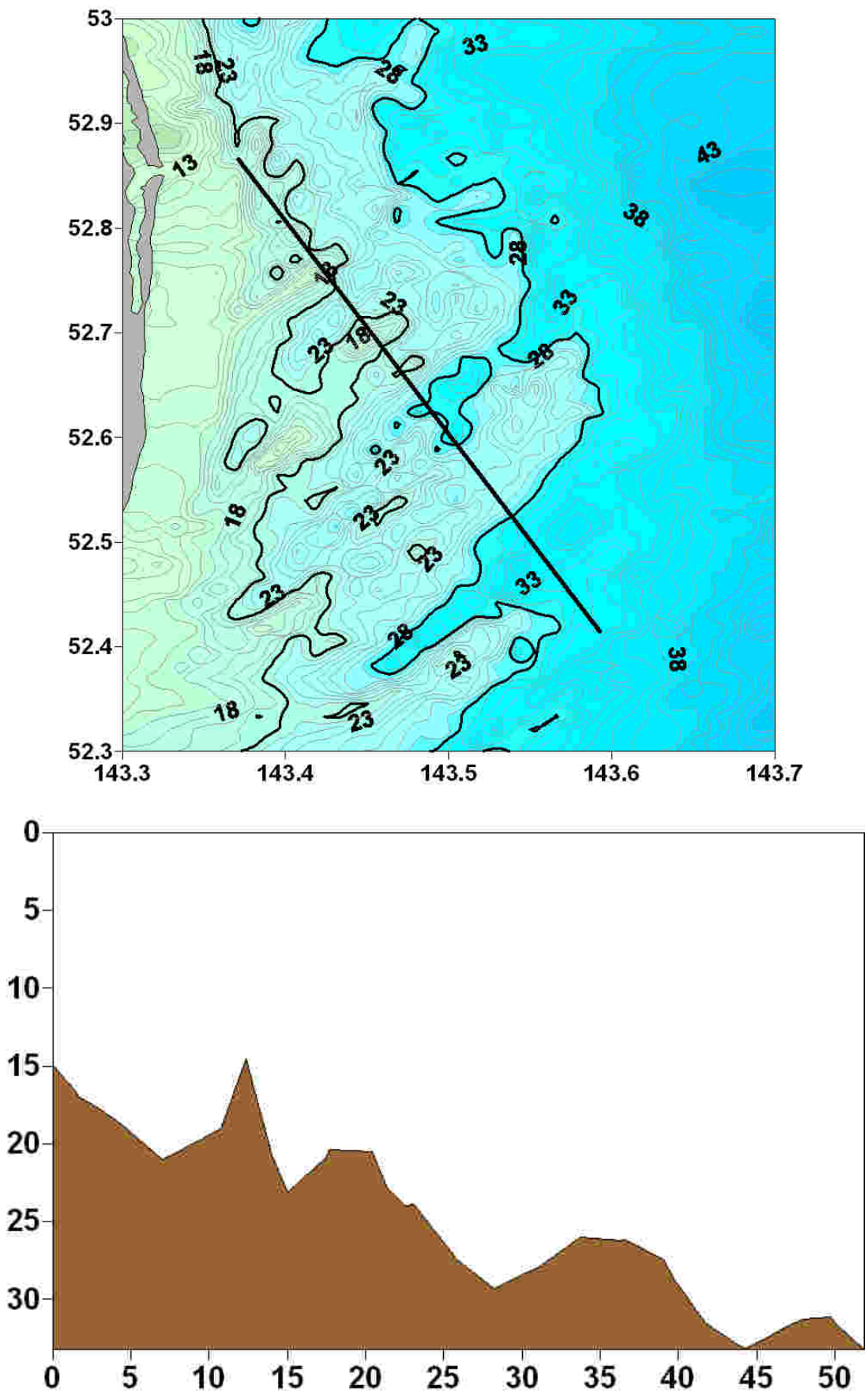


Figure 3.9 - (a) Section of the bathymetric grid used to generate the selected profile; (b) corresponding bathymetric profile.

AVERAGE TSC.db	Nom	Level	Average of T	Average of S	Average of C					
<input type="checkbox"/>	<input checked="" type="checkbox"/> join1	<input type="checkbox"/> 0	<input checked="" type="checkbox"/>	<input checked="" type="checkbox"/>	<input checked="" type="checkbox"/>					
<div><div></div><div></div></div>										
STATION.db	nom	Code st	Year	Mon	Day	Lat	Lon	Phasa	time	max
<input type="checkbox"/>	<input checked="" type="checkbox"/> join1	<input type="checkbox"/>	<input type="checkbox"/>	<input type="checkbox"/> 8	<input type="checkbox"/> 14	<input checked="" type="checkbox"/> >52.2	<input checked="" type="checkbox"/>	<input type="checkbox"/>	<input type="checkbox"/>	<input type="checkbox"/>

Nom	Level	Average of T	Average of S	Average of C	Lat	Lon
25	0.00	7.68	29.40	1 474.81	52.33	143.73
26	0.00	8.24	29.16	1 475.92	52.35	143.59
27	0.00	7.94	28.71	1 474.25	52.40	143.47
28	0.00	7.98	27.76	1 473.15	52.45	143.35
29	0.00	8.29	27.55	1 474.46	52.45	143.35
30	0.00	7.21	28.27	1 471.18	52.52	143.37
31	0.00	7.32	28.15	1 471.14	52.60	143.38
32	0.00	7.54	28.01	1 471.82	52.60	143.38
33	0.00	7.55	27.83	1 471.58	52.67	143.37

Figure 3.10 - Result of a request to the hydrology database.

STATION (**Nom** - number of measurement point;

Code st. - name of measurement point;

Year, Month, Day - date of measurement;

Time - time of measurement;

Lat - latitude;

Lon - longitude;

Phase - phase of tide;

Max - maximum depth horizon);

DATA_TSC (**Nom** - number of measurement point;

Level - measurement horizon;

T - water temperature at the depth horizon;

S - water salinity at the depth horizon;

C - sound speed at the depth horizon);

AVERAGE_TSC (**Nom** - number of measurement point;

Level - upper integer value of one-meter layer;

Average T - average temperature in the layer;

Average S - average salinity in the layer;

Average C - average sound speed in the layer).

A special program was used to convert the 321 random access files containing the hydrologic measurements at each of the 321 stations into two files, one of which corresponds to the table **STATION** and the second to the table **DATA_TSC**.

Table 3.4 - Parameters of hydrology measurements taken on 22 September 2004.

Number	Station Code	Time	Latitude	Longitude	Phase
247		13.00	52.73	143.43	'min'
248	Z1	13.30	52.73	143.48	'min'
249	PTL-6-C	14.00	52.72	143.55	'min'
250	PTL-6-B	14.20	52.72	143.61	'min'
251	PTL-6-B	16.00	52.72	143.61	'min'
252	PTL-6-A	16.30	52.72	143.66	'max'
253	PTL-6-A	18.00	52.72	143.66	'max'
254	PTL-6-C	19.00	52.72	143.55	'max'
255	Z1	19.20	52.72	143.49	'max'
256	a.5	19.40	52.73	143.43	'max'
257	PTL-7-C	20.10	52.71	143.47	'max'
258	PTL-7-C	21.00	52.71	143.47	'max'
259	a.5	21.30	52.73	143.43	'max'
260	Z1	22.10	52.69	143.54	'max'
261	PTL-7-A	23.00	52.64	143.66	'max'

For the **AVERAGE_TSC** table the data values were averaged for each 1 m layer. One of the goals of the study was to tie the hydrologic data to the phase of the tide. The tide phase was calculated using the program TideComp (demo, v. 8.01, www.pangolin.co.nz). The following classifications were defined for phase of the tide at the time of the hydrologic measurement:

- Low water 'min' - minimum tide for hydrologic measurements, tide is below 1 m⁶¹; and
- High water 'max' – maximum tide for hydrologic measurements, tide is equal to or above 1 m.

⁶¹ The maximum tidal range in the area is ± 1 m.

Figure 3.11 shows the phases of the tide for hydrologic measurements taken on 22 September 2004 (the key parameters of the hydrologic measurements are given in Table 3.4).

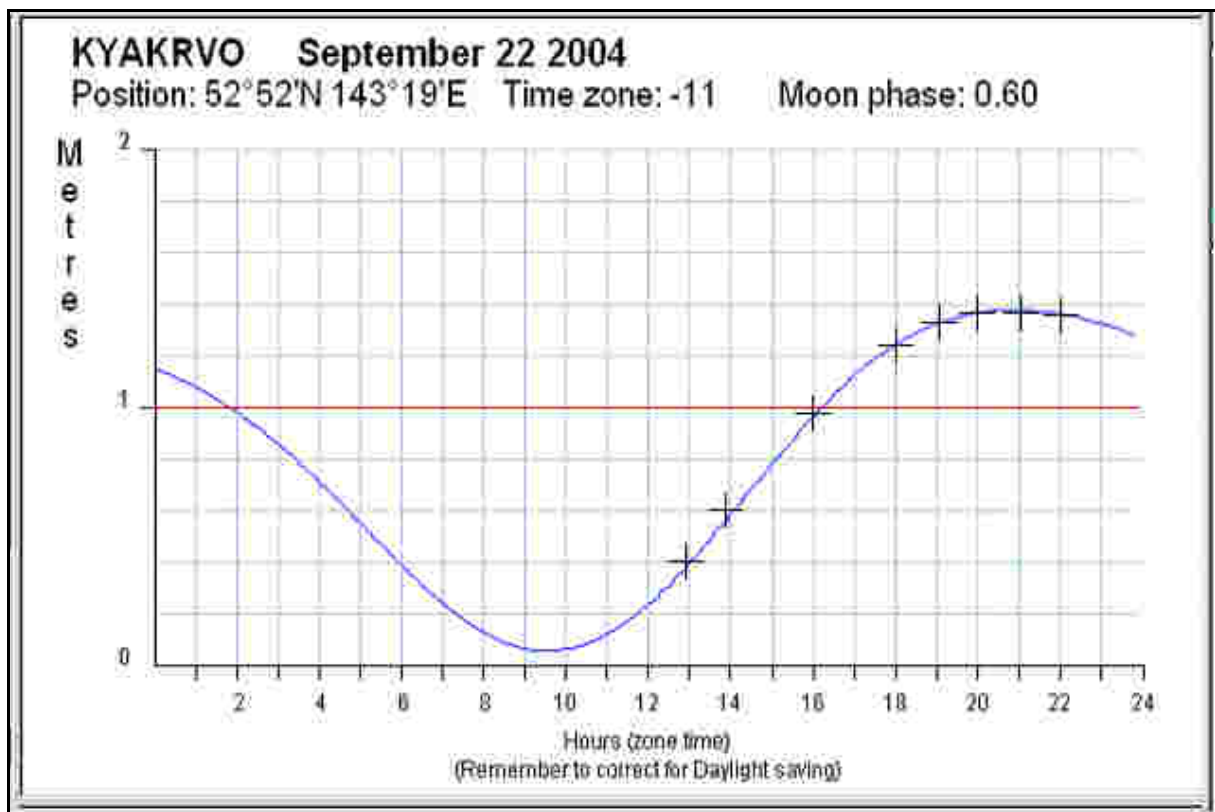


Figure 3.11 - Tide phase for hydrologic measurements made on 22 September 2004 (hydrology measurements are in Table 3.4).

3.5.3 Methodology for building hydrologic sections

Profiles were selected to analyze the spatial variation of hydrologic parameters in the area, these profiles were tied to the phase of the tide. Tables 3.5 and 3.6 contain data corresponding to hydrologic measurements acquired in August and September. The tables contain data about the number, distance from the first measurement in kilometers (R), name, longitude, latitude, depth and time of the hydrologic measurement. Figure 3.12 shows the profiles generated from hydrologic data acquired in August (Figure 3.12(a)) and September (Figure 3.12(b)).

Figure 3.13(a) shows a map of profile 2.2. Figures 3.13(b) to 3.13(d) show the distribution of temperature $T(z,r)$, salinity $S(z,r)$ and sound speed $C(z,r)$ along the profile generated using averaged data. The X-axis is the distance from the first hydrologic measurement and the Y-axis is depth in meters. Data for all the other sections shown on Figure 3.12 are in Appendix F⁶².

Table 3.5 - Profiles generated using August hydrology measurements.

#	R (km)	Station Code	Longitude	Latitude	Day	Phase	Time
2.1	0	Z1	143.45	52.9	19	'min'	21
2.1	4.09	PTL-2-C	143.51	52.91	19	'min'	21.3
2.1	9.33	PTL-2-B	143.59	52.91	19	'min'	22
2.1	11.69	PTL-2-A	143.62	52.92	19	'min'	19.2
2.2	0	TLP-9-C	143.40	52.90	19	'max'	12
2.2	3.4	Z1	143.45	52.90	19	'max'	12.5
2.2	7.4	PTL-2-C	143.51	52.90	19	'max'	13.2
2.2	12.69	PTL-3-B	143.59	52.90	20	'max'	10.2
2.2	0	8	143.39	52.90	30	'min'	14.4
2.2	4.02	Z1	143.45	52.90	30	'min'	23.3
2.2	8.12	PTL-2-C	143.51	52.91	30	'min'	15.3
2.2	9.45	PTL-2-C	143.53	52.91	30	'min'	23
2.2	12.79	PTI-2-B	143.58	52.91	30	'max'	21.3
2.2	16.24	PTL-2-A	143.63	52.92	30	'min'	18.5
3	0	PTL-13	143.35	143.35	14	'min'	17.4
3	8.5	Z1	143.37	143.37	14	'min'	18.3
3	17.27	PTL-11-C	143.38	143.38	14	'min'	21.1
3	25.37	5	143.37	143.37	14	'min'	22.1
3	29.61	A.4	143.37	143.37	14	'max'	23.1
4	0	Orlan	143.59	52.35	18	'min'	19.1
4	6.89	Z1	143.55	52.41	18	'min'	19.5
4	13.79	Z2	143.52	52.47	18	'min'	20.2
4	21.51	PTL-10-A	143.47	52.53	18	'min'	21
5	0	PTL-8-C	143.45	52.71	28	'min'	18.5
5	11.15	Z1	143.56	52.64	28	'min'	20.1
5	14.3	PTL-8-B	143.59	52.62	28	'min'	20.4
5	20.38	PTL-8-A	143.65	52.58	28	'min'	21.1

⁶² Every Figure consists of four plots: (a) A map showing the profile; (b) The sound velocity field; (c) The temperature field and (d) The salinity field. The plots were generated using Surfer.

Table 3.6 - Profiles generated using September hydrology measurements.

#	R (km)	Station Code	Longitude	Latitude	Day	Phase	Time
1	0	Odoptu-S-10	143.3	53.06	10	'min'	20.4
1	0.84	TLP-14-B	143.32	53.06	10	'min'	21
1	1.72	Odoptu-S-20	143.33	53.06	10	'max'	22.4
1	2.31	TLP-14-C	143.34	53.06	10	'max'	23
1	2.57	TLP-14-D	143.35	53.06	12	'max'	19
1	3.27	TLP-14-G	143.36	53.06	10	'max'	23.2
1	5.96	TLP-14-C	143.4	53.06	12	'min'	21.1
1	7.72	TLP-14-E	143.42	53.06	12	'min'	22.4
1	9.18	TLP-14-F	143.45	53.06	11	'max'	2
2	0	8	143.4	52.9	18	'max'	23.4
2	3.6	Z1	143.45	52.91	18	'max'	23.2
2	7.55	PTL-2-C	143.51	52.9	18	'max'	23
2	12.68	PTL-2-B	143.59	52.91	18	'max'	22.3
2	15.2	PTL-2-A	143.62	52.92	18	'max'	22
3	0	PTL-12	143.32	52.47	27	'min'	20.5
3	3.35	PTL-13	143.35	52.45	27	'min'	18.5
3	5.42	Z4	143.37	52.43	27	'min'	21.2
3	8.01	Z3	143.42	52.43	27	'min'	21.4
3	12.36	Z2	143.47	52.41	27	'max'	22
3	16.72	Z1	143.52	52.38	27	'max'	22.3
3	21.22	Orlan	143.58	52.36	27	'max'	23
3.1	0	PTL-12	143.32	52.47	27	'min'	19.2
3.1	3.35	PTL-13	143.35	52.45	27	'min'	17.2
3.1	8.08	Z3	143.41	52.43	27	'min'	17
3.1	12.31	Z2	143.47	52.41	27	'min'	16.4
3.1	16.51	Z1	143.52	52.39	27	'min'	16.2
3.1	21.59	Orlan	143.58	52.36	27	'min'	15.5
4	0	P-Orlan	143.38	52.4	7	'min'	18.4
4	6.42	H	143.48	52.38	7	'min'	16.5
4	10.53	G	143.53	52.37	7	'min'	16.2
4	13.39	E	143.57	52.36	7	'min'	15.08
4	14.31	Orlan	143.59	52.37	7	'min'	9.44
4	17.58	D.1	143.63	52.35	7	'min'	14.3
4	21.52	C	143.68	52.33	7	'min'	12.5
4	24.39	A	143.72	52.32	7	'min'	11.3

Table 3.6 (continued) - Profiles generated using September hydrology measurements.

#	R (km)	Station Code	Longitude	Latitude	Day	Phase	Time
5.1	0	a.5	143.43	52.72	22	'min'	13
5.1	3.45	Z1	143.48	52.73	22	'min'	13.3
5.1	8.06	PTL-6-C	143.55	52.72	22	'min'	14
5.1	11.7	PTL-6-B	143.61	52.72	22	'min'	14.2
5.2	0	a.5	143.43	52.72	22	'max'	19.4
5.2	2.56	PTL-7-C	143.47	52.71	22	'max'	20.1
5.2	3.53	Z1	143.49	52.72	22	'max'	19.2
5.2	7.77	PTL-6-C	143.55	52.72	22	'max'	19
5.2	14.93	PTL-6-A	143.66	52.78	22	'max'	18
6	0	a.5	143.43	52.726	11	'max'	20
6	2.9	Z1	143.47	52.72	11	'max'	20.4
6	7.93	PTL-6-C	143.55	52.72	11	'max'	21.1
6	11.73	PTL-6-B	143.61	52.72	11	'max'	23.1
6	15.07	PTL-6-A	143.65	52.72	11	'max'	23.5
7	0	Odoptu-S-10	143.38	52.40	7	'min'	18.4
7	10.52	a.8	143.38	52.5	4	'max'	20.5
7	13.85	6	143.38	52.53	4	'max'	20.2
7	29.43	5	143.37	52.67	4	'max'	17.3
7	46.12	PTL-11-B	143.36	52.82	6	'min'	4.18
7	58.34	PTL-11-A	143.36	52.93	5	'min'	7.59
7	72.95	P-Orlan	143.31	53.06	10	'min'	20.4

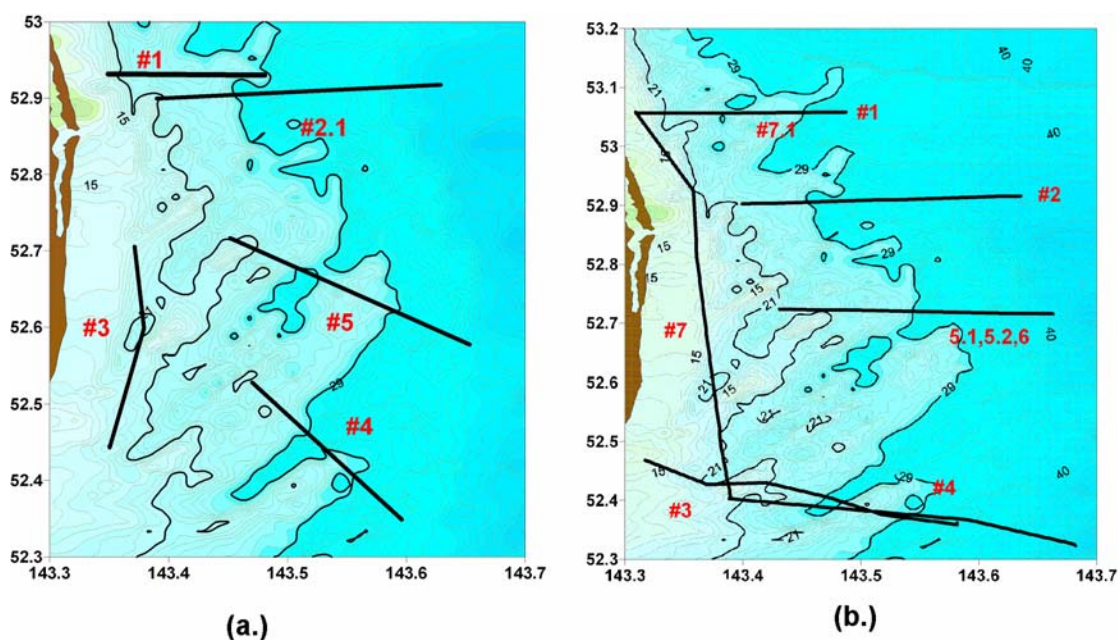


Figure 3.12 - Profiles generated from hydrology acquired in: (a) August and (b) September.

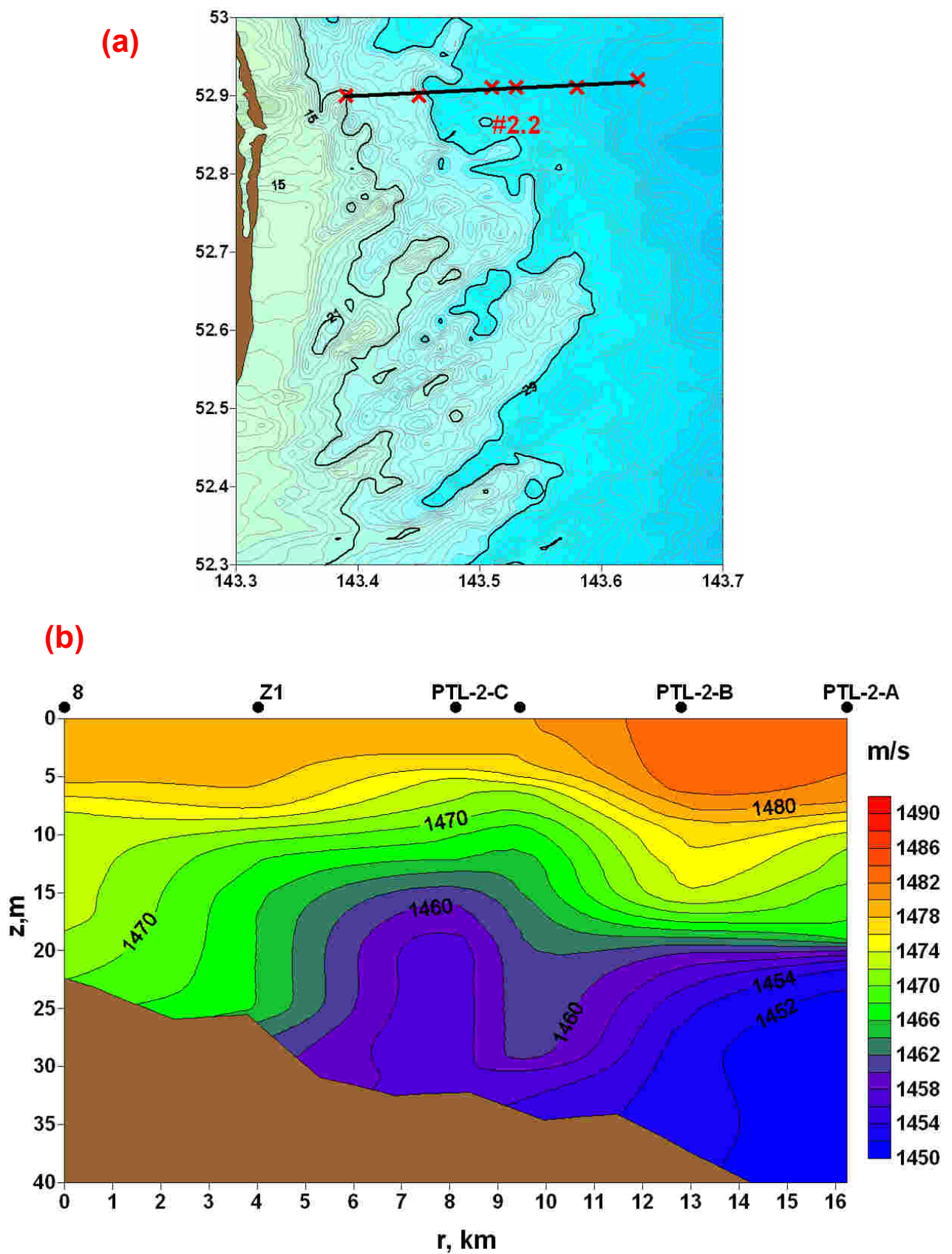


Figure 3.13 - (a) Map showing profile 2.2 generated using data acquired on the 30 August, 2004; (b) Sound velocity field $C(z,r)$ for profile 2.2.

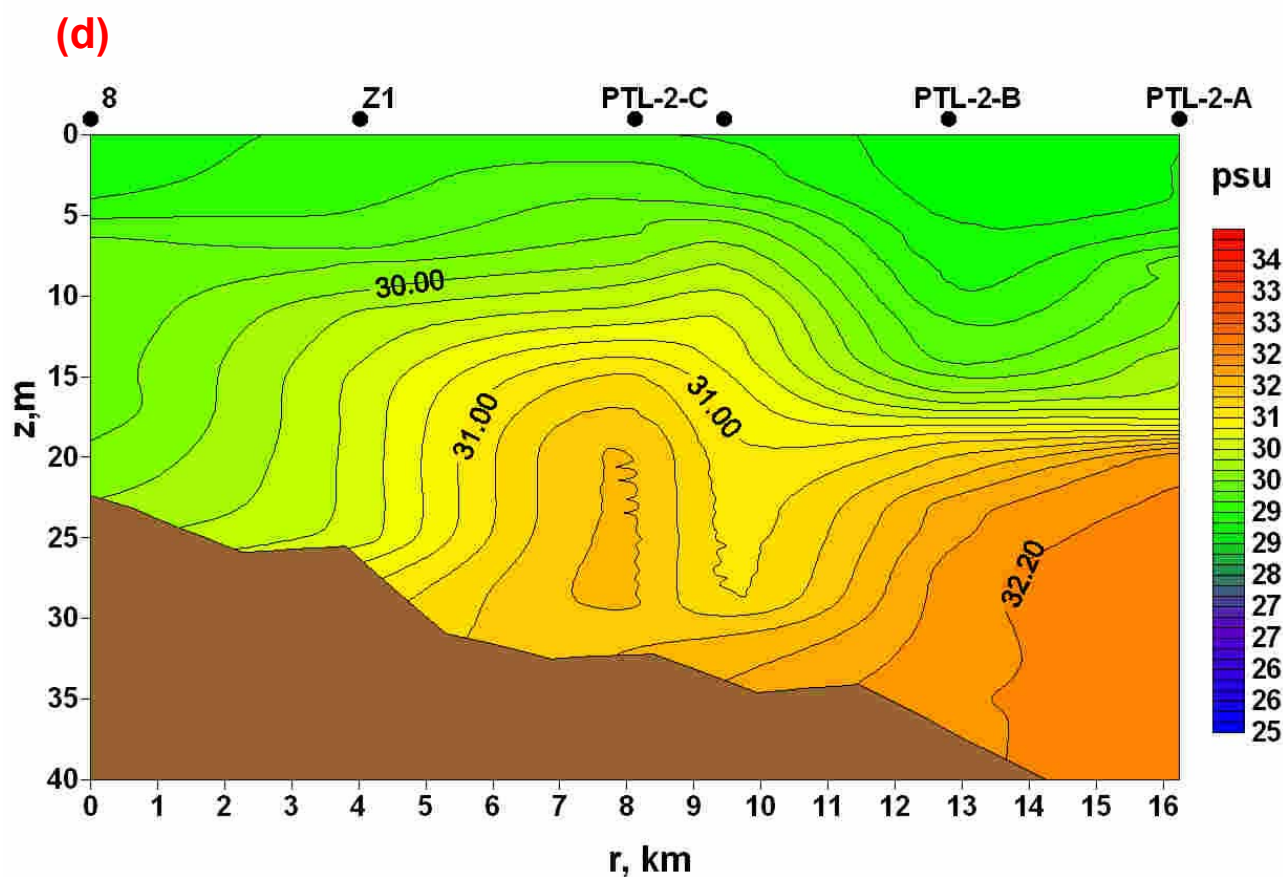
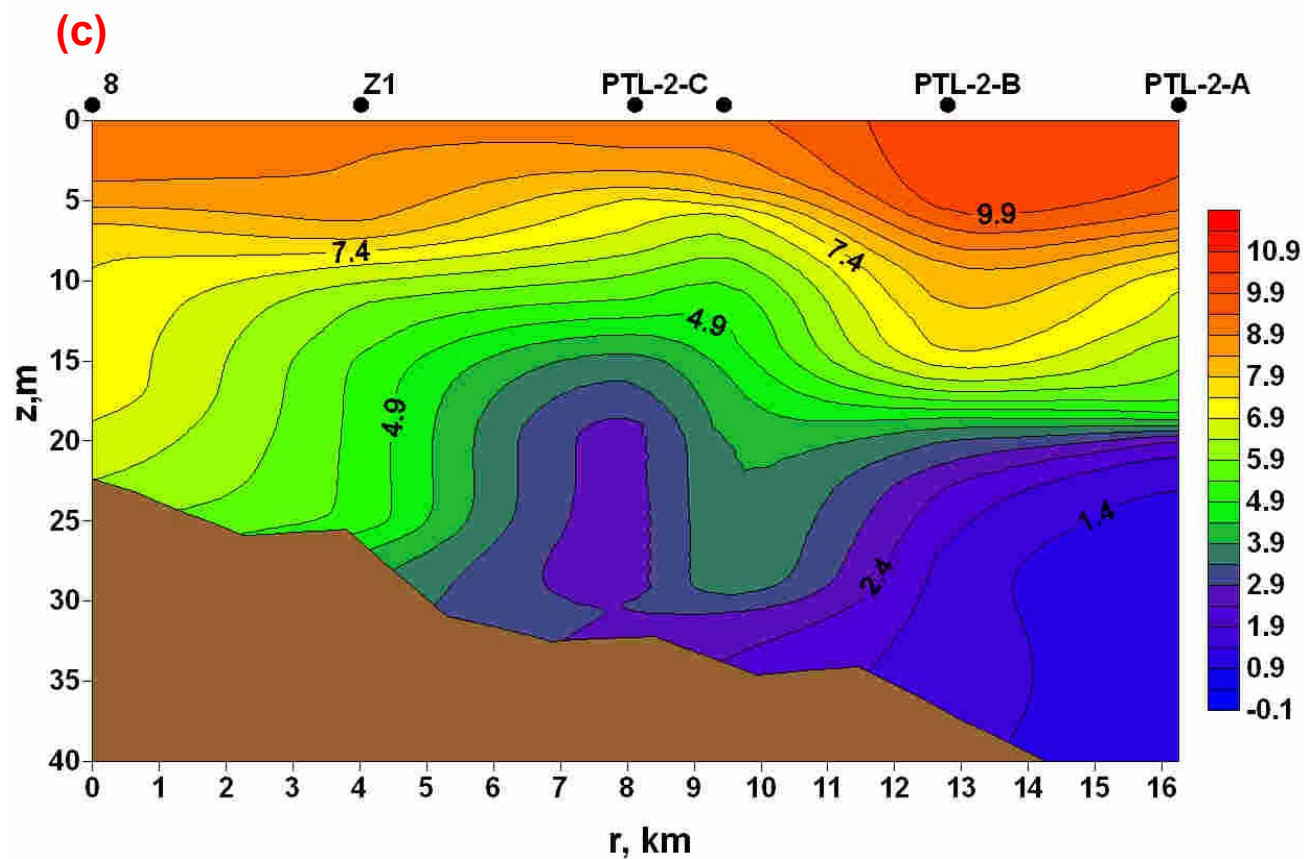


Figure 3.13 - (c) Temperature field $T(z,r)$; (d) Salinity field $S(z,r)$ for profile 2.2.

4 ACKNOWLEDGEMENTS

The authors would like to thank the V.I. Il'icev Pacific Oceanological Institute, FEB Academy of Sciences of Russia (POI), (Тихоокеанский океанологический институт им. В.И. Ильичева ДВО РАН), for assistance in performing this work.

The authors wish to thank the crew of the *Academik Oparin* for their hospitality and assistance while conducting acoustic measurements on the NE Sakhalin shelf. They would also like to thank the leader of the expedition Yuri Yakovlev (IBM) for the management of the safety program for the 2004 field season and all the scientists participating in the expedition.

Finally the authors would like to express their gratitude to Dr. Sc. G.I. Dolgih (Долгих Г. И.)(POI), Dr. Sc. V.G. Petnikov (Institute of general physics, Moscow), Drs. Richard T. Houck, H. Rodger Melton, and Markku Santala (ExxonMobil Upstream Research Co.), as well as Dr. C.I. Malme (LGL) for reviewing this report.

Our special thanks go to the investment companies, their employees and consultants, without whom the present work could not have been conducted. These include:

LGL Limited - S.R. Johnson, S. Meier, and S.B. Yazvenko.

Exxon Neftegas Limited - M.R. Jenkerson, and H.R. Melton.

Sakhalin Energy Investment Company Limited - L. Aerts, T. Konovalova.

5 AUTHORS

From the V.I. Il'icev Pacific Oceanological Institute, FEB, Academy of Sciences of Russia:

Sc. S.V. Borisov (Борисов С.В.)

Sc. A.V. Gritsenko (Гриценко А.В.)

Dr. E.V. Dmitrieva (Дмитриева Е.В.)

Dr. A.A. Karnauhov (Карнаухов А.А.)

Sc. M.V. Kruglov (Круглов М.В.)

Dr. Sc. A.N. Rutenko (Рутенко А.Н.)

6 BIBLIOGRAPHY

1. Allen J.S. (1973). Upwelling and coastal jets in a continuously stratified ocean // J. Phys. Oceanography. Vol. 3, pp. 245 – 257.
2. Bondar` L.F., Gritsenko A.V., Zakharov V.A., Kovzel` D.G. and Rutenko A.N. (1993). Digital radio telemetry system for the collection and results of its application in studies of sea reverberation characteristics // Acoustical Physics, Vol.39, no.2, pp.118-122.
3. Borisov S.V., Gritsenko A.V., Jenkerson M.R., Rutenko A.N., and Hodzevich A.V. (2002) Evaluating and Monitoring Acoustic Transmission from the Odoptu 3D seismic Survey 5 August - 9 September, 2001; Sakhalin, Russian Federation // Pacific Oceanological Institute (FEB RAS) report for Exxon Neftegas Ltd.
4. Borisov S.V., Gritsenko A.V., Rutenko A.N., and Hodzevich A.V. (2003) Results of Acoustic Studies Within and Adjacent to the Piltun-Astokh License Area 1-6 August, 2001 and 17-24 September, 2001; Sakhalin, Russian Federation // Pacific Oceanological Institute (FEB RAS) report for Exxon Neftegas Ltd. and Sakhalin Energy Investment Co.
5. Borisov S.V., Gritsenko A.V., Kruglov M.V., Korotchenko R.A., and Rutenko A.N. (2003) Results of Acoustic Studies on the North-East Sakhalin Shelf, 12 September to 23 September, 2002; Sakhalin, Russian Federation // Pacific Oceanological Institute (FEB RAS) report for Exxon Neftegas Ltd. and Sakhalin Energy Investment Co
6. Borisov S.V., Gritsenko A.V., and Rutenko A.N. (2004) Acoustic Studies on the North East Sakhalin Shelf, Volume 1: Equipment, Methodology and Data; 15 August to 20 September, 2003; Sakhalin, Russian Federation // Pacific Oceanological Institute (FEB RAS) report for Exxon Neftegas Ltd. and Sakhalin Energy Investment Co.
7. Borland Paradox for Windows, version 1.0, User's Guide. USA: Borland International, Inc., 1993. 640 p.
8. Defant A. (1961) Physical oceanography. Vol. I and II. Pergamon Press, Oxford.
9. Hooge P.N. and Eichenlaub B. (1997). Animal movement extension to arcview. Ver. 1.1. Alaska Science Center - Biological Science Office // U.S. Geological Survey, Anchorage, AK, USA.
10. Kruglov M.V., and Rutenko A.N. (2003) Transmission Loss Studies on the North-East Sakhalin Shelf 2001 and 2002; Sakhalin, Russian Federation // Pacific Oceanological Institute (FEB RAS) report for Exxon Neftegas Ltd. and Sakhalin Energy Investment Co.
11. Kruglov M.V., and Rutenko A.N. (2004) Acoustic Studies on the North-East Sakhalin Shelf, Volume 2: Analysis, Conclusions and Recommendations; 15 August to 20

- September 2003; Sakhalin, Russian Federation // Pacific Oceanological Institute (FEB RAS) report for Exxon Neftegas Ltd. and Sakhalin Energy Investment Co.
12. Powell R. A. (2000). Animal home ranges and territories and home range estimators // Research techniques in animal ecology: controversies and consequences. Edited by Boitani L. and Fuller T.K. // Columbia University Press, New York. pp. 65-110.
 13. Richardson W.J., Greene C.R., Malme C.I. and Thomson D.H. (1995). Marine mammals and noise. Academic Press Limited. 576 p.
 14. Sobolevsky E.I., et.al. (Соболевский Е.И. и др.) (2000). Report for Sakhalin Energy Investment Company (Отчет для «Сахалин Энерджи Инвестмент Компани Лтд.»).
 15. Worton B.J. (1989). Kernel methods for estimating the utility distribution in home-range studies // Ecology, Vol.70, pp. 164-168.
 16. Yozhida K. (1967). Circulation in the eastern tropical oceans with special reference of upwelling and undercurrents // Japanese. J. Geophysics, Vol.4, pp. 1 – 75.
 17. Атлас океанов. Тихий океан. - М. (1974). Гл. упр. навигации и океанографии, 1974. - XIV.- 302 С.: с ил. и картами.
 18. Дмитриева Е.В., Ростов И.Д. (2004) Разработка и реализация баз океанографических данных по Северной части Тихого океана. Владивосток: Даль наука. 143 с.
Dmitrieva E.V., Rostov I.D. (2004) Development and realization of oceanographic data base for the Northern Pacific. Vladivostok. Dalnauka. 143 p.)